Mechanical and Drainage Performance Characterization of Unbound Granular Materials

by

Amin Mneina

A Thesis

Submitted to the Faculty of Graduate Studies in Partial Fulfillment of the Requirements for the Degree of

Master of Science

Department of Civil Engineering

University of Manitoba

Winnipeg, Manitoba

Abstract

The drainage performance of unbound granular material (UGM) is an important consideration in pavement design because the presence of excess moisture in UGM layers can eventually lead to premature failures. Recently, transportation agencies have been evaluating their granular base and subbase drainage and mechanical performance to ensure sufficient drainage capacity while maintaining adequate structural support to produce more sustainable pavement structures. Linking performance to UGM construction specification requires accurate characterization of UGM's mechanical and drainage performance and how physical and gradation parameters affect such performance. These evaluations led to an update of the specification requirements of UGM in many jurisdictions including Manitoba. In this research, constant head hydraulic conductivity, resilient modulus, permanent deformation, double ring infiltrometer, and falling weight deflectometer test methods were used in laboratory and field investigations. These tests were conducted to characterize the drainage and mechanical performance of ten UGM samples representing four different gradation bands. The laboratory test results were also used to investigate the reliability of the estimated hydraulic conductivity from the Moulton prediction model and from the Enhanced Integrated Climatic Model (EICM). Test results showed an improvement in resilient modulus and drainage quality for samples in gradation bands that specify larger maximum aggregate size and limited fines. A statistical analysis of the test results showed that D_{10} larger than 0.2mm and D_{60} larger than 8mm would guarantee higher stiffness and better drainage performance with a time-to drain of less than 5days for typical pavement cross-sections and a resilient modulus value exceeding 200MPa. The Moulton prediction model was found to provide a better approximation of hydraulic conductivity of the materials included in this study, while the EICM model was found to significantly overestimate the hydraulic conductivity for most of the samples.

Acknowledgements

I would like to thank my academic advisor, Dr. Ahmed Shalaby for his technical and academic guidance through this research. I would also like to thank the members of the examination committee, Dr. Hartmut Holländer, Dr. Mohammad Alauddin Ahammed, and Dr. Ahmed Ghazi for volunteering their valuable time and effort in the review and examination of this thesis. Special thanks to my colleagues and the staff at the University of Manitoba's Pavement Research Group.

I like to acknowledge the support of this research by Manitoba Infrastructure, and The Yukon Department of Highways and Public Works.

Finally, I would like to express my sincere gratitude to my family, my in-laws, and my lovely wife for their limitless support and continuous encouragement throughout my studies.

Table of Contents

List of Figures

List of Tables

Chapter 1 Introduction

1.1 Background

Road transportation plays a significant role in the economic and social development through mobilization of goods and people. The safety and efficiency of road transportation rely heavily on the quality of transportation network. Vast amounts of money have been and are continuously being invested annually in the construction and in maintenance of pavement structures to maintain satisfactory level of service. Such large investments indicate the importance of reliable pavement design through proper mechanical and hydraulic characterization of materials.

In a typical pavement structure, the foundation layers (base/subbase) are usually constructed of unbound granular materials (UGM) for the purpose of providing structural support through load distribution, and for providing sufficient drainage of water that infiltrates the pavement system during different environmental events (Gu et al. 2017; Nishizawa 2012). The presence of excess moisture in the pavement system is related to most pavement distresses (Christopher & McGuffey, 1997). The stiffness reduction due to presence of excess moisture would cause buildup of tensile stresses in the bottom of the surface layer which results in premature fatigue cracking under traffic loads, (Hall & Crovetti 2007; Nishizawa, 2012). When moisture is trapped in a pavement system, it would cause significant reduction in the shear strength of the supporting base and subgrade layers. In a more comprehensive perspective, applying traffic loads on pavements with saturated sublayers would decrease their service life up to 10 times faster than if the same loads are applied on a pavement with well drained sublayers, (Cedergren 1988). Therefore, a subsurface drainage system is an important component of a pavement structure. The different approaches of subsurface drainage all depend on the drainage performance of the base layer, which is significantly

influenced by the hydraulic conductivity of the UGM. The hydraulic conductivity is affected by UGM physical properties, gradation, and type and amount of fines.

In addition to high quality drainage, base layers should also possess adequate mechanical properties such as stability during construction, stiffness, and resistance to permanent deformation under traffic loading. Historically, the California Bearing Ratio (CBR) test method has been widely used to provide an index of UGM stability as a road base material. However, such empirical method do not characterize mechanical behaviour based on fundamental engineering properties. They rather quantify mechanical behaviour based on comparison with historical behaviour of existing UGM material. Advanced mechanistic testing methods such as the Repeated Load Triaxial testing (RLT) is more accurate in characterizing the mechanical behaviour of UGM through quantifying stiffness, or resilient modulus, and permanent deformation behaviour.

The resilient modulus is a material property that is considered in the design of pavements by the 1993 American Association of State Highway and Transportation Officials (AASHTO) Design Guide. Resilient modulus is also the primary material input parameter for the Mechanistic-Empirical Pavement Design Guide (MEPDG). The resilient modulus captures the nonlinear elasto-plastic response of UGM under repeated loading in different stress conditions. Pavement structures experience rutting failure when pavement materials accumulate excessive amount of permanent deformation. Laboratory assessment of plastic behaviour is an essential performance parameter for UGM.

Aggregate gradation is the most prominent UGM property that influence performance (Bilodeau et al. 2009). It is beneficial to engineer an optimized gradation range that is bound by performance related parameters. Most transportation agencies have base/subbase UGM specifications that are established decades ago which are not linked to mechanistic performance (Bilodeau et al. 2009).

Optimization of UGM base/subbase in terms of drainage and stiffness guarantees the efficient use of resources, since suboptimal base/subbase stiffness would result in designing thicker pavement structures.

To produce a more sustainable cost-effective pavement design, unbound granular layers in pavement structures need to be based on locally available UGM with optimized characteristics for mechanical (structural) and hydraulic performance.

1.2 Research Objectives

This research aims to:

- Investigate the effect of different physical properties such as porosity, nominal maximum size, gradation, and angularity on the mechanical behaviour of compacted UGM

- Obtain laboratory measured range of values for performance related parameters, (hydraulic conductivity, resilient modulus, and permanent deformation), for locally available UGM to enhance the reliability of design outputs for both Manitoba and Yukon.

- Evaluate the drainage quality of different UGM and study the effect of physical properties on subsurface drainage.

- Evaluate the performance of Manitoba's newly adopted drainable base through laboratory and field investigation of mechanical and hydraulic properties.
- Evaluate prediction models for hydraulic conductivity based on the laboratory measurements.

- Provide recommendations on gradation controls that link aggregate size distribution to the base layer's mechanical and hydraulic performance.

1.3 Research Scope

The update of UGM gradation specifications to include coarser UGM gradations with limited fines (Classes: Granular Base Course-"GBC", and Drainable Stable Base-"DSB") for use in base layers in Manitoba provided a need to investigate the mechanical and hydraulic properties of the newly adopted gradation bands. The Yukon Department of Highways and Public Works were also reviewing their UGM Specifications regarding the mechanical and drainage performance. Laboratory and field testing programs were developed to quantify the base layer performance in terms of stiffness (resilient modulus), permanent deformation, and drainage quality of different representative gradation bands of locally available UGM. Effects of gradation parameters on performance were investigated to provide recommendations on gradation controls in order to link UGM gradation specifications to mechanical and hydraulic performance.

1.4 Research Significance

This research provides laboratory-evaluated range of values for UGM performance related parameters such as hydraulic conductivity, resilient modulus, and permanent deformation. The provided values would provide reliable pavement design input parameters in Yukon and in Manitoba. The research would provide testing data to support recommendations on gradation controls which would lead to improved mechanical and drainage performance of pavement structures. Improving pavement design reliability would reduce uncertainties in performance.

Improving material performance would reduce the possibility of premature distresses in pavements, leading to sustainable, safe, and cost-effective roads.

1.5 Thesis Organization

The flow of the thesis is organized as follows:

- Chapter 1 Introduction

  This chapter provides a general background, contexts, problem statement, research objectives, and research scope.

- Chapter 2 Literature Review

  This chapter presents a literature review related to drainage and mechanical characterization of UGM. The review included 1) The effect of subsurface drainage on pavement structures and a summary of factors affecting UGM drainage, 2) A summary of the current practice for time-to drain calculations, 3) A summary of existing prediction models for estimating permeability of UGM, and 4) Current knowledge on UGM mechanical performance in terms of resilient modulus and permanent deformation.

- Chapter 3 Experimental Program

  This chapter provides details on the material properties, current agency specifications, sampling procedures, and test methods used for characterization of drainage and mechanical behaviour of UGM.

- Chapter 4 Drainage Performance of UGM

  This chapter presents the results of lab and field hydraulic conductivity tests. Provides thorough discussion of effect of different material properties on the quality of drainage, and comparisons between hydraulic conductivity prediction models.

- Chapter 5 Mechanical Performance of UGM

  This chapter presents test results of resilient modulus and permanent deformation testing, in addition to falling weight deflectometer test results. Results provide characterization of the effect of material properties on mechanical performance.

- Chapter 6 Conclusions and Recommendations

  This chapter provides a summary of the research, conclusion points, and recommendations for future research.

Chapter 2 Literature Review

2.1 Introduction

A typical pavement structure consists of three layers being subgrade, base/subbase, and pavement surface as simplified in Figure 2.1 (Davich et al. 2004; and Hossain & Lane, 2015). The base/subbase layer is usually constructed of unbound granular materials (UGM) for the purpose of providing structural support through load distribution, as well as providing sufficient drainage of water that infiltrates the pavement system from different environmental events (Gu et al. 2017). The UGM base/subbase layers have both elastic and plastic responses to traffic loading. Such mechanical response or behaviour is characterized through both resilient modulus testing and permanent deformation testing which will be discussed in detail in this chapter.

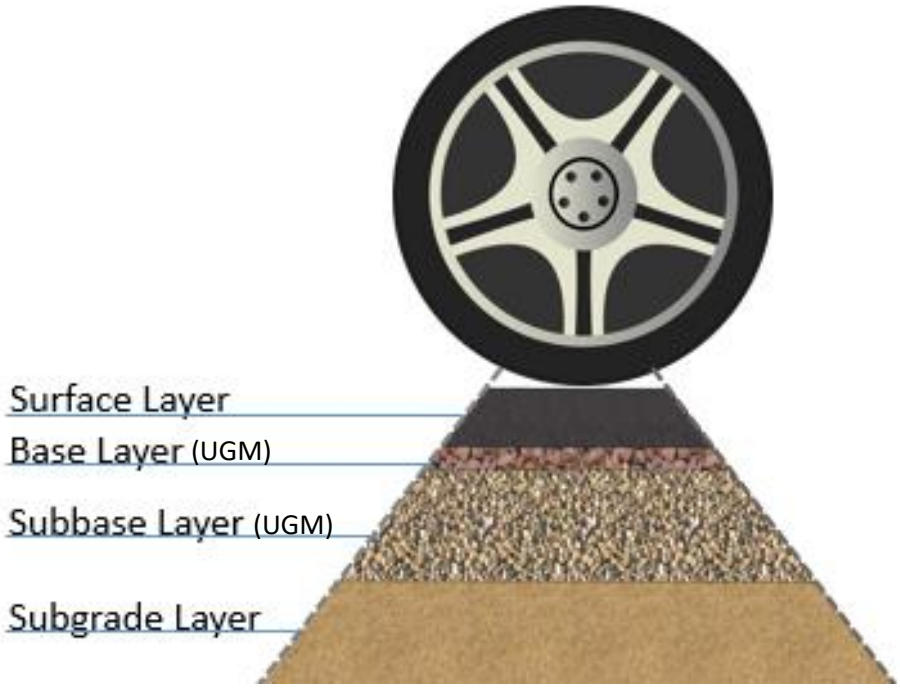

Figure 2.1 Typical Pavement Structure. Traffic loads get distributed across a larger area as they transmit down from the surface layer.

During the life span of the pavement structure, the unbound base/subbase layers accumulate damage under repeated traffic loading in the form of permanent deformation, which translates to surface distresses and reduced serviceability of the pavement structure. Though foundation layers are designed to resist such damage throughout the service life, the presence of excess moisture in pavement sublayers accelerate the damage caused by traffic loading which decreases the expected service life of the structure (Bouchedid & Humphrey, 2005). According to Abhijit & Patil, (2011) the interaction between water and aggregate grains often translates to road damage in different ways that include:

- Strength reduction due to excess pore water pressure
- Pumping of fines and void creation
- Deformation caused by frost heave and thaw weakening
- Increase in differential swelling of expansive subgrade soils

Therefore, a reliable characterization of drainage properties in aggregate bases is essential in evaluating the performance of pavement structures.

2.2 Drainage in Pavement Structures

In pavement structures, it is recognized that many surface distresses are related to the presence of moisture in sublayers either directly or indirectly (Suits et al. 1999). For instance, if water is trapped in a pavement system, it will cause significant reduction in the shear strength of the supporting base and subgrade layers,(Liang 2007; Soliman 2015). Cedergren, (1974) concluded that applying traffic loads on pavements with saturated sublayers would decrease their service life up to 10 times faster than if the same loads are applied on a pavement with well drained sublayers.

The effect would be even more severe when freeze/thaw cycles are considered (Cedergren 1988). Erlingsson et al. (2009) demonstrated the increase of the rate of rutting due the heavy vehicle passes when groundwater table was raised.

Mitigation of moisture related distresses can be achieved by quickly draining excess moisture out of the pavement structure through a good drainage system. Although there are three components of pavement drainage: (Surface drainage, subsurface drainage, and groundwater drainage), subsurface drainage is considered the most effective (Mallela et al. 2000). Various subsurface drainage techniques have been developed and adapted over the years and can be classified as;

- Daylighting of permeable bases
- Edge drains

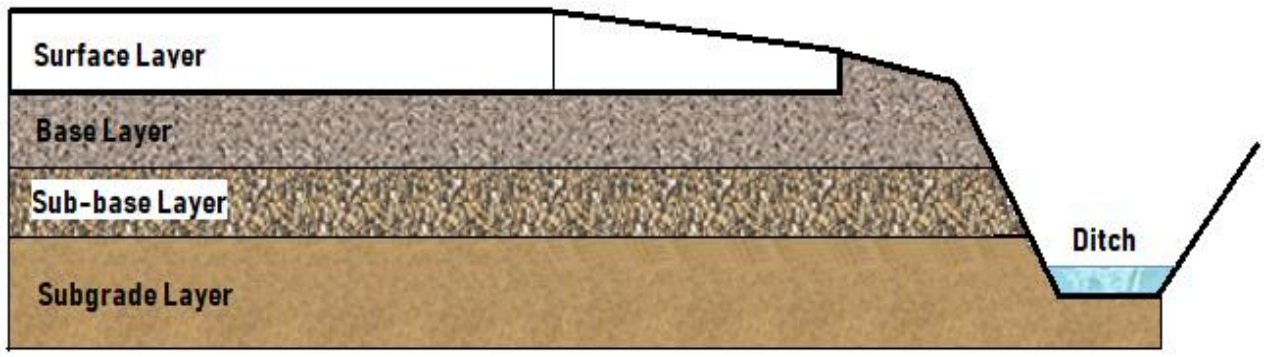

Figure 2.2 Typical AC pavement with a daylighted base

In either technique, a base layer with sufficient drainage capability is an essential requirement. Subsurface drainage quality has direct effect on pavement construction costs as well as maintenance costs. AASHTO 1993 pavement design guide accounts for layer drainage through the classification of drainage quality. The value of the drainage quality has a direct effect on layer thickness calculations and the pavement structural number through the drainage coefficient (Cd)

for rigid pavements, and the drainage modifier (m) for flexible pavements (Blaschke et al. 1993). Moreover, decreasing maintenance costs and efforts would require more attention to drainage as a design parameter in pavement structures. For example, in areas with high precipitation, a given pavement structure could have the thickness of its base layer reduced by a factor of 2 if excellent drainage vs poor drainage was provided (Christopher & Zhao 2001).

Pavement drainage quality can be improved by enhancing the structural geometry through increasing surface slope or increasing base layer thickness. However, a more cost-effective way of enhancing pavement drainage quality is to improve the characteristics of base materials by using engineered aggregate blends with properties that allow for better drainage through connected voids, while maintaining proper structural stability through stone-on-stone contact.

2.3 Factors Affecting UGM Drainage

Subsurface drainage performance in pavement systems is affected by the material properties as well as the geometry of the pavement structure. This research focused on the effect of material properties on subsurface pavement drainage.

The main material properties that influence drainage in granular layers are; effective porosity (N_e), and hydraulic conductivity (K), (Federal Highway Administration, 1992).

2.3.1 Effective Porosity

The effective porosity of a granular material is a measure of the pores ability to drain water. In other words, a granular material with high effective porosity is more capable of storing water than of draining it under the effect of gravity(Federal Highway Administration, 1992; Mallela et al.

2000). The effective porosity is influenced by material properties including void ratio, gradation, and type of course and fine materials. It is negatively proportional to the drainability of the granular layer. The effective porosity can be measured by recording the amount of water that drains from a saturated sample. It can also be estimated by Equation 2.1 (Federal Highway Administration, 1992)

$$N_e = N\ WL \qquad \textbf{(Eq. 2.1)}$$

Where: (N) is the porosity, and (WL) is the water loss factor which accounts for amount and type of fines.

2.3.2 Hydraulic Conductivity

Hydraulic conductivity is a measure of how fast water can travel through a material's pores under the effect of gravity (Klute 1965). It is also defined in Darcy's law as the proportional factor of the relationship between the flow through porous media and the hydraulic gradient (Lal & Shukla 2004; Simmons 2008). The hydraulic conductivity of UGM is influenced by grain size distribution and the density of the material, as well as the viscosity of the permeant fluid and the degree of saturation (Randolph et al. 1981, and Boadu et al. 2000). Since the conductivity decreases when the degree of saturation increases, for transportation applications it is usually recorded at 100% saturation to obtain a conservative measure.

Pavement's subsurface drainage is influenced by various material and geometric factors, but the hydraulic conductivity of compacted UGM has the most significant effect on subsurface drainage. For that reason, numerous research studies focused on linking material properties to the hydraulic conductivity in an effort to improve subsurface drainage. Table-2.1 presents a summary of material

properties that have been reported in the literature to influence the hydraulic conductivity of a compacted UGM layer.

According to (Federal Highway Administration, 1992), a large effective diameter (D_{10}) has a positive effect on the permeability of the material. Increasing the effective diameter is usually achieved by limiting the amount of material passing #8 sieve or #16 sieves. The coefficient of uniformity is a shape parameter, which is an indication of how close the blend is to a uniform gradation which is also reported to have influence on the hydraulic conductivity of compacted UGM (Tao & Abu-Farsakh 2008; Bennert & Maher 2005; Hoppe 1996).

The coefficient of uniformity (Cu) is negatively proportional to hydraulic conductivity. The smaller the value of C_u, the higher the uniformity of the grain sizes which results in higher permeability. (Hoppe 1996) reported that hydraulic conductivity increased significantly in samples with small C_u than in samples with larger C_u while the fines content remained constant. The fines content has been well reported in the literature to be negatively correlated to the hydraulic conductivity of the granular material (Soliman 2015; Moulton 1980; Bennert & Maher 2005).

Table 2.1 Material parameters affecting hydraulic conductivity as found in the literature

Parameter	Definition	Relationship to hydraulic conductivity	References
P_{200}	Percentage of particles smaller than 0.075 mm	Negatively proportional	Soliman (2015); Tao & Abu-Farsakh (2008); Bennert & Maher (2005); Moulton (1980)
D_{10}	Particle size corresponding to 10% finer in the particle-size distribution	Positively proportional	Kamal et al. (1993) ; Moulton (1980)
D_{20}	Particle size corresponding to 20% finer in the particle-size distribution	Positively proportional	Kamal et al. (1993)
G/S	Ratio between percent of gravel particles to percent of sand particles in the material according to USCS.	Positively proportional	Xiao et al. (2016)
C_u	Coefficient of uniformity of the gradation	Negatively proportional	Tao & Abu-Farsakh (2008); Federal Highway Administration (1992); Bennert & Maher (2005) ; Hoppe (1996)
N	Porosity of compacted UGM	Positively proportional	Moulton (1980)

2.3.3 Time-to Drain

According to AASHTO 1993 design guide, the drainage quality of a layer is determined using the drainage time parameter (t) which is defined as the time required to drain 50% of the free moisture in a given pavement system at saturation conditions, (Blaschke et al. 1993). The drainage time parameter is influenced by the geometrics of the pavement structure as well as the material properties of the base/subbase layers.

Table 2.2 Quantification of drainage quality (Blaschke et al. 1993).

Quality of Drainage	Time to Drain
Excellent	2 hrs
Good	1 day
Fair	7 days
Poor	1 month
Very poor	Does not drain

Drainage time in days can be calculated by using Equation 2.2, where $\boldsymbol{T}$ is a time factor that accounts for the structure's geometry and $\boldsymbol{m}$ is a material factor that accounts for base/subbase material and gradation.

$$\boldsymbol{t = T\, m\, 24} \qquad \textbf{(Eq. 2.2)}$$

The time factor ($\boldsymbol{T}$) is determined from the nomograph in Figure 2.4 based on the slope factor (S_1). The slope factor in the nomograph is calculated from Equation 2.3, where $\mathbf{S_R}$ and $\mathbf{L_R}$ are the resultant slope and resultant flow path, respectively and **H** is the base thickness in feet.

$$\boldsymbol{S_1 = \frac{L_R\, S_R}{H}} \qquad \textbf{(Eq. 2.3)}$$

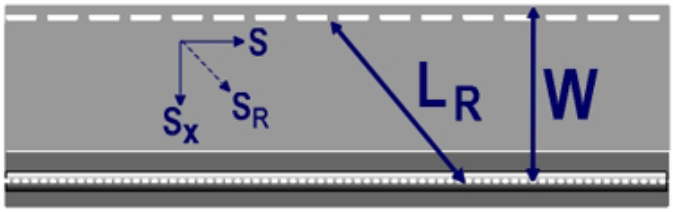

Figure 2.3 Pavement geometry parameters (Plan view of a typical pavement surface)

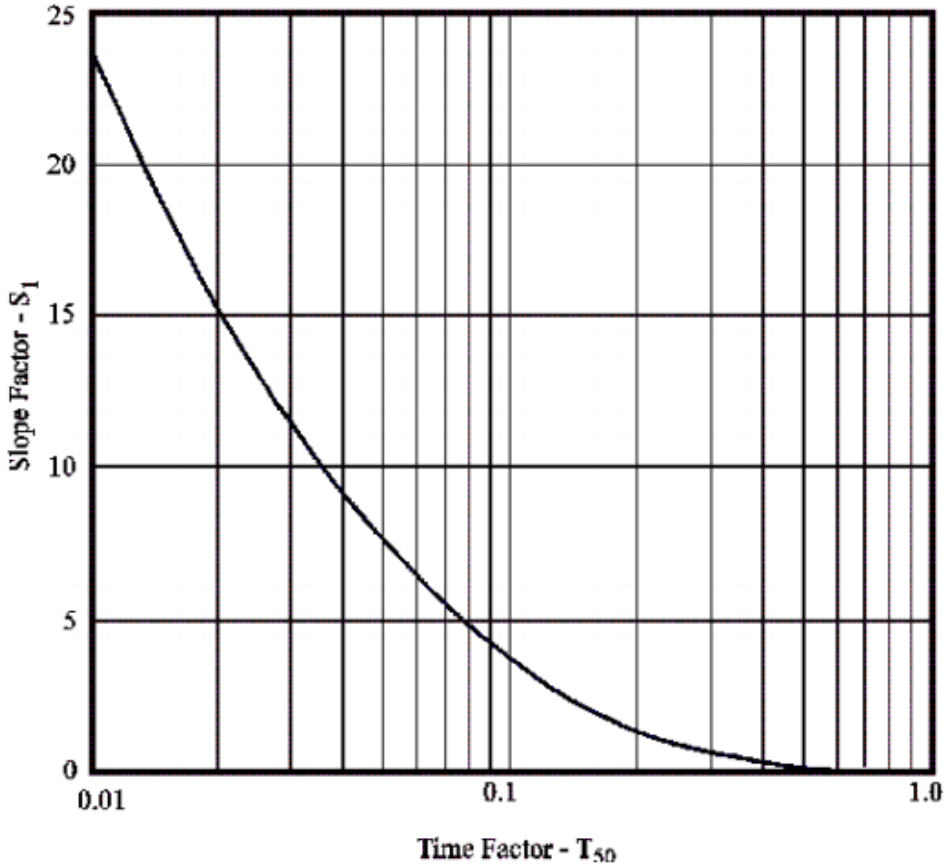

Figure 2.4 Time factor for 50% drainage (Federal Highway Administration 1992)**.**

The material factor $\boldsymbol{m}$ is calculated from Equation 2.4, where $\boldsymbol{N_e}$ is the effective porosity, and $\boldsymbol{K}$ is the hydraulic conductivity of the base layer.

$$\boldsymbol{m = \frac{N_e\, L_R^2}{K\, H}} \qquad \textbf{(Eq. 2.4)}$$

2.4 Modeling of Hydraulic Conductivity

Since drainage is a significant factor in pavement performance, it is beneficial to include it in the design process. However, measuring the hydraulic conductivity of UGM for a specific project after the UGM is crushed and produced can not be considered as an effective design practice. Therefore, using a reliable prediction model for hydraulic conductivity is a better design practice. Numerous models have been developed over the years to estimate the saturated hydraulic conductivity of soils based on correlation with material properties.

One of the earliest attempts to estimate hydraulic conductivity based on granular size distribution was by Hazen (1911).

$$K = C\,D_{10}^2 \qquad \textbf{(Eq. 2.5)}$$

Where C is a regression coefficient. The limitation of this model is it being based on clean noncompacted sands and does not include the influence of degree of packing or void ratio. Another widely used prediction model that has similar limitation as the Hazen equation is developed by Sherard, et al, (1984) which is based on results from silty soils.

$$K = 0.35\,D_{15}^2 \qquad \textbf{(Eq. 2.6)}$$

The Moulton model was developed in 1980 and was based on a statistical analysis of material properties on a large sample size (Moulton 1980). The result of such analysis showed that effective size ($\mathbf{D_{10}}$), porosity (**N**), and fines content ($\mathbf{P_{200}}$) explained over %91 in the variation in hydraulic conductivity. The model that best fit that data was presented by Moulton as shown in Equation 2.7, where **K** is in units of ft/day, and $\mathbf{D_{10}}$ in units of mm. The Moulton model is used in the FHWA subsurface drainage design computer program, DRIP2.0, which is recommended by NCHRP's guide for mechanistic empirical pavement design (ARA 2004).

$$K = [(6.214\ x\ 10^5)D_{10}{}^{1.478} * N^{6.654}] \,/\, P_{200}^{0.597} \quad \textbf{(Eq. 2.7)}$$

Moulton described the fines content, (P_{200}), as the most significant factor that influence hydraulic conductivity. This agrees with findings from (Elsayed & Lindly 1996) where they produced a model to predict hydraulic conductivity of dense graded granular material based on void ratio, percent passing #30 and #200 sieves. However, a study of UGM from 19 quarry samples in Virginia, (Hoppe 1996) found that fines content alone does not exert a significant influence on hydraulic conductivity. They recommended the use of more aggregated parameters such as C_u and D_{85}/D_{15}. This suggests that a combination of material and gradation parameters should be used to produce reliable estimates of the hydraulic conductivity of compacted UGM.

$$K = -0.251 + 0.92 * e + {}^{2.68}/_{P_{30}} - 0.005 * P_{200} \quad \textbf{(Eq. 2.8)}$$

Table 2.3 Comparison of several prediction models for unbound granular materials' hydraulic conductivity

Reference	Model	Comments
(Hazen 1911)	$K = C(D_{10})^2$	For predicting permeability of clean sands (K in cm/s, C in s^{-1}, D_{10} in cm)
(Sherard et al. 1984)	$K = 0.35D_{15}^2$	Does not account for aggregate packing through porosity or void ratio (K in cm/s, D_{15} in mm)
(Moulton 1980)	$K = [(6.214 \times 10^5)D_{10}{}^{1.478}\, N^{6.654}] \,/\, P_{200}^{0.597}$	Used in DRIP2.0 to calculate time-to drain (K in ft/day, D in mm)
(Elsayed & Lindly 1996)	$K = -0.251 + 0.92e + {}^{2.68}/_{P_{30}} - 0.005\ P_{200}$	Based on void ratio and grain sizes (K in 10^{-2} m/s, D in mm)

K = hydraulic conductivity, D_x = Effective diameter of *x*% passing, e = void ratio of compacted sample, N = porosity, P_{200} = Percent passing sieve# 200, C = Empirical coefficient

2.5 Mechanical Properties of UGM under Repeated Loading

In flexible pavement structures, the primary role of a granular base layer is to distribute and spread traffic loads to a magnitude that would not cause significant damage to the subgrade layer (Ashtiani 2009). These loads are transferred throughout the base layer by particle to particle contact where the stress concentrates in the meeting points between particles (Dantu 1957; Oda 1974). However, the stresses in UGM produced by traffic loads are more complex. Considering an element in the UGM layer, it would undergo varying magnitudes of principal and shear stresses which results in the rotation of the principal axes as a reaction to the moving wheel load, as shown in Figure 2.5 (Lekarp et al. 2000a).

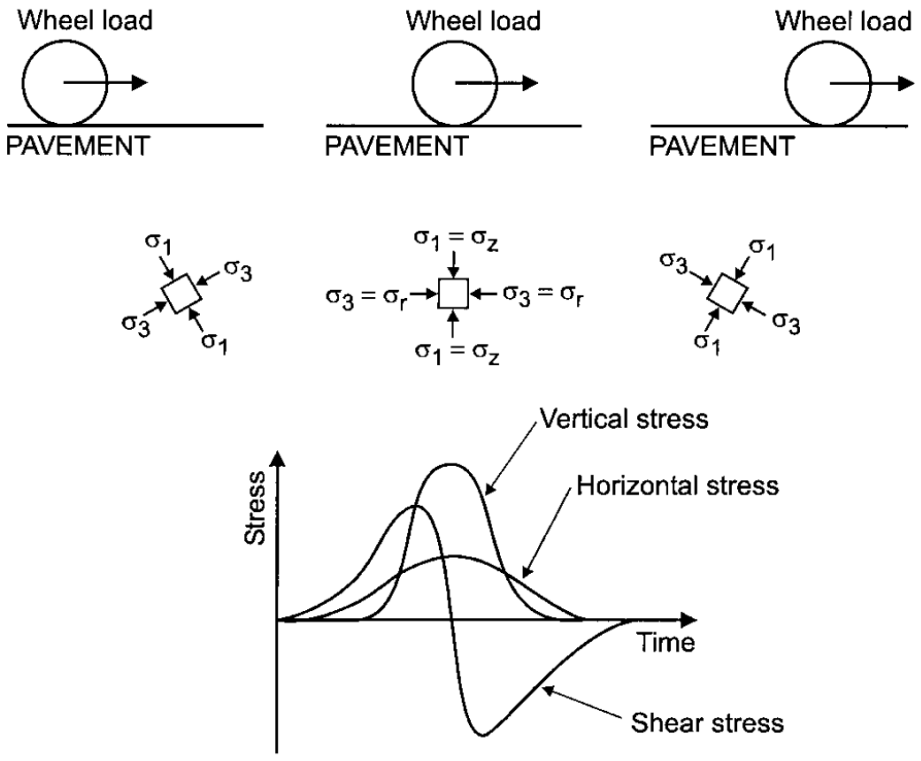

Figure 2.5 Stress development in UGM under moving traffic loads (Lekarp et al. 2000a).

As a reaction of the induced stress, the base layer undergoes a vertical deformation. Part of that deformation is recovered (resilient) by the elasticity of the interlocked particles, and the remaining part is permanent (plastic) deformation. Such behaviour is characterized by the resilient modulus (M_R) and by permanent deformation (ε_p) of the UGM. The mechanical behaviour of the base layer is a function of several performance indicators such as; mineralogy, density, moisture, particle size, and gradation of the UGM. A good understanding of the mechanical behaviour of the UGM used in pavement base layers eliminates unexpected maintenance costs due to unforeseen granular base related premature distresses. Therefore, to produce reliable pavement designs it is vital to base it on accurate laboratory characterization of the material's performance related properties.

2.5.1 Resilient Response

In pavement structures, UGM layers undergo a combination of plastic and elastic strains due to repeated traffic loading. The stress vs. strain relationship in granular materials is non-linear, and can be described by a hysteresis loop which provides values of the resilient and permanent strain for each load cycle.

The resilient response or stiffness of UGM is quantified by the resilient modulus. The value of the resilience modulus of granular aggregate base can be used for an accurate evaluation of pavement performance, specifically, in terms of its capacity to handle repeated traffic loads and to dissipate strains. The resilient modulus is a characterization of the stiffness of the material, and is calculated by Equation 2.9, where $\boldsymbol{\sigma_d}$ is the deviatoric stress, $\boldsymbol{\varepsilon_r}$ is the recoverable strain.

$$\boldsymbol{M_R = \frac{\sigma_d}{\varepsilon_r}} \qquad \textbf{(Eq. 2.9)}$$

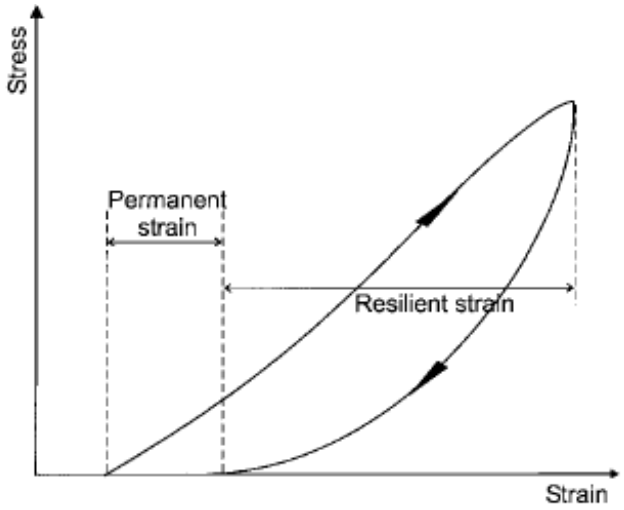

Figure 2.6 Stress-strain relationship in UGM (Lekarp et al. 2000a).

2.5.1.1 Resilient Modulus and CBR Correlation

California Bearing Ratio (CBR) is a standardized test method that was developed by the California Department of Transportation in the 1930s. The test provided an empirical value of the strength of granular materials by comparing a static load penetration resistant of the tested material to the penetration resistant of a standard material. Since then, CBR has been widely used in the design and quality control of pavement structures for its simple and quick laboratory procedure (Uz et al. 2015). However, resilient modulus provides a more reliable characterization of UGM performance as it accounts for the number and magnitude of load applications, as well as the varying stress state conditions acting on pavement sublayers.

Several researchers have studied the relationship between CBR and resilient modulus, since resilient modulus requires a more complex apparatus and testing procedures than CBR. (Thompson & Robnett 1979) studied the M_R-CBR relationship and suggested that the two properties cannot be correlated as justified by the fact that M_R is a measure of stiffness while CBR is a measure of

shear strength. However, other researchers agree on the validity of correlating M_R and CBR since both are affected by many similar material properties.(ARA 2004; Heukelom & Klomp 1962).

One of the earliest attempts to develop a relationship between M_R and CBR was made by Heukelom & Klomp, (1962) based on in-situ measurements using road vibration machine. The relationship was used in the AASHTO Design Guide (Blaschke et al. 1993) for estimating the subgrade modulus based on CBR measurements.

$$\boldsymbol{M_R}(MPa) = \boldsymbol{CBR} * \mathbf{10} \qquad \textbf{(Eq. 2.10)}$$

Van Til, et al (1972) performed extensive literature review of the different research attempts that were taking place at the time to quantify base layer support coefficient. They recommended a correlation chart based on their findings that the modulus of crushed aggregate base was reported to be ranging from 103.4 MPa to 206.8 MPa (15,000 psi to 35,000 psi) which corresponded to CBR values of 20 to 80 as shown in Figure **2.7**. This chart is used by AASHTO Design Guide (Blaschke et al. 1993) for linking aggregate base layer support to the different quantification parameters.

Angell (1988) noted that the relationship presented by Heukelom & Klomp (1962) over estimates the modulus value when the value of CBR is greater than 5%. Powell et al. (1984) Studied wave propagation based on in-situ CBR test and presented an M_R-CBR relationship with boundary condition of <12% CBR. This relationship is recommended by NCHRP Mechanistic Empirical Design Guide for unbound granular base materials (Division 2004).

$$\boldsymbol{M_R}(MPa) = \boldsymbol{CBR^{0.64}} * \mathbf{17.6} \qquad \textbf{(Eq. 2.10)}$$

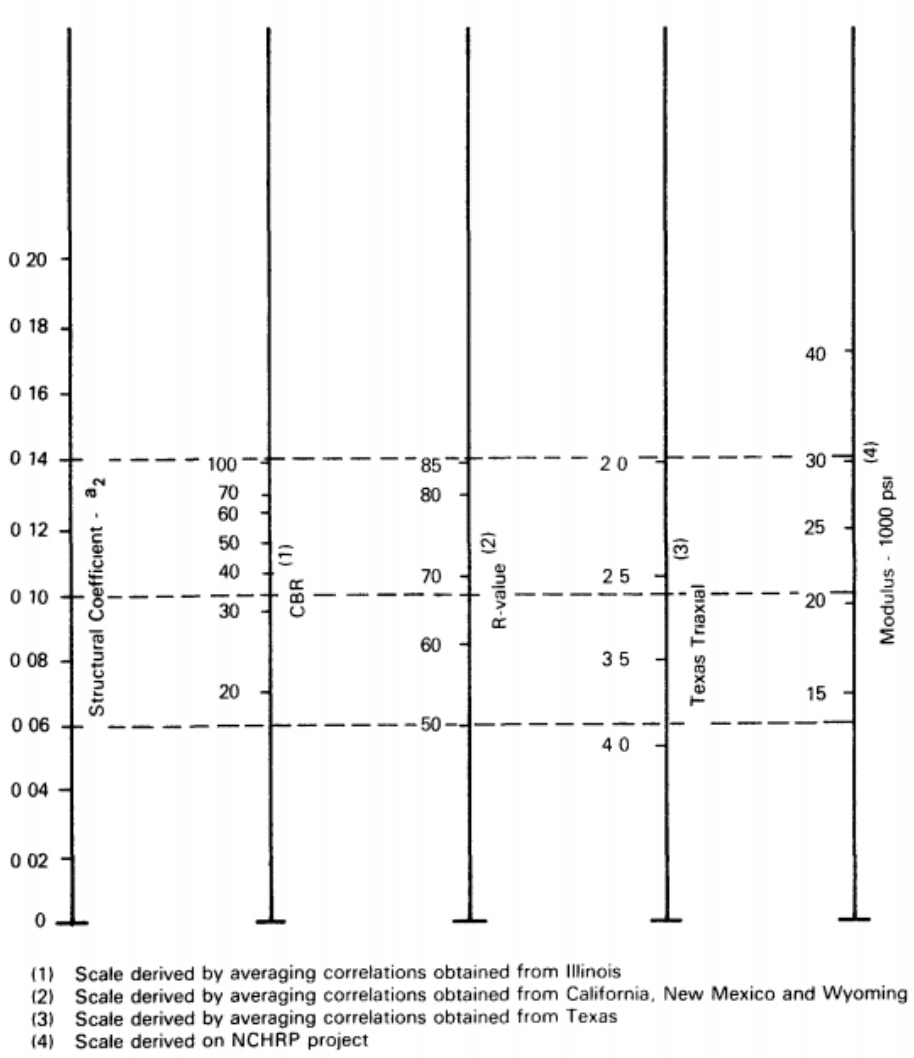

Figure 2.7 Relationship between granular base layer coefficient and various base strength parameters (Van Til et al. 1972)

2.5.1.2 Estimating Resilient Modulus from Material Properties

Resilient modulus is a key material input in AASHTO 1993 Design Guide and in National Cooperative Highway Research Program (NCHRP) Mechanistic Empirical Pavement Design that has a direct influence on layer thickness, (Blaschke et al. 1993; ARA 2004). Due to the complexity of the resilient modulus testing procedure and testing instruments, several agencies rely on estimating resilient modulus based on easily obtained material properties (Yau & Quintus 2002).

Particle size distribution is the most pointed UGM property that influences performance (Arnold et al. 2007; Bilodeau et al. 2009; Xiao et al. 2016). Multiple researchers have studied the effect of UGM gradation on mechanical performance of base/subbase layers through utilizing different gradation parameters and quantification methods. Kim et al. (2005) proposed a modified gradation parameter model which presented gradation parameters ($\mathbf{g_a}$, $\mathbf{g_n}$, $\mathbf{g_m}$) that would indicate the shape of the gradation curve as shown in Figure 2.8 and Figure 2.9.

Furthermore, Kim et al. (2007) validated the application of the model by studying the response of the subgrade layer using Falling Weight Deflectometer testing. They succeeded in linking field performance to gradation through a resilient modulus prediction model that was based on gradation quantification parameters from Kim et al. (2005).

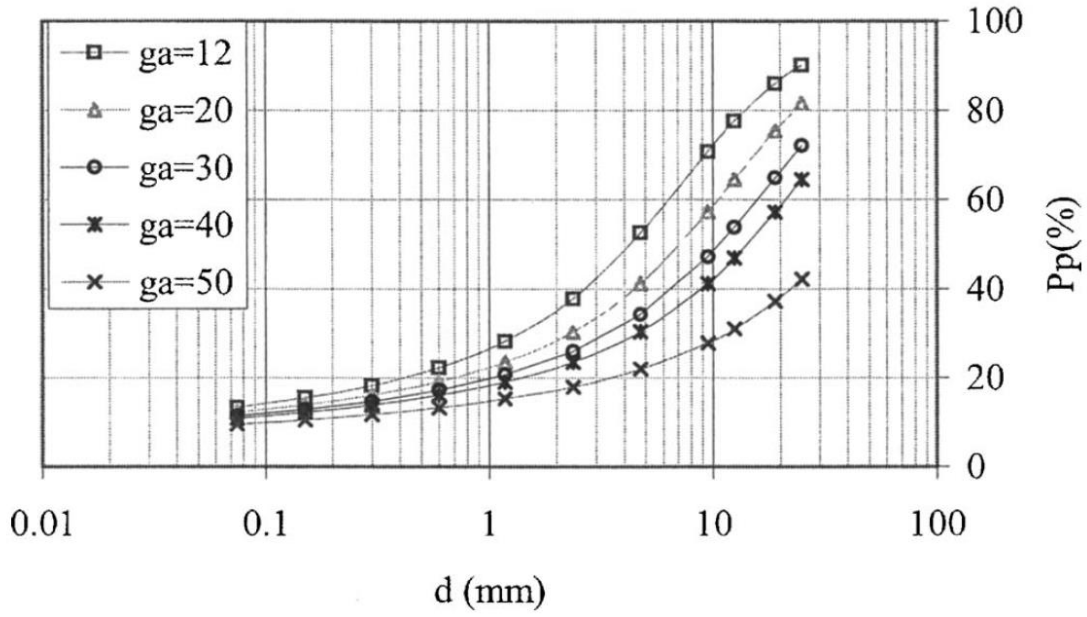

Figure 2.8 Gradation parameter (ga) corresponding to the initial break in the grain-size curve (Kim et al. 2005)

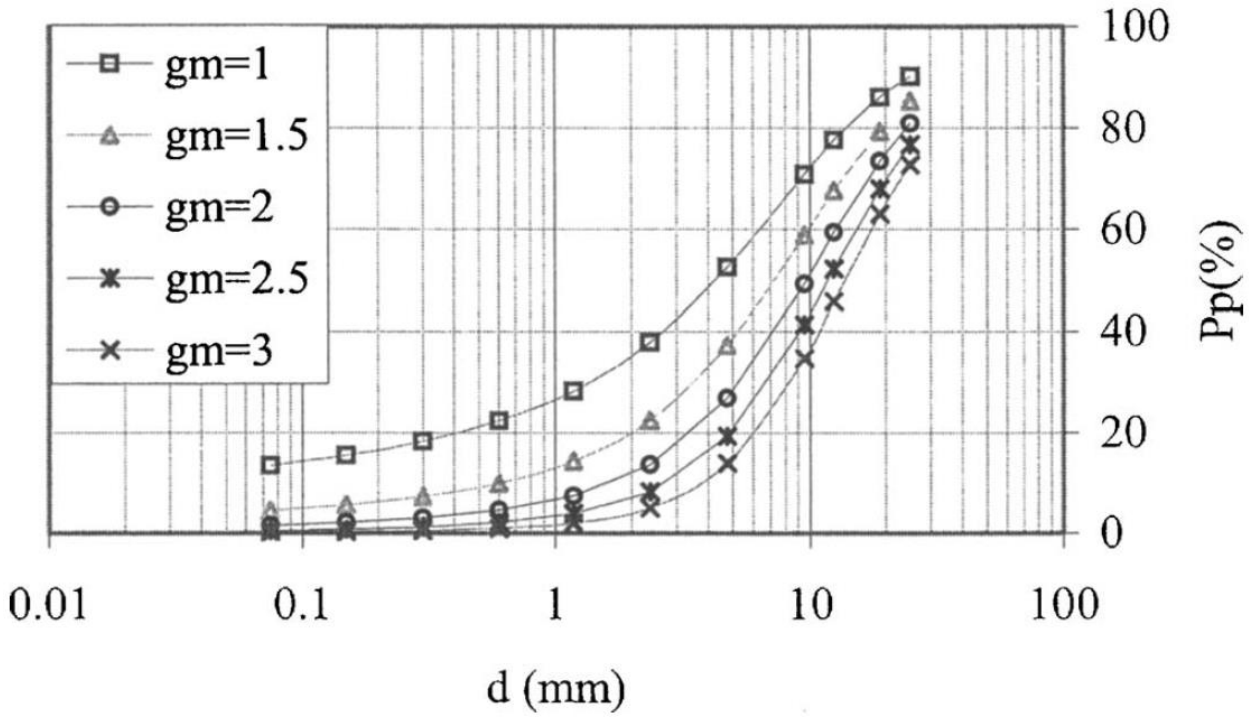

Figure 2.9 Gradation parameter (gm) corresponding to the curvature of the grain-size curve (Kim et al. 2005)

Though the move towards linking aggregate gradation to performance parameters is widely studied, there seem to be no agreement in the literature on a single model for linking stiffness performance with UGM gradation. The Bailey method was originally proposed by Vavrik et al. (2002) for controlling HMA volumetric mix through studying aggregate packing. Bilodeau & Doré. (2012) applied the Bailey method in investigating the effects of aggregate packing on the resilient modulus of 18 test specimens. This study found that the Bailey method is an effective way in understanding UGM aggregate interlock and can be linked to resilient modulus of compacted UGM. However, Xiao et al. (2012) used several gradation quantification methods, including the Bailey method, on a database of 376 different UGM specimens tested by MNDOT. The study proved that the parameters from the Bailey method do not have significant statistical relationship with UGM strength.

2.5.2 Plastic Response

The plastic response of UGM under traffic loading is characterized by the rate of accumulation of permanent strain. The permanent strain is defined as the non-recoverable portion of the strain induced by cyclic loading. Load distribution in granular aggregate skeleton is achieved through grain-to-grain contact or interlock. Under repeated loading, a freshly compacted layer will keep densifying and acquiring more contact points between its grains in the post compaction stage. In this phase, the UGM layer will accumulate plastic strain in a high rate with load repetitions until no further densification could be achieved. In the second phase, gradual accumulation of permanent deformation would occur in constant rate under repeated loads due to particle attrition and particle distortion (Werkmeister et al. 2004). Therefore, grain angularity and abrasion resistance are important criteria for selecting the desired quality source of UGM in terms of rutting resistance, (Kolisoja 1997; Lekarp et al. 2000b; Rahman & Erlingsson 2015).

2.5.2.1 Permanent Deformation Models

Pavement structures failure occur gradually and is attributed to accumulation of plastic strain (Sharp, 1985). Several researchers developed models to predict the permanent deformation behaviour of UGM and according to the literature, Equation 2.11 provides the best permanent deformation fit for all flexible pavement materials (subgrade, UGM, and asphalt concrete) (Ba et al. 2015; ARA 2004; Schreuders 1989). This permanent deformation model is used in mechanistic pavement design to estimate the structure's service life according to the estimated severity of rutting distresses.

$$\boldsymbol{\varepsilon_p = \varepsilon_o\, e^{-[\frac{\rho}{N}]^{\beta}}} \qquad \textbf{(Eq. 2.11)}$$

ε_p = *Permanent Strain*
$\rho, \varepsilon_o, \beta$ = *Regression coeffecients*
N = *Load Cycles/Repetitions*

2.5.2.2 Shakedown Theory

The shakedown concept was originally proposed to analyse the behaviour of elastic materials under repeated thermal flux (Bree 1967). Later it was applied to analyse the behaviour of different elastic materials under different conditions of cyclic loading. The concept states that materials subjected to repeated loading would undergo different deformation responses. Those responses are categorized into four different types, according to the shakedown concept: purely elastic, elastic shakedown, plastic shakedown, and incremental collapse.

The shakedown concept was utilized to study the behaviour of UGM under repeated traffic loading (Nazzal et al. 2011; Garcia-Rojo & Herrmann 2005; Gu et al. 2017; Werkmeister et al. 2005). According to Sharp (1985), pavements subjected to lighter traffic loads or ones with UGM of higher shakedown limits had longer service life. UGM shakedown behaviour can be described using the following phases depending on stress level, plastic strain, and load repetition which is also presented in Figure 2.10 (Werkmeister et al. 2004):

- Plastic Shakedown: The material response is plastic for a finite number of load cycles. A rapid decrease in permanent strain rate is noticeable after which the response becomes elastic.
- Plastic Creep: When transitioning towards the Plastic Creep range, the material experiences high permanent strain rate that declines to a constant rate after a few cycles. In this range,

the material achieves a long-term steady state. However, after a large number of load cycles, the material transitions towards incremental collapse where it starts showing high and increasing permanent strain rates.

- Incremental Collapse: In this range, the UGM would experience high amounts of permanent strain with each load repetition. The permanent strain would keep accumulation until failure is achieved after relatively low number of load repetitions.

It is worth noting that the desirable shakedown behaviour of UGM base material is to be within the plastic shakedown range or the plastic creep range, (Sharp 1985).

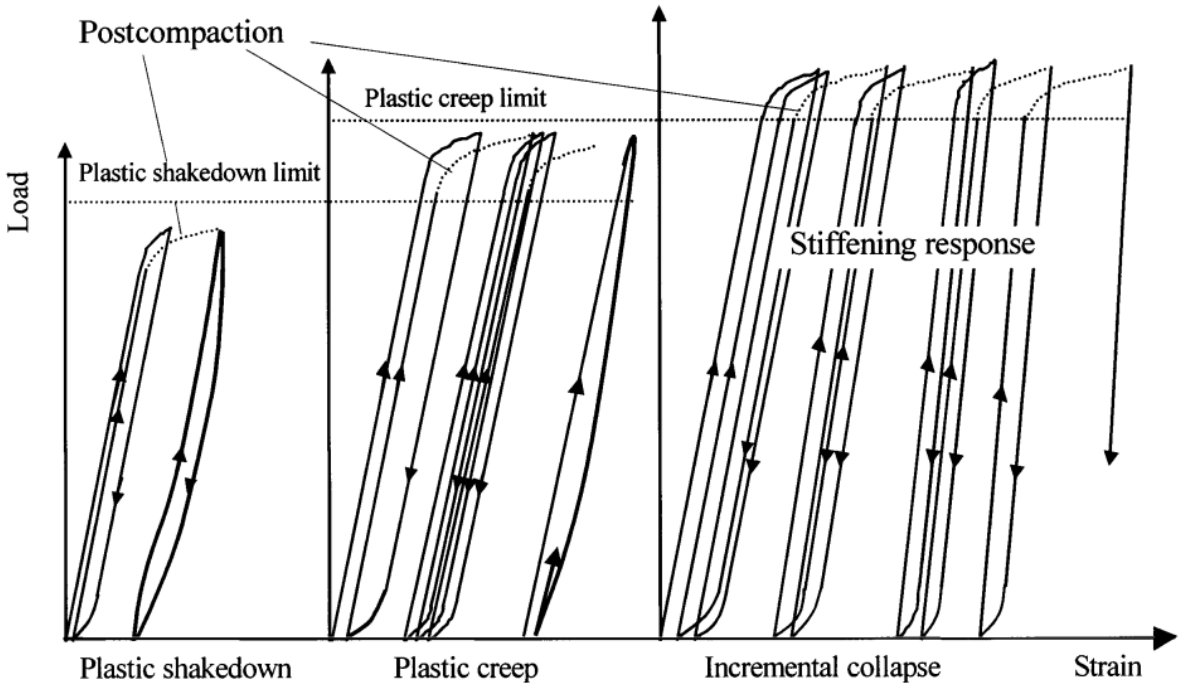

Figure 2.10 Behaviour of granular material under repeated cyclic pressure load (Werkmeister et al. 2005)

2.6 Non-Destructive Deflection Testing

The mechanical properties of UGM and other pavement layers can be characterized based on measurements of deflections under dynamic loads. Pavement non-destructive deflection testing that are performed on in-situ conditions have become more widespread for their reliability in representing field conditions, and for their speed and ease of operation compared to advanced laboratory testing.

2.6.1 Falling Weight Deflectometer

The falling weight deflectometer is a non-destructive testing device that characterizes pavement mechanical response by applying a dynamic impulse load on the pavement surface that resembles a moving truck loading in its impact magnitude and duration (Sharma & Das 2008). FWD is advantageous for its ability to produce large amount of data in short period of time and with no sample collection required (ARA 2004; Hoffman & Thompson 1982).

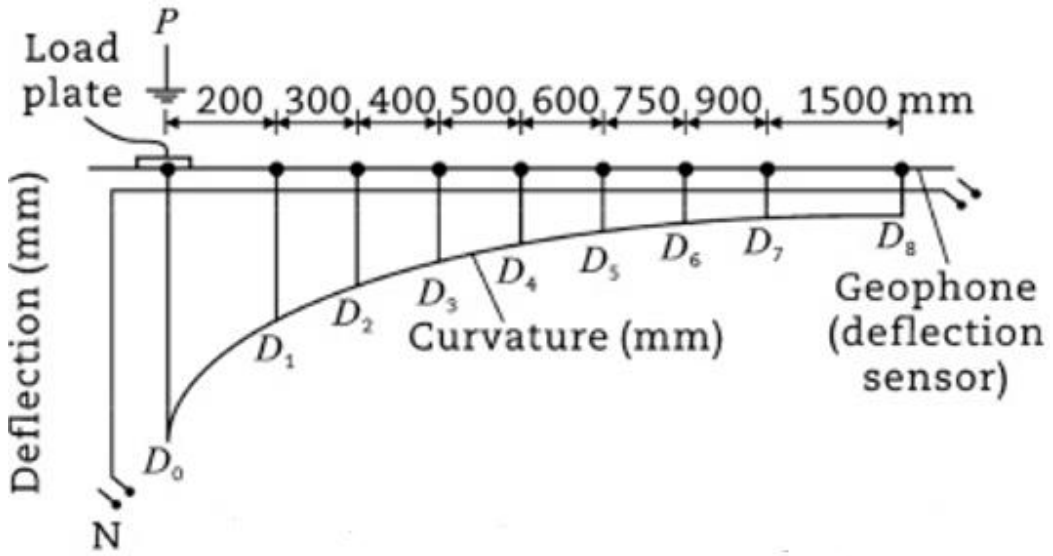

Figure 2.10 FWD typical geophone configuration and deflection basin

The device utilizes a set of geophones to measure load induced deflections at different spacing from the load center to create what is called the deflection basin of the pavement as shown in Figure 2.11. The magnitude of the falling load paired with the deflection basin are used to calculate the stiffness modulus of each layer of the pavement structure. In addition, the results of FWD testing are using to:

- Evaluation of structural capacity of pavement structures
- Estimating load transfer efficiency in rigid pavements
- Detecting the presence of voids under pavement surface
- Designing overlay thickness
- Backcalculation of layer moduli for pavement layers

In analyzing deflection data from FWD testing, the surface modulus is usually calculated based on Boussinesq's half-space solution using surface deflections (Ullidtz 1987).

$$\boldsymbol{E = \frac{2\,(1-\mu^2)\;\;\sigma\;\;a}{D_0}} \qquad \textbf{(Eq. 2.12)}$$

E is the surface elastic modulus at the center of the loading plate (MPa)

μ is poisson's ratio

σ is the contact stress under the loading plate (MPa)

a is the radius of the loading plate (mm)

D_0 is the deflection at the center of the loading plate (mm)

To document the decrease in stiffness resulted by flooding in Missouri, Vennapusa & White (2015) used central deflections from FWD tests on unpaved gravel roads and calculated surface modulus using Equation 2.12.

2.6.2 Correlating Resilient Modulus to Layer Modulus for UGM

The resilient modulus backcalculated from FWD data is found to be inconsistent due to factors such as the simplifying assumption that FWD loading is static rather than dynamic, and the different confining conditions (George & Uddin 2000). Several researchers have studied the relationship between laboratory measured resilient modulus and FWD backcalculated modulus for base layers to recommend an adjustment/correction factor between backcalculated and laboratory measured resilient modulus as shown in Equation 2.13.

$$M_R = C\, E_{FWD} \qquad \textbf{(Eq.2.13)}$$

The AASHTO 1993 guide recommends an adjustment factor of 0.33 for subgrade such that the backcalculated modulus is 3 times larger than resilient modulus (Blaschke et al. 1993). Ping et al. (2001) concluded that the adjustment factor should be 0.55, such that FWD modulus is 1.8 times greater than the laboratory measured resilient modulus. Moreover, findings from a study done on four different roads in Indiana Ji et al. (2012) reported that the correction factor C ranges from 0.2 to 0.62. In another study that involved ten pavement projects in Louisiana, Nazzal & Mohammad (2010) concluded that the E_{FWD} / M_R ratio ranges from 0.51 to 8.1 for local subgrade soils. They also compared several backcalculation softwares and found that ELMOD5.1 had the most consistent results.

Chapter 3 Experimental Program

3.1 Introduction

The experimental testing program for this study was developed for the purpose of characterizing UGM for their mechanical and drainage behaviour. Laboratory resilient modulus, and permanent deformation testing were conducted to evaluate the mechanical performance dependency on aggregate gradation parameters. Constant head permeability tests were conducted to evaluate the drainage performance of UGM with different gradation parameters. As a quality control measure, two specimens were tested for each material at a minimum. Testing a third specimen was deemed necessary if high variability in results of the first two specimens was recorded.

In addition to laboratory testing, the reconstruction project of Provincial Trunk Highway PTH-10 north of Brandon was assigned to be an experimental road test to evaluate the in-situ mechanical and drainage performance of typical and modified UGM base specifications using Falling Weight Deflectometer (FWD), and Double Ring Infiltrometer (DRI) tests. Presented in Table 3.1 is a summary of the experimental testing program for this study.

Table 3.1 Experimental Program

Sample ID	Retrieved From	Laboratory Testing			Field Testing	
		Constant Head Hydraulic Conductivity	Resilient Modulus	Permanent Deformation	FWD	DRI
UGM-1(9.7)	Silver City, Yukon	2	2	2	-	-
UGM-1(12.3)	PTH-10, Abase, MB	2	4*	2	x	x
UGM-2(3.5)	Ibex, Yukon	2	2	2	-	-
UGM-2(4.9)	Silver City, Yukon	2	-	-	-	-
UGM-2(6.4)	South Klondike, Yukon	2	2	2	-	-
UGM-3(3.9)	Carmacks, Yukon	2	2	2	-	-
UGM-3(6.9)	PTH-10, GBC, MB	2	4*	2	x	x
UGM-3(7.1)	PTH-13, GBC, MB	2	2	2	-	-
UGM-4(3.3)	PTH-75, DSB, MB	2	2	2	x	x
UGM-4(7.8)	PTH-8, -50LS, MB	2	2	-	-	-

* Test was performed at OMC and at OMC+2%

3.2 Materials and Physical Properties

Ten granular material samples were collected for this study to evaluate the effect of different physical and gradation properties on mechanical and drainage performance of base layers. The selected materials were collected from different highway construction sites to represents different UGM specifications, and to eliminate variabilities that might arise from producing UGM mixes in laboratory environment. Materials were categorized in four groups according to their fines content and maximum aggregate size. In addition, test data from Soliman (2015) were used in this research.

Table 3.2 Materials groups according to their gradation range

UGM Group	Fines content (%)	Maximum aggregate size (mm)
UGM-1	8-17	19
UGM-2	3-8	19
UGM-3	3-8	25
UGM-4	0-8	37.5

3.2.1 Sampling

The materials were collected and delivered to the University of Manitoba by both Manitoba Infrastructure and Yukon Department of Highways. Around 100kg of blended aggregates were provided for each material source. The following procedures were followed upon receiving materials:

- All aggregates were oven dried for 24 hours and prepared for sample splitting
- Aggregates were portioned, according to AASHTO-T248, into ~5kg specimens
- Portioned specimens were bagged and organized with a naming convention until testing

3.2.2 Gradation and Physical Properties

The granular material samples collected for this study represent a range of aggregate gradations and source properties. Maximum aggregate size ranged from 19mm to 37.5mm, and fines content ranged from 3.3% to 12.3%. Also, the uniformity of the gradations measured by the Coefficient of Uniformity (Cu) ranged from 18 to 98. Sieve analysis and standard proctor testing were performed by each transportation agency. A summary of the results of the gradation and density tests, for UGM samples used in this study as well as data retrieved from Soliman (2015) are presented in Table 3.3 and Table 3.4.

Table 3.3 Materials' grain size distribution

Sample ID	Passing 37.5 mm (%)	Passing 25 mm (%)	Passing 19 mm (%)	Passing 16 mm (%)	Passing 12.5 mm (%)	Passing 9.5 mm (%)	Passing 4.75 mm (%)	Passing 2 mm (%)	Passing 0.425 mm (%)	Passing 0.075 mm (%)
UGM-1(9)	100	100	100	96	85	76	56	39	19.5	9
UGM-1(9.7)	100	100	100	N/A	81.5	71.2	43	31.6	11.8	9.7
UGM-1(12.3)	100	100	100	97	86.8	77.3	60.4	45.6	23.7	12.3
UGM-1(14.5)	100	100	100	95	85	76	57	41	22.5	14.5
UGM-1(10.5)	100	100	100	91	86	75	52.5	37.5	17.5	10.5
UGM-1(16)	100	100	100	95	88	77.5	56	42.5	22	16
UGM-2(3.5)	100	100	100	N/A	85.2	78.6	56.6	46.3	12	3.5
UGM-2(4)	100	100	100	90	80	70	48	32	15	4
UGM-2(4.9)	100	100	100	N/A	80.4	71.1	40.1	28.3	7.8	4.9
UGM-2(6.4)	100	100	100	N/A	85.2	73.5	47.7	33.1	11.5	6.4
UGM-2(4.5)	100	100	100	95	87.5	76	52	35	10	4.5
UGM-3(3.9)	100	100	98.4	N/A	81.7	72	39.8	27.2	7.8	3.9
UGM-3(6.9)	100	100	88.5	81.1	72	63.9	49.6	36.8	12.8	6.9
UGM-3(7.1)	100	100	93.2	86.3	71.7	59.2	39.3	25.3	13.9	7.1
UGM-4(3.3)	100	98.3	83.7	74.4	61.2	52.3	38	27.7	10.1	3.3
UGM-4(7.8)	100	88	75.5	70.1	57.8	48	29.6	17.6	9.5	7.8

* N/A = sieve size was not included in sieve analysis

Table 3.4 Materials properties

Sample ID	Material Type	Maximum dry density (Kg/m^3)	Optimum moisture content (%)	D_{10} (mm)	D_{60} (mm)	Coefficient of uniformity "Cu"	Crush count (%)
UGM-1(9)	Gravel	2223	7.0	0.08	5.56	67.5	n/a
UGM-1(9.7)	Gravel	2362	6.4	0.09	7.37	78.0	64
UGM-1(12.3)	Gravel	2156	8.7	0.05	4.65	98.3	55
UGM-1(14.5)	Gravel	2203	8.3	0.03	5.38	163.0	n/a
UGM-1(10.5)	Limestone	2277	7.0	0.07	6.14	14.4	100
UGM-1(16)	Limestone	2305	6.5	0.03	5.50	208	100
UGM-2(3.5)	Gravel	2206	9.0	0.22	5.67	24.6	67
UGM-2(4)	Gravel	2170	7.9	0.18	7.12	38.4	n/a
UGM-2(4.9)	Gravel	2237	8.6	0.40	7.59	19.1	64
UGM-2(6.4)	Gravel	2287	8.5	0.23	6.79	29.9	83
UGM-2(4.5)	Limestone	2202	7.5	0.43	7.00	14.4	100
UGM-3(3.9)	Gravel	2221	9.2	0.41	7.52	18.6	76
UGM-3(6.9)	Gravel	2053	10.1	0.23	8.03	35.1	62.6
UGM-3(7.1)	Limestone	2226	6.9	0.21	9.68	46.6	100
UGM-4(3.3)	Gravel	2220	7.8	0.42	12.07	28.7	73.8
UGM-4(7.8)	Limestone	2065	6.8	0.52	13.23	25.4	100

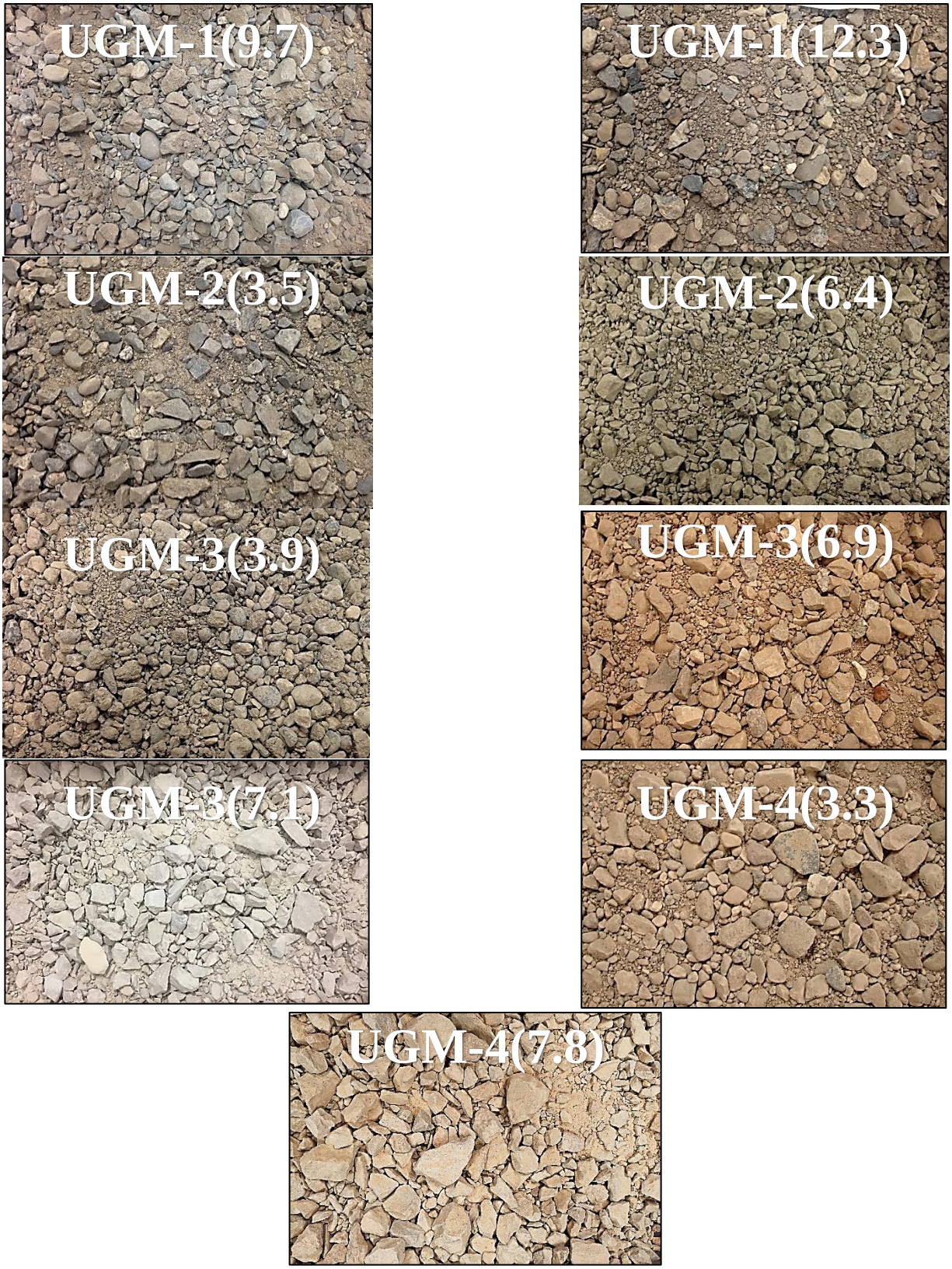

Figure 3.1 UGM samples

3.2.3 Agency Specifications

Manitoba Infrastructure provides three different classes of UGM specifications for usage as base/subbase layers in Manitoba Provincial Highways, namely (Class-A, Class-B, and Class-C). In addition, MI provided two experimental modified specifications to potentially replace the existing class "A" gradation band. The experimental specifications were named Drainable Stable Base (DSB), and Granular Base Coarse (GBC) to be used under rigid and flexible pavements, respectively.

Figures 3.2 to 3.5 present the particle size distribution of the materials included in this research with respect to each gradation bands for UGM-1 to UGM-4 respectively.

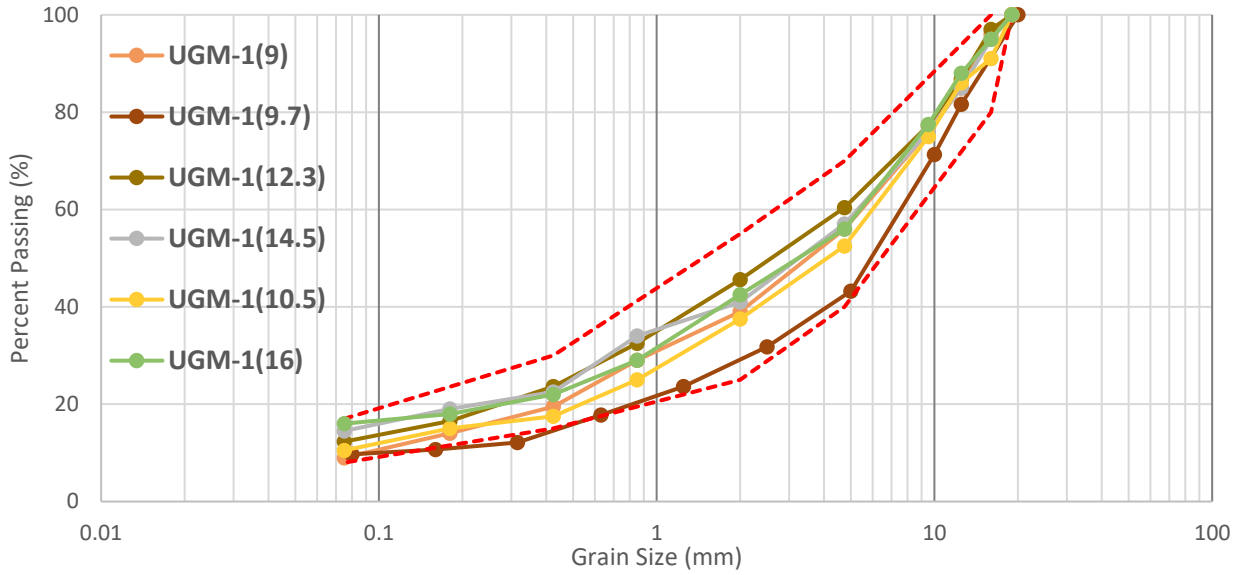

Figure 3.2 Particle size distribution for UGM-1 samples representing Manitoba Class "A" gradation range

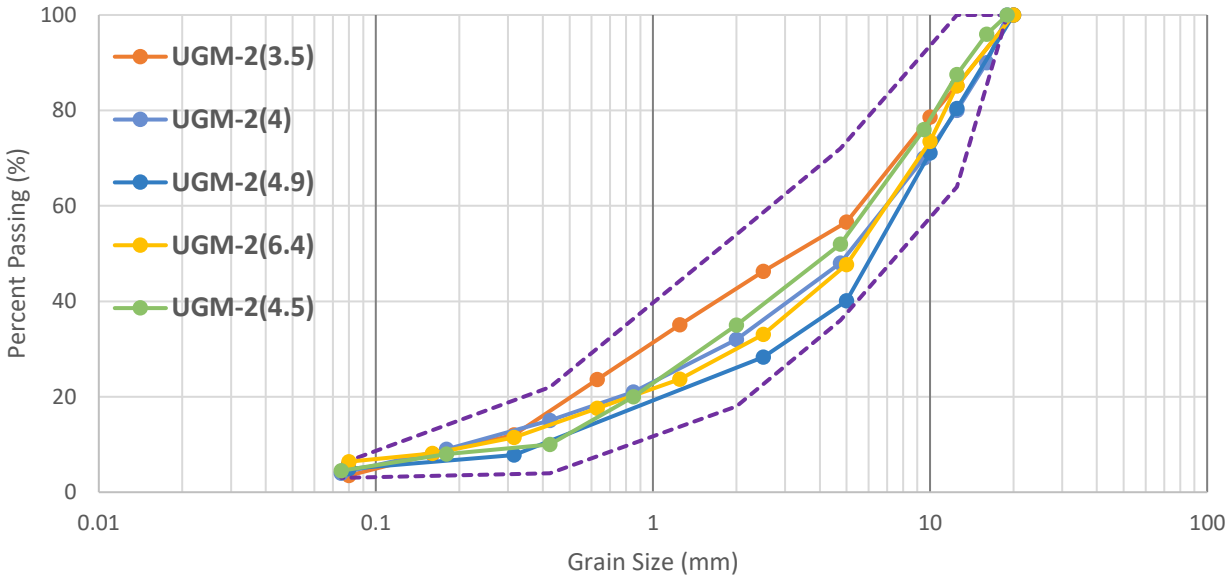

Figure 3.3 Particle size distribution for UGM-2 samples representing Yukon Gran "A" gradation range

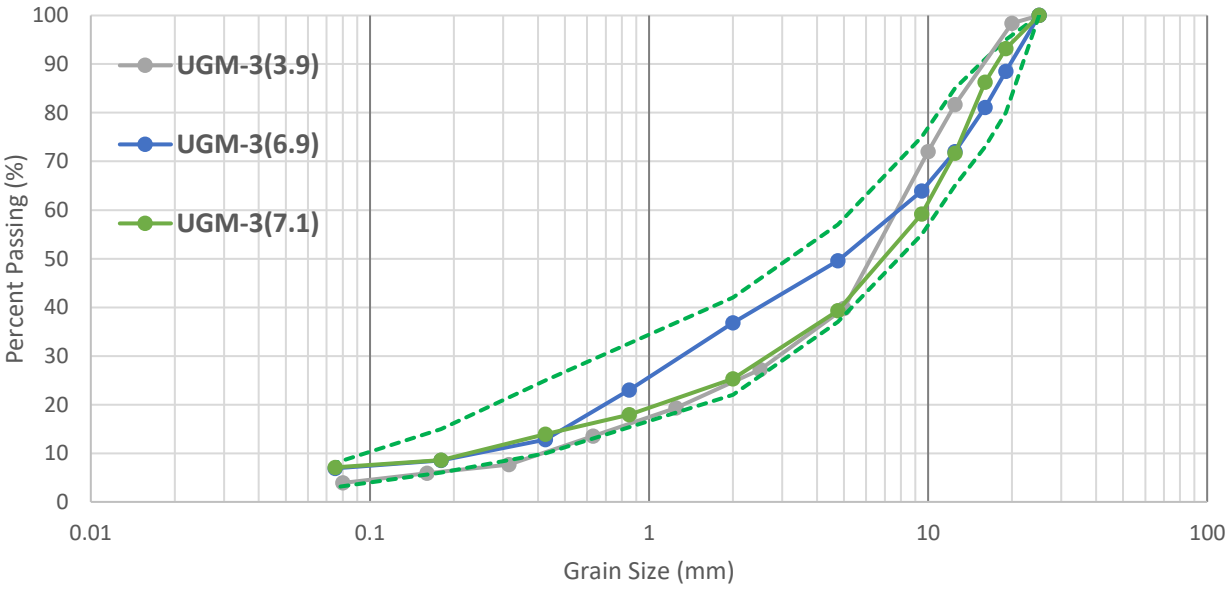

Figure 3.4 Particle size distribution for UGM-3 samples representing Manitoba Class "GBC" gradation range

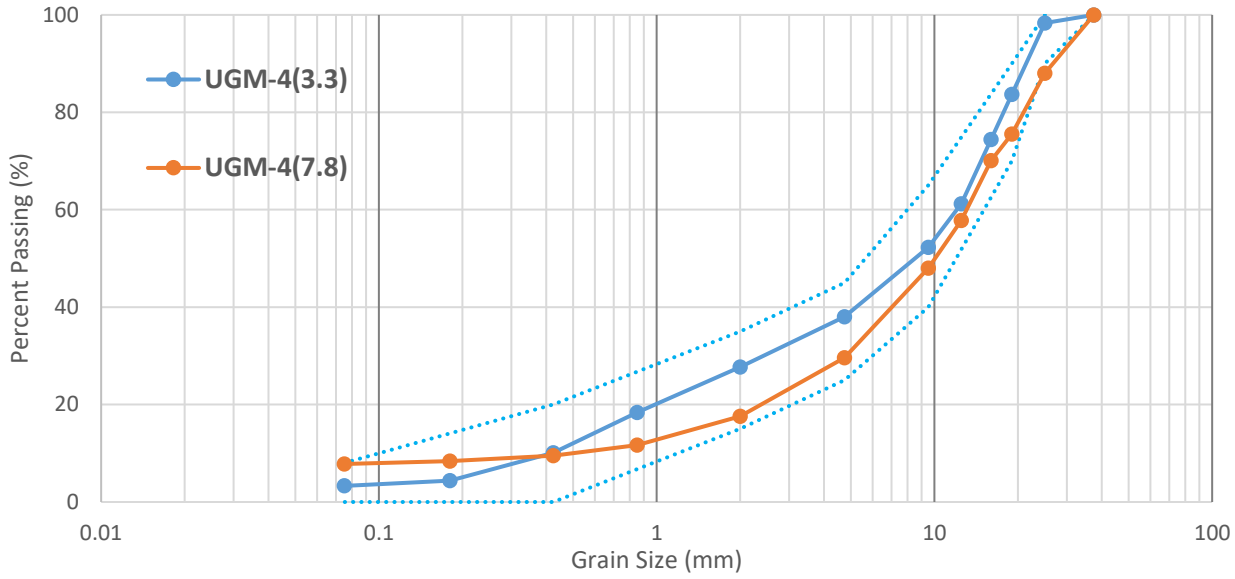

Figure 3.5 Particle size distribution for UGM-4 samples representing Manitoba Class "DSB" gradation range

Table 3.5 UGM specification for base/subbase

MI								Yukon
Passing Sieve (mm)	Class "A"		Class "B"	Class "C"		DSB	GBC	Gran "A"
	Gravel	Limestone	Gravel or Limestone	Gravel	Limestone	Gravel or Limestone	Gravel or Limestone	Gravel or Limestone
37.5				100%		100%		
25				80-100%	100%	90-100%	100%	
19	100%	100%	100%			70-90%	80-95%	100
16	80-100%						73-91%	
12.5								64-100%
9.5						40-65%	55-75%	
4.75	40-70%	35-70%	30-75%	25-80%	25-80%	25-45%	37-57%	36-72%
2	25-55%		25-65%			15-35%	22-42%	18-54%
0.425	15-30%	10-30%	15-35%	15-40%		0-20%	10-25%	4-22%
0.075	8-15%	8-17%	8-18%	8-18%	8-20%	0-8%	3-8%	3-6%
Minimum Crush Count	35%	100%	25%	15%	100%	60%	60%	60%
Max LA	35%	35%	35%	40%	40%	60%	60%	35%
Max Shale Content	12%	N/A	12%	20%	N/A	0%	0%	N/A
Max Clay Balls	10%	N/A	10%	N/A	N/A	0%	0%	N/A
Max Plasticity Index	6%	NP	N/A	N/A	NP	6%	6%	6%

3.3 Drainage Performance Testing

As explained in section **2.3.3**, the laboratory and field measured hydraulic conductivity are used to characterize the drainage performance of base layer using time-to drain calculations.

3.3.1 Hydraulic Conductivity

The studied UGMs were tested for their hydraulic conductivity in accordance with ASTM-D5856 standard test method for measuring hydraulic conductivity using a rigid-wall compaction-mold permeameter (ASTM, 2015). In preparation, materials were compacted at OMC in three equal lifts in a steel permeameter mold with a vibratory compactor adjusted at about 2000 blows per minute. The compacted sample in the permeameter was 101.6mm in diameter, and 116.4mm in height. A vacuum pump was used to achieve 100% saturation for tested specimens. After saturation, the permeameter was connected to constant head water source and allowed to drain under gravity, while ensuring laminar flow by guaranteeing that the hydraulic gradient (i) did not exceed five. The volume of collected water, elapsed time, and the water temperature were recorded in order to calculate a temperature corrected value of hydraulic conductivity. Equation 3.1 and Error! Reference source not found. are used for temperature correction. Test apparatus is presented in Figure 3.7.

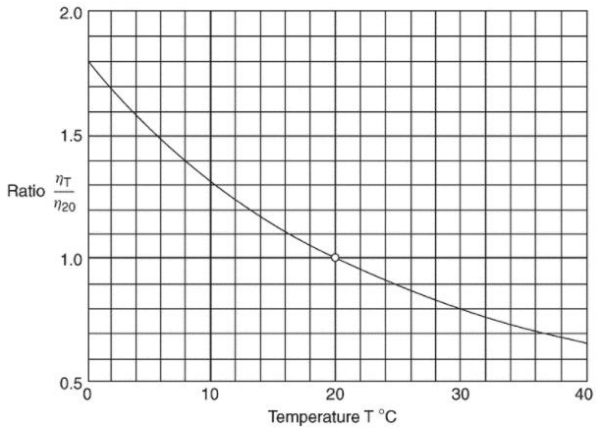

Figure 3.6 Relationship between dynamic viscosity and temperature of water for correcting hydraulic conductivity measurements based on data from Kaye & Laby, (1995)

$$K_{20} = K_T \frac{\eta_T}{\eta_{20}} \quad \textbf{(Eq. 3.1)}$$

K_{20} = Hydraulic conductivity at 20 degrees Celsius

K_T = Hydraulic conductivity at temperature (t)

η_T = Viscosity of the used liquid at temperature (t)

η_{20} = Viscosity of the used liquid at 20 degrees Celsius

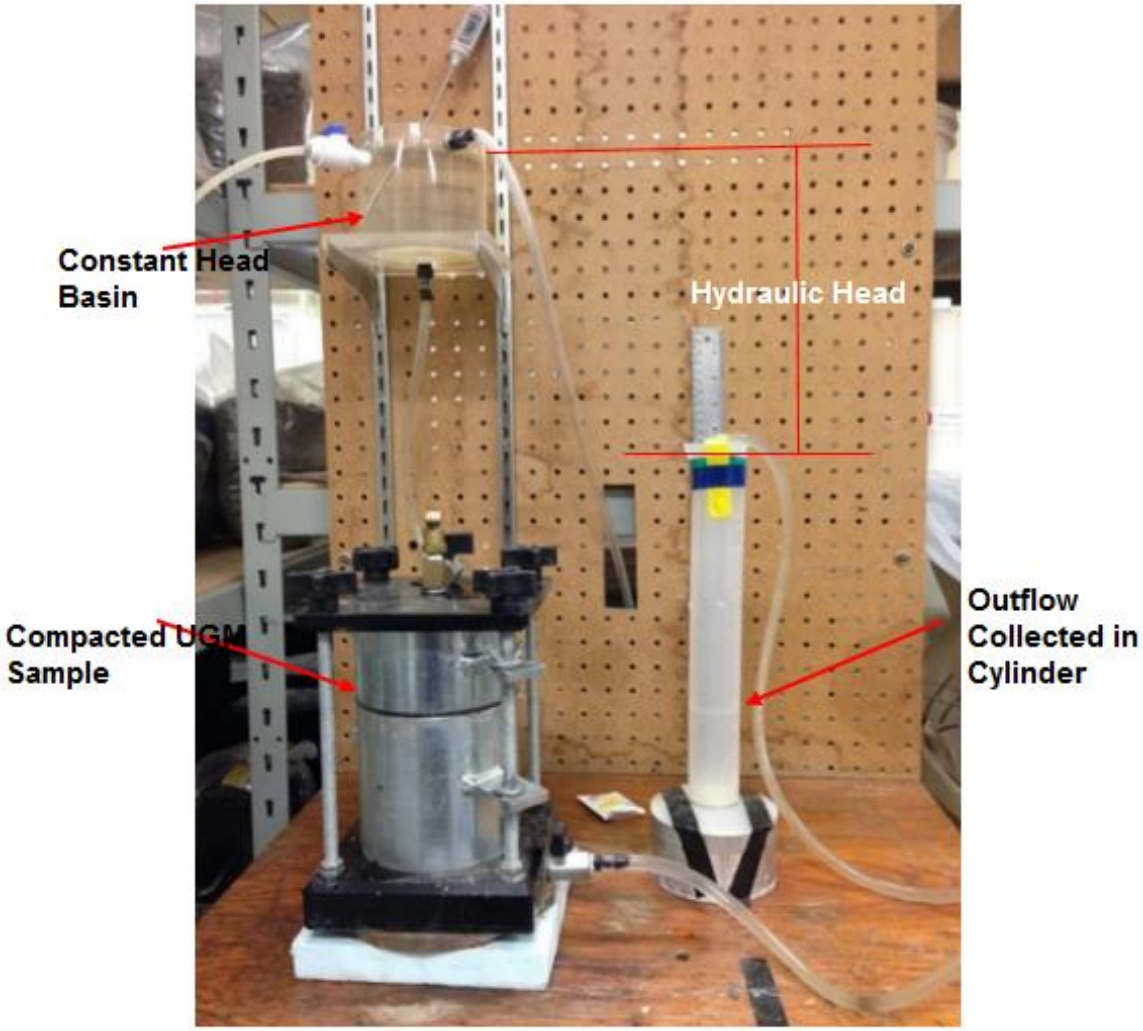

Figure 3.7 Hydraulic conductivity test setup

3.3.2 Double Ring Infiltrometer (DRI)

The field testing for hydraulic conductivity was done using the double ring apparatus according to ASTM D3385 standard test method for infiltration rate of soils in field using double-ring infiltrometer (ASTM, 2009). The test apparatus consisted of two steel rings of diameters 278mm and 530mm, a steel plate for driving the rings, and a floating measure which are shown in Figure 3.9. For test preparation, the two steel rings were driven 50mm into the compacted base layer. That was achieved by using a sledgehammer on the driving plate as shown in Figure 3.8.

Once the rings were installed and were level, a paste mix of bentonite and water was used to seal the soil near the rings' edges. This is to keep water drainage restricted to a path in the base layer only. The test is started by filling the two rings to the same level with clean water and installing the measuring rod and float. Caution was used during this step to prevent soil disruption resulting from pouring water in the rings. Measurements were taken from the inner ring while the outer ring insured that water in the inner ring had strict vertical infiltration.

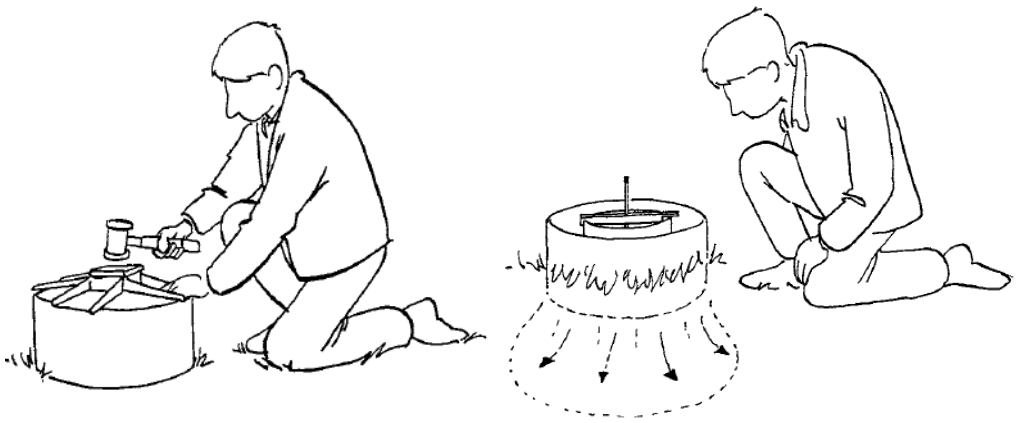

Figure 3.8 Preparation and measurement (Eijkelkamp Agrisearch Equipment, 2015)

Readings of elapsed time, water level, and water temperature were recorded periodically. This provided a direct measurement of the infiltration rate of the tested material. However, under steady state infiltration at saturation, it can be assumed that the infiltration is equal to the hydraulic conductivity. Such assumption is based on a hydraulic gradient of 1 which results from the equilibrium between the difference in ponded water level and the difference in the wetting front depth when the base layer is saturated.

Figure 3.9 Double Ring Infiltration apparatus (Eijkelkamp Agrisearch Equipment, 2015)

$$K = \frac{Q}{i \cdot A} \qquad \textbf{(Eq. 3.2)}$$

$$I = \frac{Q}{A} \qquad \textbf{(Eq. 3.3)}$$

K = Hydraulic conductivity (m/s)

Q = Flow (m^3/s)

i = Hydraulic gradient

A = Cross sectional area of infiltration (m^2)

I = Rate of infiltration (m/s)

3.4 Mechanical Properties Testing

3.4.1 Resilient Modulus

The resilient modulus test was performed according to NCHRP 1-28A standard test method for laboratory determination of resilient modulus, (Harrigan & Witczak 2004). The test consisted of

30 loading sequences at different states of stress. Each sequence consisted of 100 pulse load cycles. The NCHRP 1-28A test procedure for M_R testing was followed in this study instead of the more recent AASHTO T-307 Test Standard (AASHTO 2013), because the larger number of loading sequences, required by NCHRP 1-28A, allowed for more thorough investigation of UGM resilient behaviour under varying stress conditions. The test simulates cyclic traffic loading under various stress states and measures the deformation at each load cycle to allow calculation of the stiffness of tested UGM at any given stress state. After testing, the data was fitted to the universal model in order to predict the value of the modulus at stress conditions that resemble typical traffic loading at base layer. A minimum regression coefficient of determination of 0.9 was used to accept fitted results. At least two tests were performed per gradation to ensure reliability of results.

The test procedures included preparing a test specimen to the desired moisture content and compacting it in a split mold using a vibratory compactor. The split mold produced a specimen with 102.6mm in diameter and 202.3mm in height. The vibratory compactor used was a BOSCH SDS demolition hammer and was set to 2,000 blows/minute following the testing standard. The sample was compacted in eight layers of 25.4mm, with the surface of each layer scarified prior to placing the next layer.

The compacted specimen cylinder was then put in a triaxial cell and subjected to 30 loading sequences of 100 load cycles with drainage allowed from top and bottom of specimen. Each load pulse followed a Haversine wave shape and had 0.1 second of load duration and 0.9 second of rest. The deformation from each load repetition was measured and recorded using four LVDTs, (Linear Variable Differential Transducer). As shown in Figure 3.10 and Figure 3.11, LVDTs were mounted in a way that they take their measurements from the top surface of the specimen, and in the inside of the triaxial cell.

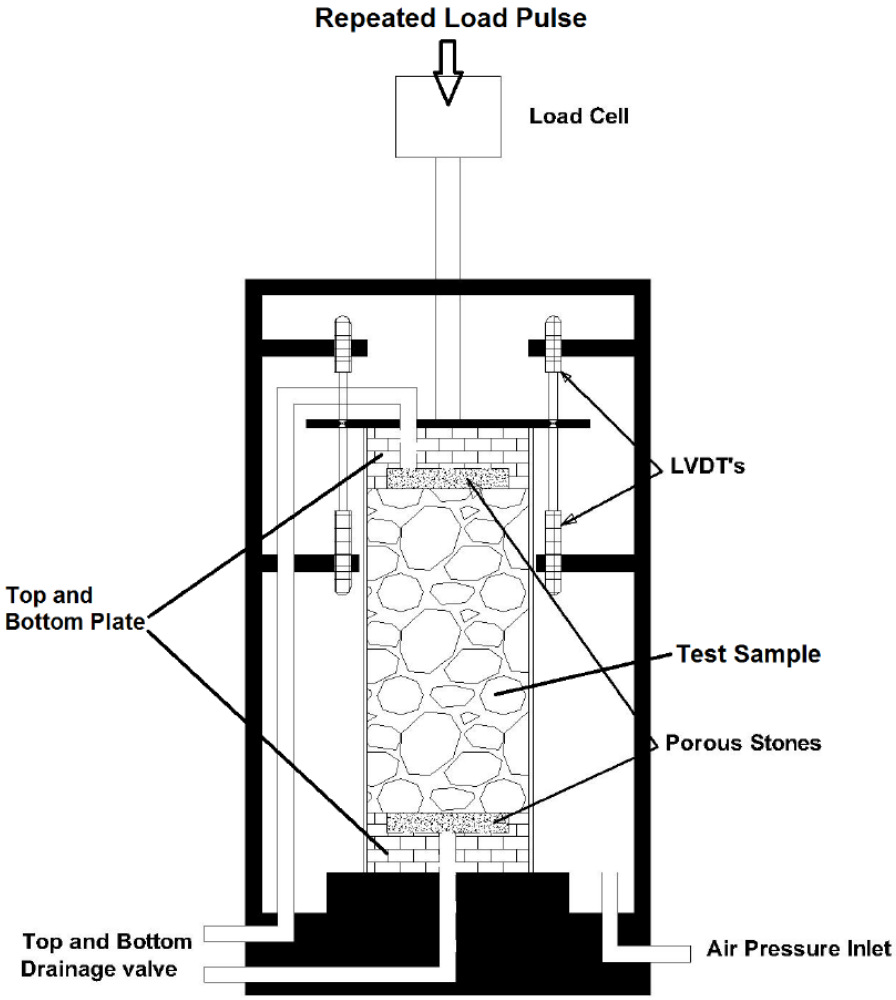

Figure 3.10 Setup for repeated load triaxial testing, (resilient modulus and permanent deformation)

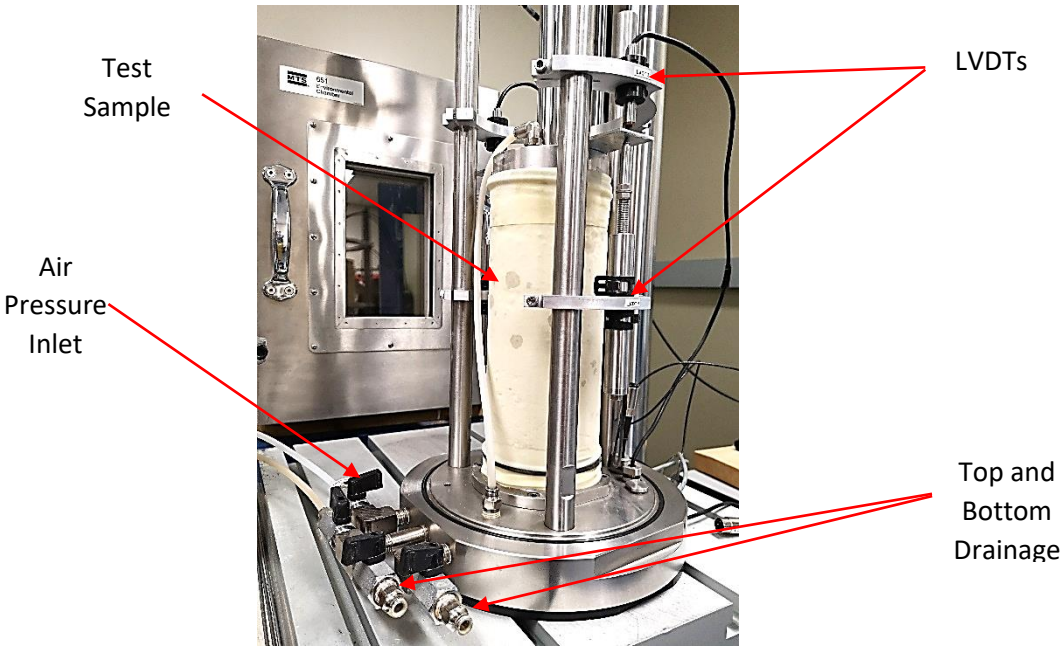

Figure 3.11 Compacted UGM specimen in the repeated load triaxial test setup to run resilient modulus test

A computer programming code was developed using MATLAB programing software to analyze the recorded test data and to calculate bulk stress, octahedral stress, and resilient modulus for each recorded load cycle. The calculated resilient modulus values from each of the 30 sequences were used to fit the universal constitutive model in order to obtain the resilient behaviour for the tested UGM using Equation 3.4. The reported M_R values were calculated based on confining pressure of (σ_3) =35kPa, and cyclic stress of ($\sigma_1 - \sigma_3$)=103kPa.

$$\boldsymbol{M_R = K_1 * P_a * \left[\frac{\theta}{P_a}\right]^{K_2} * \left[\frac{\tau_{oct}}{P_a} + 1\right]^{K_3}} \qquad \textbf{(Eq. 3.4)}$$

M_R = Resilient Modulus (kPa)

θ = Bulk Stress (kPa) = $\sigma_1 + \sigma_2 + \sigma_3$

τ_{oct} = Octahedral Stress (kPa) = $\frac{1}{3} * \sqrt{(\sigma_1 - \sigma_2)^2 + (\sigma_3 - \sigma_1)^2 + (\sigma_2 - \sigma_3)^2}$

σ_1 , σ_2 , $and\ \sigma_3$ = Principal Stresses (kPa)

$K_1, K_2, and\ K_3$ = Regression Constants

P_a= Atmospheric Pressure (101.35 kPa)

Table 3.6 Loading configurations for resilient modulus testing according to NCHRP 1-28A

Sequence	Confining Pressure (kPa)	Contact Stress (kPa)	Cyclic Stress (kPa)	Total Stress (kPa)	No. of Cycles
Conditioning	103.5	20.7	207	227.7	1000
1	20.7	4.1	10.4	14.5	100
2	41.4	8.3	20.7	29	100
3	69	13.8	34.5	48.4	100
4	103.5	20.7	51.8	72.5	100
5	138	27.6	69	96.6	100
6	20.7	4.1	20.7	24.8	100
7	41.4	8.3	41.4	49.7	100
8	69	13.8	69	82.8	100
9	103.5	20.7	103.5	124.2	100
10	138	27.6	138	165.6	100
11	20.7	4.1	41.4	45.5	100
12	41.4	8.3	82.8	91.1	100
13	69	13.8	138	151.8	100
14	103.5	20.7	207	227.7	100
15	138	27.6	276	303.6	100
16	20.7	4.1	62.1	66.2	100
17	41.4	8.3	124.2	132.5	100
18	69	13.8	207	220.8	100
19	103.5	20.7	310.5	331.2	100
20	138	27.6	414	441.6	100
21	20.7	4.1	103.5	107.6	100
22	41.4	8.3	207	215.3	100
23	69	13.8	354	358.8	100
24	103.5	20.7	517.5	538.2	100
25	138	27.6	690	717.6	100
26	20.7	4.1	144.9	149	100
27	41.4	8.3	289.8	298.1	100
28	69	13.8	483	496.8	100
29	103.5	20.7	724.5	745.2	100
30	138	27.6	966	993.6	100

3.4.2 Permanent Deformation

Repeated load triaxial testing (RLT) was used to assess permanent deformation behaviour for UGM. Several studies performed permanent deformation testing and had load cycles ranging from 10,000 to around one million cycles (Bilodeau et al. 2011; Werkmeister et al. 2004). Samples in this study were subjected to 13,250 Haversine load cycles at one stress state. This number of loading cycles was chosen as a balance between accuracy and testing duration (Ahmeduzzaman, 2016; Soliman and Shalaby 2016). The stress state in this test, (σ_3 =35kPa, $\sigma_1 - \sigma_3$=103kPa), represents the average stress state at the middle of the base layer in a pavement structure (Bilodeau et al. 2011).

Sample preparation and testing procedures were the same as that of resilient modulus testing with the exception of number of loading cycles and magnitude of principal stresses. Permanent strain and load cycles results were fitted using Equation 2.11 to obtain the permanent deformation properties of the tested UGM. The permanent deformation behaviour of tested materials was characterized based on the shakedown concept.

3.4.3 Falling Weight Deflectometer (FWD)

Dynatest's truck mounted FWD was used to evaluate the in-situ layer stiffness of UGM. The test was carried out after laying and compacting of base material onsite at 10m intervals using 30kN and 40kN drops on PTH-10 north of Brandon, MB. For testing UGM, the 450mm load plate for unpaved roads was used. Deflections at the center of the loading plate were measured and used in Equation 2.12 to calculate the in-situ resilient modulus which is referred to as E_{FWD}.

Figure 3.12 Location of FWD runs at the UGM base test site on PTH-10 north of Brandon, MB.

Figure 3.13 FWD testing on DSB at PTH-75 in Manitoba

Chapter 4 Drainage Performance of UGM

4.1 Introduction:

Pavement sublayers approach saturation conditions due to seasonal environmental events such as rainfall and snow melting. It has been proven that when moisture is trapped in a pavement system and saturation levels are approached, the stiffness and bearing capacity of that layer become significantly reduced which negatively affects the pavement's response to traffic loading causing premature distresses. Therefore, using UGM with proper drainage properties would ensure quicker regain of layer strength and stiffness after rainfall events. Improvement in drainage quality leads to extended pavement service life and reduced required layer thickness. Laboratory characterization of UGM allowed to quantify the improvements in drainage associated with different gradation and physical properties which allowed for optimizing gradation for drainage performance.

4.2 Hydraulic Conductivity Test Results

Results of hydraulic conductivity tests are presented in Table 4.1. The resulted hydraulic conductivity values were used as an input parameter to calculate the time required to drain a given pavement section for each UGM. To facilitate comparison, all calculations for time-to drain were made using an arbitrary pavement geometry consisting of 2x3.65m lanes and 2% crown slope sitting on 300mm thick base layer. The reported hydraulic conductivity values are at a water temperature of 20^{o}C.

Hydraulic conductivity was observed to improve by increasing aggregate sizes, which are captured by the D_{10} and D_{60} gradation parameters. Reducing the fines content also had a positive effect on the hydraulic conductivity. The time-to drain decreased as particle sizes increased, as grain sizes

increased and as fines content decreased, resulting in an improvement in the drainage quality. In general, Limestone materials showed superior drainage performance to gravel materials of similar gradation characteristics. The difference in drainage behaviour between limestone and gravel can be due to the difference in the plasticity of fine particles, and to the difference in amount of voids between a 100% crushed aggregate matrix in limestone and partially crushed aggregate matrix in gravel.

Sample ID	Material Type	D10 (mm)	D60 (mm)	G/S	K* (m/s)x10^{-7}	Time-to drain (days)	Drainage Quality
UGM-1(9)	G	0.08	5.6	0.94	8.50	15	Poor
UGM-1(9.7)	G	0.10	7.4	1.71	1.56	21	Poor
UGM-1(12.3)	G	0.05	4.7	0.82	0.01	>30	Poor
UGM-1(14.5)	G	0.03	5.4	1.01	4.20	17	Poor
UGM-1(10.5)	L	0.07	6.1	1.13	17.5	5	Fair
UGM-1(16)	L	0.03	5.5	1.10	8.70	6	Fair
UGM-2(3.5)	G	0.22	5.7	0.82	17.60	5	Fair
UGM-2(4)	G	0.18	7.1	1.18	27.00	7	Fair
UGM-2(4.9)	G	0.40	7.6	1.70	7.47	10	Poor
UGM-2(6.4)	G	0.23	6.8	1.27	1.36	>30	Poor
UGM-2(4.5)	L	0.43	7.0	1.01	45.50	3	Fair
UGM-3(3.9)	G	0.41	7.5	1.68	14.00	6	Fair
UGM-3(6.9)	G	0.23	8.0	1.18	15.50	5	Fair
UGM-3(7.1)	L	0.21	9.7	1.89	39.60	1	Good
UGM-4(3.3)	G	0.42	12.1	1.79	21.20	4	Fair
UGM-4(7.8)	L	0.52	13.2	3.23	34.40	1	Good

Table 4.1 Results of laboratory testing of hydraulic conductivity

* Hydraulic conductivity values at saturation and water temperature of 20ºC
G = Gravel, L = Limestone

Along with hydraulic conductivity, base thickness is also a factor in subsurface drainage quality as described in section 2.3.3. In order to better understand the improvement in drainage gained by modifying gradation vs modifying structure, the relationship between the time-to drain and the thickness of the base layer was plotted as shown in Figure 4.1. From the graph, it can be sees that there is a detrimental effect on the drainage capacity of the base layer from an increase in fines

content. It can also be noticed that changing the material is a much efficient approach to enhancing subsurface drainage than changing the layer thickness.

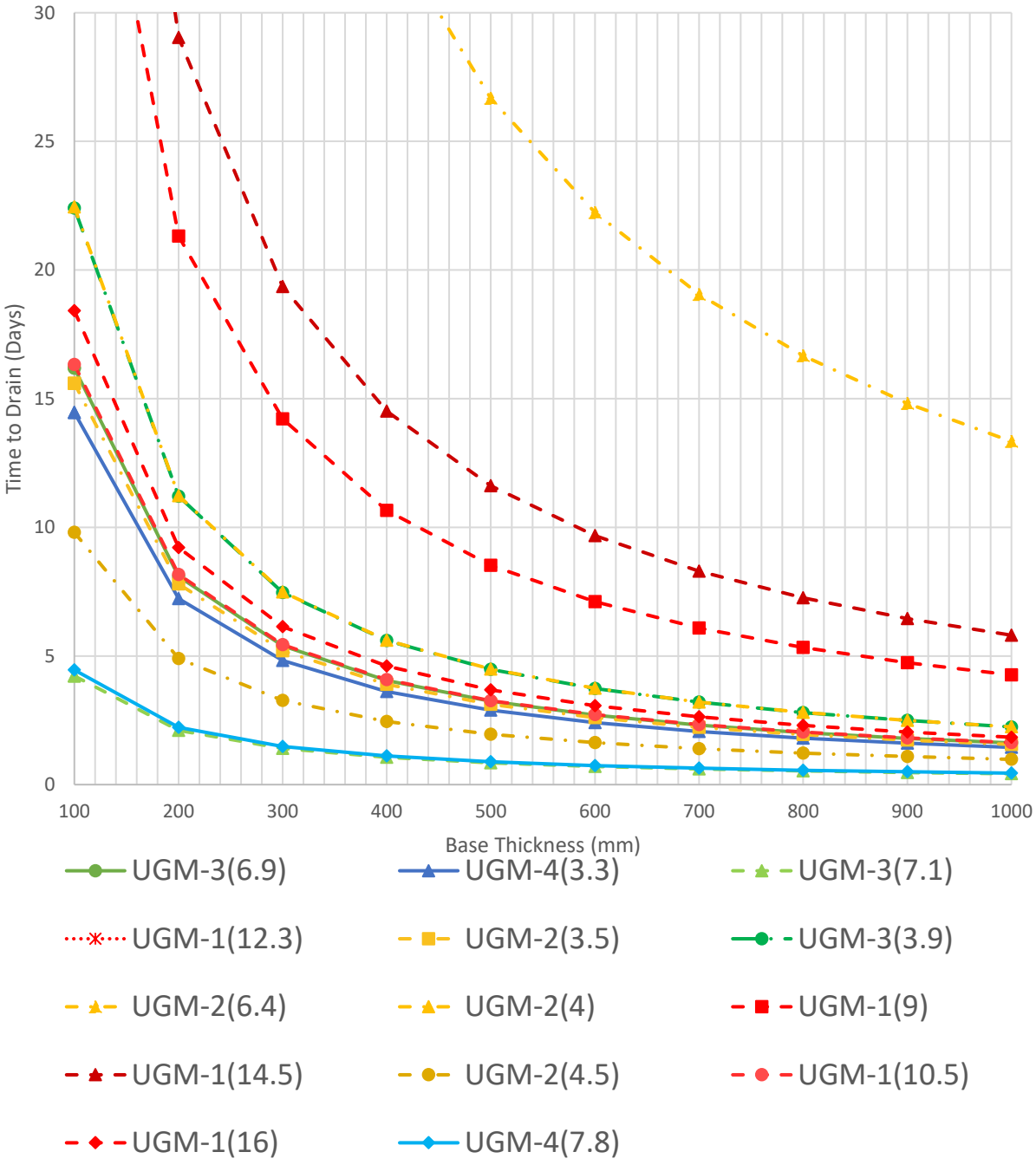

Figure 4.1 Drainage time vs. base layer thickness for UGM

4.3 Effect of UGM Gradation on Drainage Performance

To investigate the effect of gradation parameters on UGM drainage, each parameter was plotted against hydraulic conductivity values as a first step to obtain a clear picture on which factors can be considered as performance indicators of UGM drainage. Pearson correlation coefficient greater than 0.5 (strong correlation) was set as the minimum criteria for selecting gradation parameters that influence permeability of UGM. Statistical t-test was performed on the data to examine the significant level of the correlation for each parameter. A p-value less than 5% indicates that the correlation is statistically significant at a confidence level of 95% or higher. Figure 4.2, and Table 4. present a summary of the most important drainage performance indicators found in this study. Only the six parameters with the highest correlations are reported. However, the statistical analysis included dust ratio, porosity, coefficient of curvature, D_{15}, D_{30}, D_{85}, and percent passing of each sieve sizes.

Table 4.2 Correlations between gradation parameters and hydraulic conductivity of UGM

Gradation Parameter	Correlation Coefficient	p-value	Result of t-test
D10	0.65	0.006	Significant
D60	0.54	0.029	Significant
G/S	0.45	0.078	Insignificant
Cu	-0.42	0.108	Insignificant
P4	0.5	0.047	Significant
P200	-0.52	0.037	Significant

The analysis showed that aggregate sizes corresponding to 10% and 60% passing (D10 and D60), and the percent passing sieves no. 200 (P200) and no. 4 (P4) were the most significant indicators of UGM hydraulic conductivity.

The grains of the primary aggregate structure create the voids that become filled by the particles of the secondary structure. This relationship describes the creation of pores in the aggregate structure. For the studied gradation, sieve No.4 can be considered as the separator between primary and secondary aggregate structures (primary control sieve) according to the Bailey method (Vavrik et al. 2002). The gradation parameters D_{60} and D_{10} describe the particle sizes of the primary and the secondary aggregate structures. The D_{10} parameter had the strongest correlation with UGM permeability. This finding was as expected because the sand particles and fines of the granular material (secondary aggregate structure) control pore structure and therefore control permeability of UGM to a significant extent. By increasing the D_{10} value in the UGM gradation band, the desired drainage performance or quality may be reliably achieved.

The evaluation of drainage performance expected for each gradation band was carried out by comparing the average drainage test results in the four different gradation bands in this study. With this approach, an improvement in average drainage performance was noted for gradation bands that allow for coarser grain sizes and restricts fines content to low, as quantified by the parameters D10 and D60, respectively. The calculated time-to drain in days was reduced by 75% and 83% by increasing the D_{10} and D_{60} when comparing UGM-1 to UGM-3 and to UGM-4 respectively, which indicated great improvements in the drainage quality.

Table 4.3 Average Time-to drain values for gradation bands

Gradation Band	Avg. Time-to drain (days)	Std. (days)	Drainage Quality
UGM-1	15.7	8.5	Poor
UGM-2	6.9	2.6	Poor
UGM-3	4.2	2	Fair
UGM-4	2.5	1.5	Fair

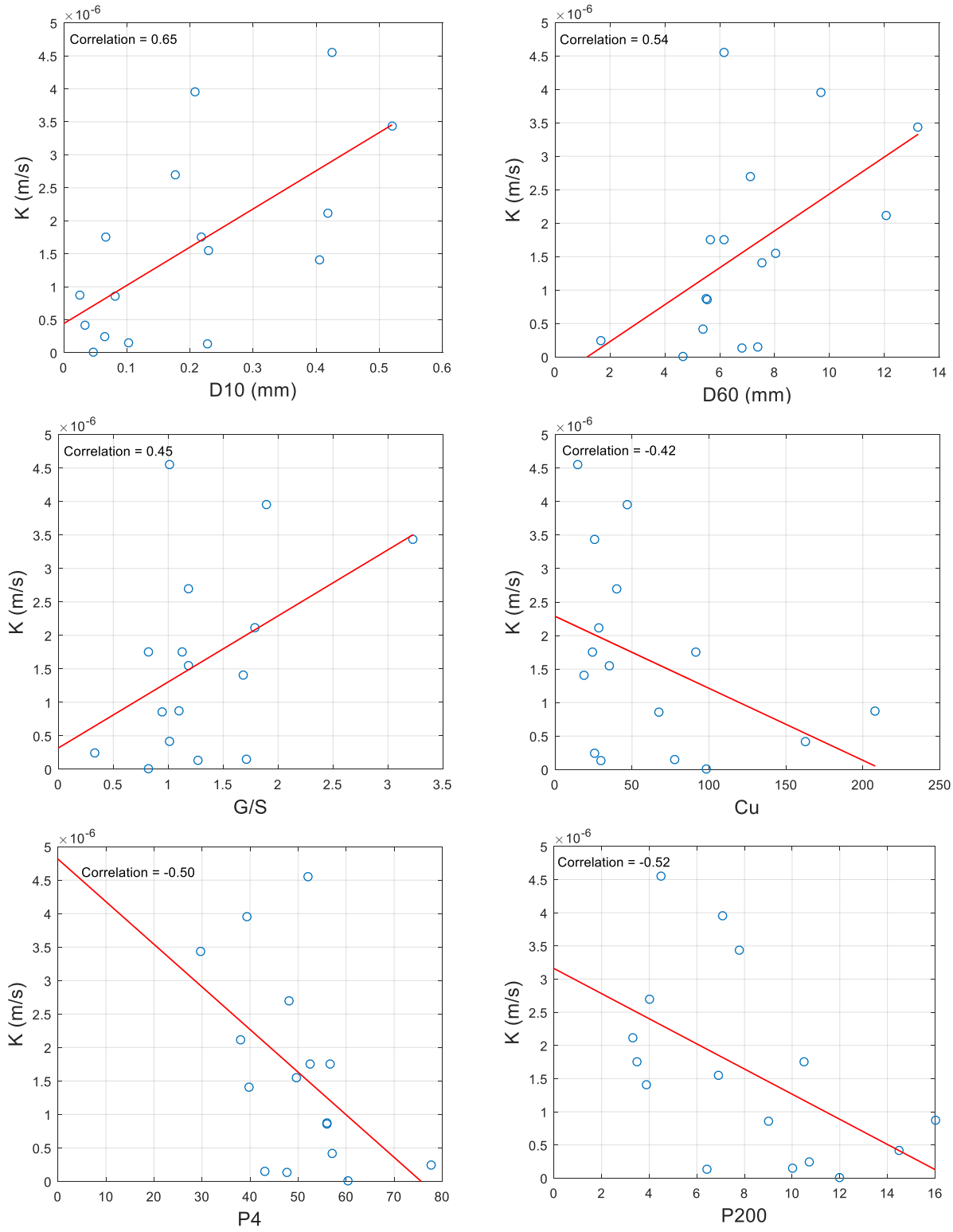

Figure 4.2 Correlations of hydraulic conductivity with gradation parameters. (a) D_{10}, (b) D_{60}, (c) gravel-to sand ratio, (d) coefficient of uniformity, (e) percent passing no.4 sieve, (f) fines content.

4.4 Prediction Models for Hydraulic Conductivity of UGM

Since subsurface drainage is a significant factor in pavement performance, it is beneficial to use appropriately representative values of UGM permeability in the design process. However, measuring the hydraulic conductivity of UGM for a specific project after the UGM is crushed and produced may not be an effective pavement design practice. Therefore, using a reliable hydraulic conductivity prediction model may be a more suitable option.

The test data from this study was used to assess the accuracy of three different hydraulic conductivity prediction models for compacted UGM. The models are discussed in detail in section 2.4 and listed in Table 4.. Correlation between measured and predicted hydraulic conductivity values, and root mean squared errors (RMSE) were used as tools for assessing the accuracy of the models in predicting hydraulic conductivity of UGM.

Table 4.4 Hydraulic conductivity prediction models

Reference	Model	Comments
(Moulton, 1980)	$K = [(6.214 \times 10^5) D_{10}^{1.478} N^{6.654}] / P_{200}^{0.597}$	K in ft/day, D_{10} in mm
(Elsayed & Lindly, 1996)	$K = -0.251 + 0.92e + {}^{2.68}/_{P_{30}} - 0.005\, P_{200}$	K in 10^{-2} m/s
(ARA, 2004) - EICM	$K = 118.11\, x\, 10^{[7.28(logD_{60}+2)-1.13(logD_{60}+2)^2-11.29]}$	K in ft/hr, D_{60} in inches

It was found that all the models, except for Moulton model, tend to overestimate the hydraulic conductivity. Table 4. shows the RMSE for each model. Table 4. shows actual vs. predicted drainage quality and it was noted that EICM hydraulic conductivity model produces overestimates for drainage quality, while the Moulton model produces drainage quality that is consistent with laboratory results. However, the Moulton predicted hydraulic conductivity of limestone materials

was significantly lower than the measured hydraulic conductivity, unlike what was observed in gravel materials. Figures 4.3 to 4.5 graphically show the trends of correlation between laboratory measured and predicted values. Poor correlations were observed for all models. The large RMSE in the Elsayed model can be explained by the different in testing materials and testing equipment. Elsayed & Lindley (1996) studied specimens from three different materials with nominal maximum aggregate sizes of 25, 37.5, and 68mm which would result in higher values of hydraulic conductivity. Also, they used a 6 inch permeameter mold due to the larger NMAS which would increase the possibility of moisture draining between the compacted specimen and the mold's wall and result in higher hydraulic conductivity. The model was based on the reported hydraulic conductivity from Elsayed & Lindley (1996), which ranged from 0.006 to 0.009 m/s. That range is significantly larger than the values found in this research.

Table 4.5 Hydraulic conductivity model evaluation

Prediction Model	RMSE (m/s)
Moulton	14.4×10^{-07}
EICM	87.3×10^{-07}
Elsayed	447.26

Table 4.6 Measured and predicted hydraulic conductivity of UGM

Sample ID	Material Type	Laboratory Measured K ($x10^{-7}$ m/s)	Predicted K ($x10^{-7}$ m/s)		
			Moulton	EICM	Elsayed
UGM-1(9)	Gravel	8.50	0.77	27.9	L*
UGM-1(9.7)	Gravel	1.56	0.03	89.0	L
UGM-1(12.3)	Gravel	0.01	0.74	12.8	L
UGM-1(14.5)	Gravel	4.20	0.21	24.2	L
UGM-1(10.5)	Limestone	17.5	0.22	42.3	L
UGM-1(16)	Limestone	8.70	0.02	26.6	L
UGM-2(3.5)	Gravel	17.60	7.65	30.3	L
UGM-2(4)	Gravel	27.00	8.46	77.5	8121
UGM-2(4.9)	Gravel	7.47	11.4	123	9247
UGM-2(6.4)	Gravel	1.36	1.46	64	4724
UGM-2(4.5)	Limestone	45.50	18.4	72.4	9227
UGM-3(3.9)	Gravel	14.00	13.5	96.4	15419
UGM-3(6.9)	Gravel	15.50	38.3	124.8	13131
UGM-3(7.1)	Limestone	39.60	3.38	254.3	5729
UGM-4(3.3)	Gravel	21.20	16.3	563.7	9842
UGM-4(7.8)	Limestone	34.40	106.6	774.1	22383

* L = Limitation in the model.

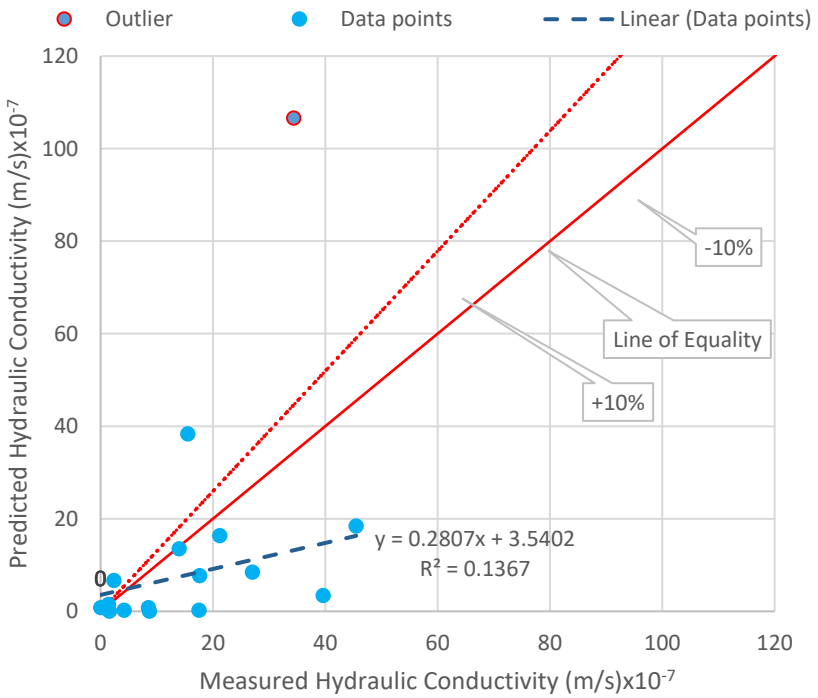

Figure 4.3 Measured vs predicted hydraulic conductivity using Moulton Model (Moulton 1980)

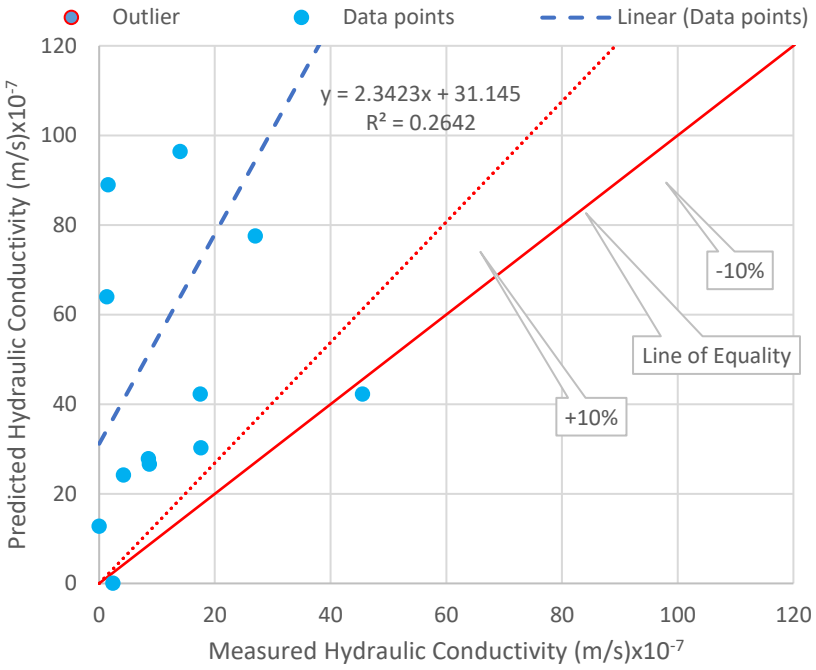

Figure 4.4 Measured vs predicted hydraulic conductivity using EICM Model (ARA 2004)

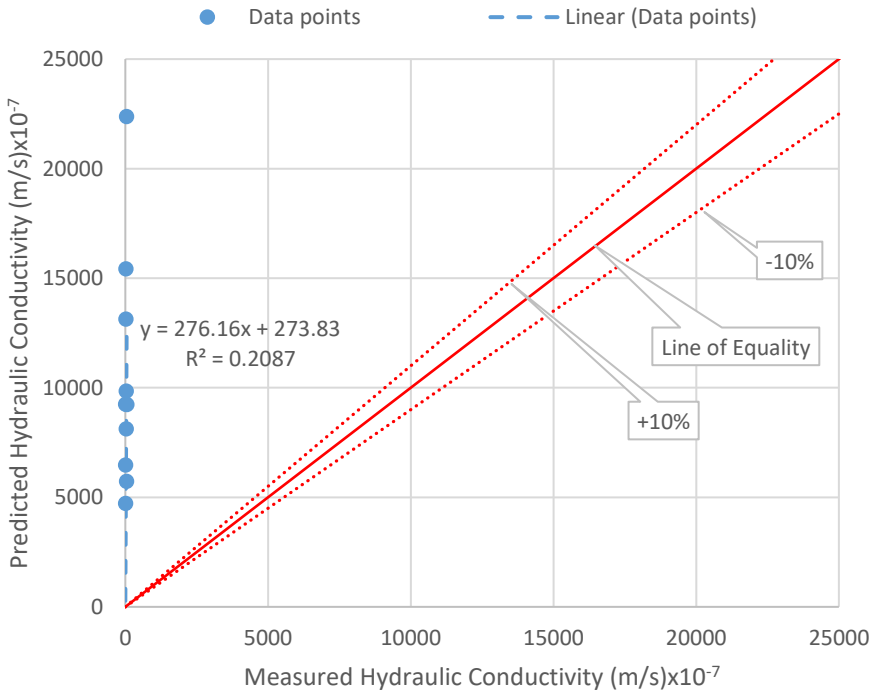

Figure 4.5 Measured vs predicted hydraulic conductivity (Elsayed & Lindly 1996)

Even though the Moulton prediction model provided better approximation of UGM hydraulic conductivity than the other two models, it seems to be consistently underestimating the hydraulic conductivity for limestone samples. Figure 4.6 shows that the error between measured and predicted hydraulic conductivity of gravel UGM is much smaller than that in limestone samples. This is because the model is sensitive to the fines content which is true in the case of gravel material. However, due to the non-plastic nature of limestone fines, the amount of fines would not affect hydraulic conductivity as much as plastic fines tend to swell and fill aggregate voids. Figures 4.3 to 4.5 graphically show the trends of correlation between laboratory measured and predicted values. Poor correlations were observed for all three models.

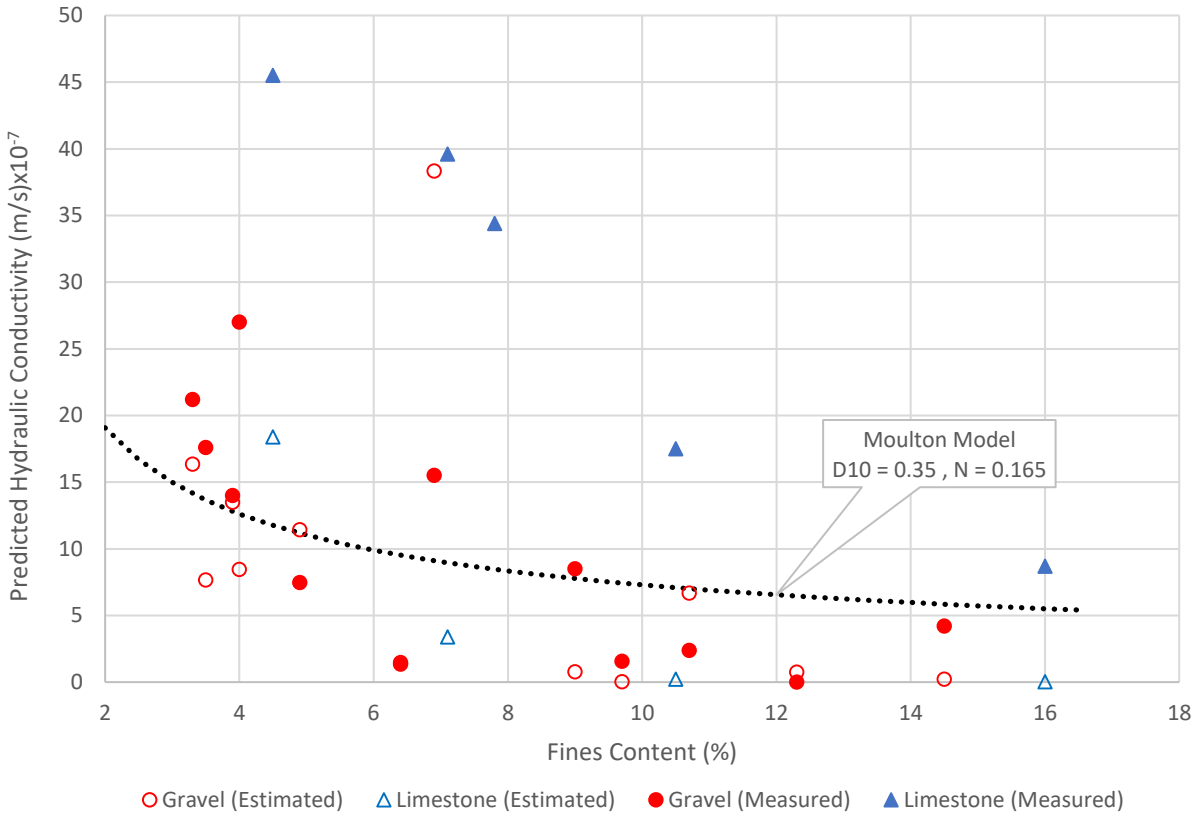

Figure 4.6 Effect of fines on prediction of hydraulic conductivity using Moulton equation

4.5 Field Testing for UGM Drainage

UGM drainage was assessed in field conditions using the Double Ring Infiltrometer test method. Tests were conducted on three PTH sections representing gradation bands UGM-1, UGM-3, and UGM-4. Table 4.2 shows the average measured hydraulic conductivity for each PTH section. The

Table 4.2 Field measurements of hydraulic conductivity and drainage quality

Material ID	Location	Field "K" ($x10^{-7}$ m/s)	Time-to Drain (days)	Field Quality of Drainage
UGM-1(12.3)	PTH-10-South	5	>30	Poor
UGM-3(6.9)	PTH-10-North	1500	0.06	Excellent
UGM-3(3.3)	PTH-75	88	1.00	Good

field measurements of hydraulic conductivity varied from laboratory measurements due to possible leakage on the sides of the rings. The variation seemed to increase as the soil became less permeable. This is explained by the flow of water seeking the easier path through the sides of the rings, instead of through the granular layer, in the case of a clogged granular layer. Even though drainage data retrieved from the field were over estimating the hydraulic conductivity, it still confirmed the gains of drainage quality achieved from modifying UGM gradation bands.

Chapter 5 Mechanical Performance of UGM

5.1 Introduction

The primary role of a granular base layer is to distribute traffic loads so that they are spread on the subgrade. These loads are transferred throughout the base layer by particle to particle contact where the stress concentrates in the meeting points between particles (Tutumluer 2013; Oda 1974). The load carrying behaviour of UGM depends on the characteristics of the primary and secondary structures of the aggregate matrix. Within this interaction, the base layer undergoes a vertical deformation. Part of that deformation is recovered (resilient) by the elasticity of the particle to particle contact, and the remaining part is permanent (plastic) deformation. This behaviour of the base layer is a function of several performance indicators such as mineralogy, density, moisture, particle size, and gradation of the UGM. Therefore, in order to produce reliable pavement designs it is vital to use accurate laboratory characterization of the proposed material's mechanical response.

5.2 Resilient Behaviour of UGM

5.2.1 Resilient Modulus Test Results

Data from each test was fitted to the universal model, (Equation.3.4), in order to predict the value of the modulus at stress conditions that match traffic loading at a typical base layer. A minimum coefficient of determination of 0.9 was used to accept fitted results. The regression model is then used to obtain the value of the resilient modulus under typical stress conditions that are experienced at the middle of a base layer (Confinement Stress = 35 kPa, Cyclic Stress = 103 kPa). Results of resilient modulus tests are reported in Table 5.1 . Resilient modulus was found to increase with increase in particle sizes and with a decrease in fines content.

Table 5.1 Resilient modulus test results

Sample ID	Material Type	D10 (mm)	D60 (mm)	G/S	M_R (MPa)	K1	K2	K3
UGM-1(9)	Gravel	0.08	5.6	0.94	168	1085	1.088	-0.913
UGM-1(9.7)	Gravel	0.10	7.4	1.71	165	941	1.210	-0.786
UGM-1(12.3)	Gravel	0.05	4.7	0.82	184*	1209	1.650	-1.960
UGM-1(14.5)	Gravel	0.03	5.4	1.01	156*	917	1.380	-1.223
UGM-1(10.5)	Limestone	0.07	6.1	1.13	155	997	0.978	-0.698
UGM-1(16)	Limestone	0.03	5.5	1.10	149	934	0.986	-0.645
UGM-2(3.5)	Gravel	0.22	5.7	0.82	217	1292	1.000	-0.544
UGM-2(4)	Gravel	0.18	7.1	1.18	138	866	1.045	-0.760
UGM-2(4.9)	Gravel	0.40	7.6	1.70	NA	NA	NA	NA
UGM-2(6.4)	Gravel	0.23	6.8	1.27	181	1025	1.150	-0.733
UGM-2(4.5)	Limestone	0.43	6.1	1.01	196	1264	0.978	-0.698
UGM-3(3.9)	Gravel	0.41	7.5	1.68	194	1173	1.190	-0.938
UGM-3(6.9)	Gravel	0.23	8.0	1.18	184	1102	1.270	-1.070
UGM-3(7.1)	Limestone	0.21	9.7	1.89	204	1230	1.448	-1.230
UGM-4(3.3)	Gravel	0.42	12.1	1.79	299	1864	0.960	-0.589
UGM-4(7.8)	Limestone	0.52	13.2	3.23	355	2290	0.75	-0.290

* Specimen accumulated more than 5% permanent strain
NA Test was not conducted

Table 5.2 Average resilient modulus values of gradation ranges

Gradation Band	Average M_R (MPa)	Standard Deviation (MPa)
UGM-1	162	11
UGM-2	183	8
UGM-3	194	29
UGM-4	327	28

Table 5.2 presents the average values of stiffness for each gradation band with the standard deviation. Reducing the allowed fines content in gradation from (8 - 17%) to (3 - 8%) resulted in 12% increase in stiffness as recorded between gradation bands UGM-1 and UGM-2 where the maximum aggregate size was 19mm for both bands. In addition to fines reduction, increasing the maximum aggregate size from 19mm to 25mm, resulted in a 20% increase in stiffness as recorded between gradation bands UGM-1 and UGM-3 where the fines content were (8 - 17%) and (3 - 8%), respectively. A further increase in maximum aggregate size from 19mm to 37.5mm and limiting fines content from (8 - 17%) to (0 - 6%) resulted in 101% increase in stiffness as recorded between gradation bands UGM-1 and UGM-4.

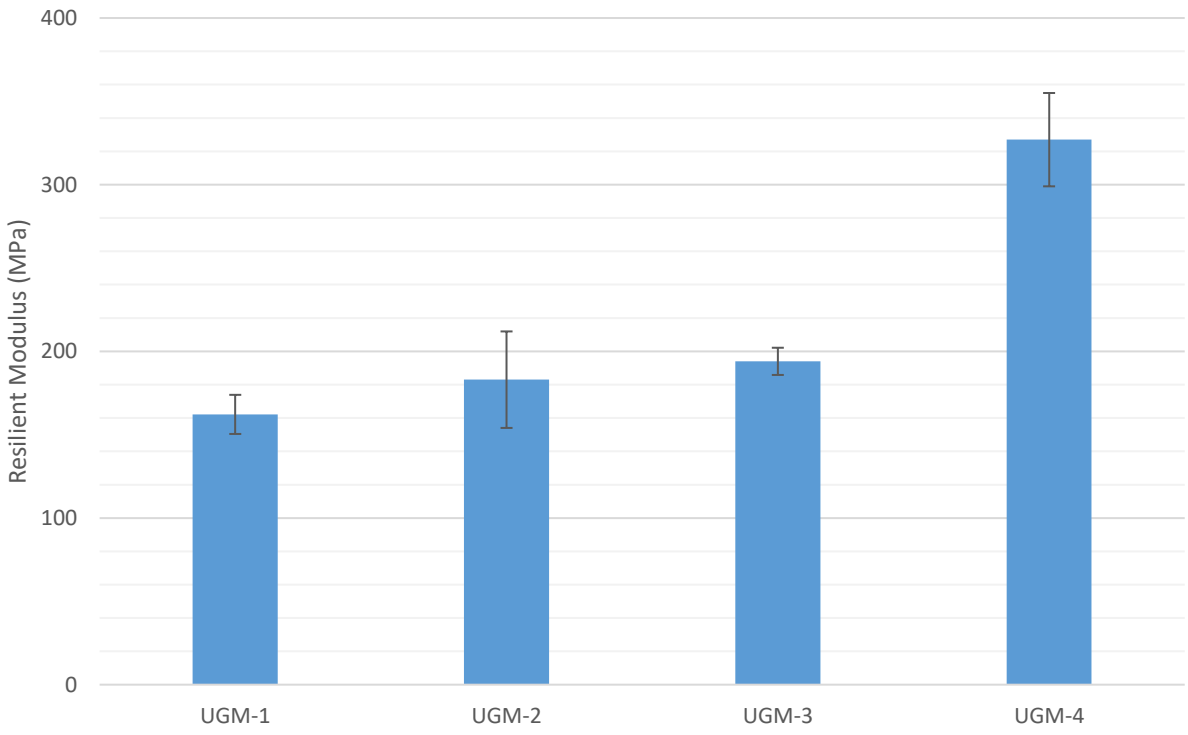

Figure 5.1 Average resilient modulus values of different gradation bands

5.2.2 Effect of Moisture on UGM Stiffness

Several researchers have studied UGM behaviour at high degrees of saturations and found that the moisture content of UGM has a significant effect on the resilient response of the material (Lekarp et al. 2000a; Soliman 2015; Stolle et al. 2009). To evaluate the sensitivity of UGM stiffness for moisture change, the two materials, UGM-1(12.3) and UGM-3(6.9), retrieved from PTH-10, were selected to be tested for resilient modulus at moisture conditions of 2% above the optimum, in addition to testing at the OMC.

The experiment resulted, as expected, in a reduction of resilient modulus in both materials when moisture was increased. This is attributed to the development of excess pore water pressure, and to the lubricating effect of moisture on particles (Lekarp et al. 2000a; Thom & Brown 1987). However, the magnitude of that reduction was much more severe in the UGM-1(12.3) material than in the UGM-3(6.9). A 32% reduction in stiffness was recorded in the UGM-2 sample, while the stiffness reduction in the UGM-1 sample was more severe and resulted in resilient modulus value that was too low to be measured by current resilient modulus testing practice.

It has been reported that the stiffness of UGM with high fines content would be more sensitive to changes in moisture (Raad et al. 1992). This can be explained by the decreased permeability of UGM with high fines. It was observed during M_R testing that the UGM-3(6.9) sample was continuously dissipating excess pore water pressure through draining its excess moisture. While the poorly draining UGM-1(12.3) sample contained its excess moisture, which allowed pore water pressure to build up until the specimen failed after only 100 out of 4,000 load cycles. Moreover, Soliman (2015) investigated the UGM stiffness sensitivity to moisture through resilient modulus testing of samples: UGM-1(9),(10.5),(14.5),(16) and UGM-2(4),(4.5), and Soliman's test results

showed that the stiffness of samples containing higher amounts of fines were more sensitive to moisture variations than samples containing limited amounts of fines.

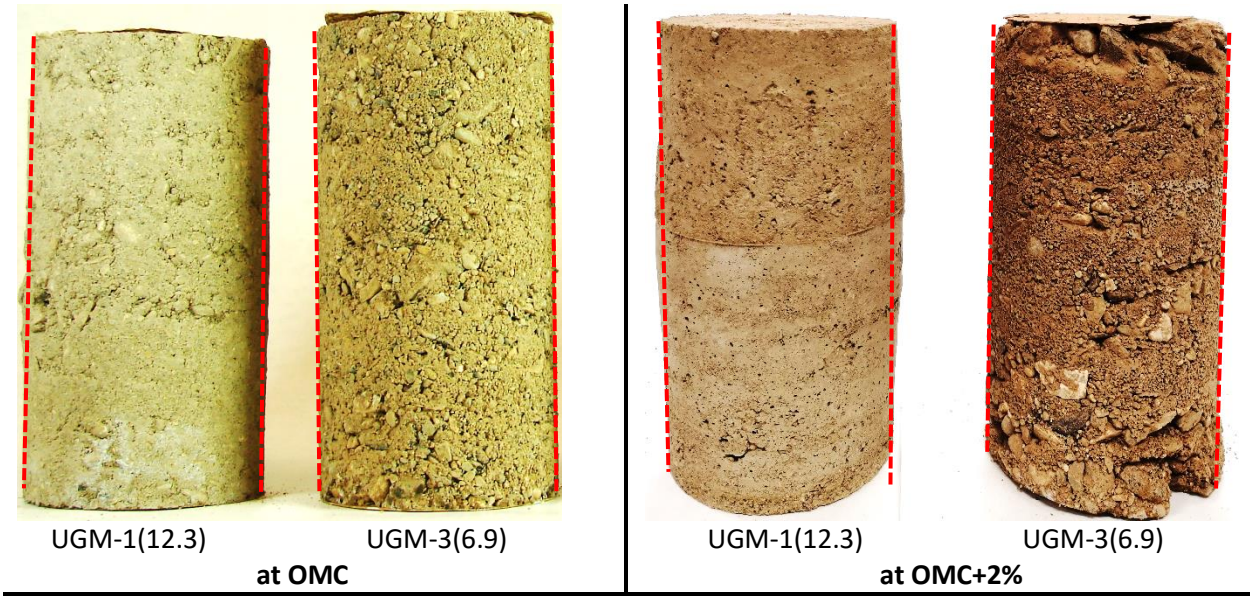

Figure 5.2 PTH-10 UGM samples after M_R testing at different moisture contents showing excessive lateral strain in UGM-1(12.3) sample in high moisture conditions

Table 5.3 Resilient modulus test results for moisture sensitivity

Sample ID	OMC (%)	Resilient Modulus at OMC (MPa)	Resilient Modulus at OMC+2% (MPa)
UGM-3(6.9)	10.1	184	125
PTH-1(12.3)	8.7	183*	Failed*

* Specimen accumulated more than 5% permanent strain

5.2.3 Relating Gradation Parameters to UGM Stiffness

To investigate the effect of gradation parameters as performance indicators of UGM stiffness, each parameter was plotted against the resilient modulus (M_R). This allowed for determining which factors could be considered as performance indicators of UGM stiffness. Pearson

correlation coefficient greater than 0.5 was set as the minimum criteria for selecting gradation parameters that influence stiffness of UGM. Statistical t-test was performed on the data to examine the significant level of the correlation for each parameter. A p-value 5% or less indicates that the correlation is statistically significant at a confidence level of 95% or higher. Figure 5.3 and Table 5.4 present a summary of the most important stiffness performance indicators found in this study. Only the six parameters with the highest correlations were reported. However, the statistical analysis included dust ratio, porosity, coefficient of curvature, D_{15}, D_{30}, D_{85}, and each percent passing of all of the sieve sizes. The result of the statistical analysis in Table 5.4 showed that D60, D10, P4, and G/S were strongly and positively correlated to UGM resilient modulus based on their coefficient of correlation and the associated p-value. Based on these observations, an increased maximum aggregate size and a limited amount of fines content would contribute to higher stiffness of UGM. However, D_{max} and P_{200} only represent the two ends of the gradation curve, while D_{60} and D_{10} represent the aggregated values of grain size distribution of both of the primary and the secondary aggregate structures, respectively. Therefore, it is understood that these parameters provide better indication of UGM stiffness.

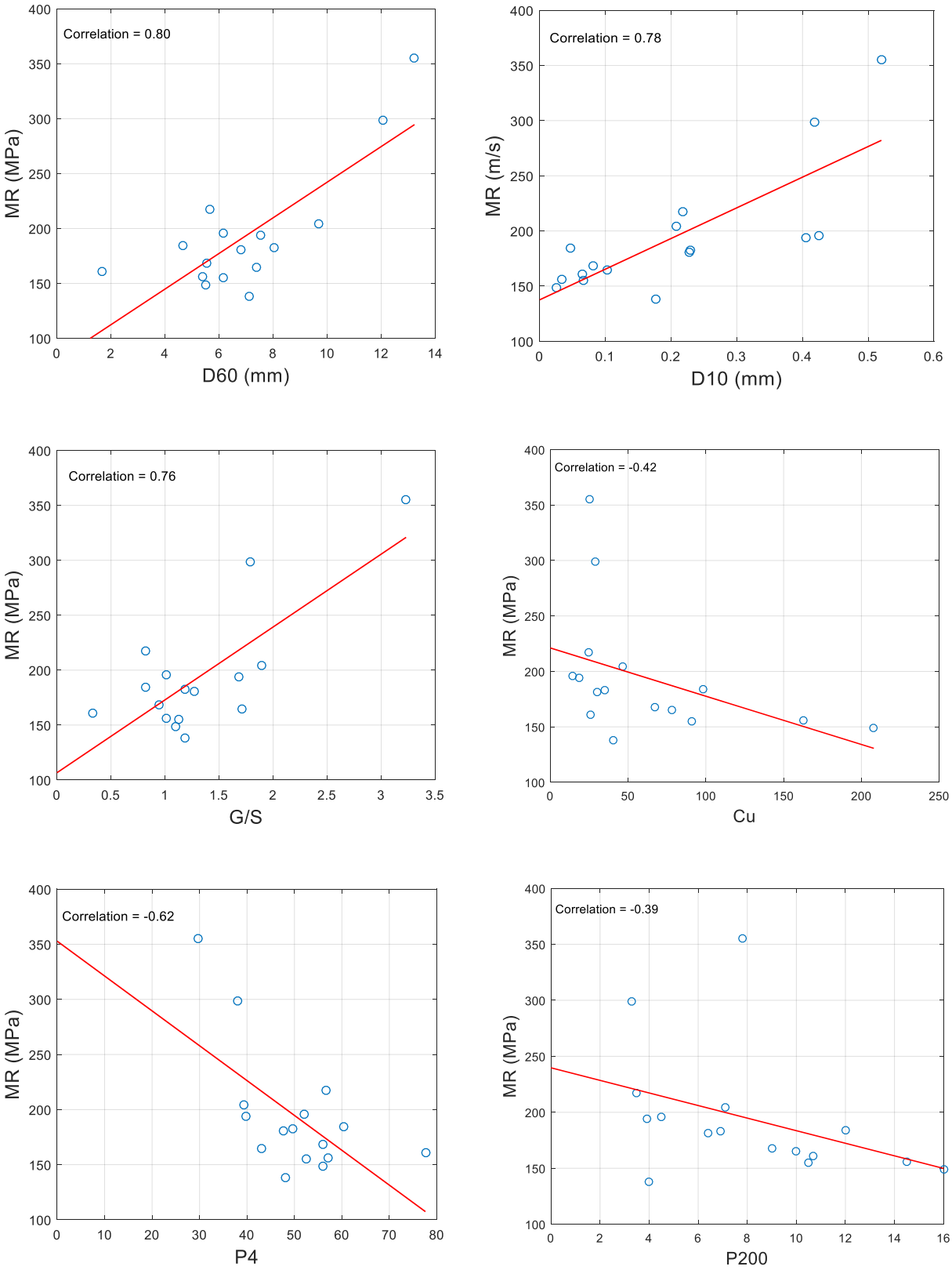

Figure 5.3 Correlations of resilient modulus with gradation parameters. (a) D_{60}, (b) D_{10}, (c) gravel-to sand ratio, (d) coefficient of uniformity, (e) percent passing sieve no.4, (f) fines content

Table 5.4 Correlations between gradation parameters and resilient modulus of UGM

Gradation Parameter	Correlation Coefficient	p-value	t-test
D10	0.78	0.0003	Significant
D60	0.80	0.0002	Significant
G/S	0.76	0.0006	Significant
Cu	-0.42	0.1038	Insignificant
P4	0.62	0.0101	Significant
P200	-0.39	0.1406	Insignificant

Osouli et al. (2019) studied the strength of UGM using CBR and staged triaxial testing and concluded that dust ratio is a significant parameter in indicating static strength. Further the study suggested that the dust ratio effect on UGM should be further investigated under cyclic loading. In this study, the dust ratio was not found to have a statistically significant correlation with M_R. It was expected that UGM with large maximum aggregate size and limited amount of fines would lead to higher stiffness. However, the fines content and maximum aggregate size were found to be statistically insignificant indicators of stiffness as they only represent the two ends of the gradation curve. Instead, D_{60} and D_{10} were found to be more significant indicators of UGM stiffness, because their aggregated values account for the size distribution of the primary and secondary aggregate structures, respectively. Therefore, using these parameters provides better indication of UGM stiffness.

5.2.4 Effect of Stress on Resilient Behaviour

For purposes of pavement design inputs and simplified comparison of base layer mechanical performance, M_R value is usually reported under the state of stress experienced in the mid-depth of a base layer in a typical pavement structure. However, studying the resilient response under

different combinations of principal stresses provide better insights on the mechanical behaviour of UGM. Samples having large aggregate sizes, represented by the value of D_{60}, showed stress hardening behaviour. This is evident by an increase in stiffness with increasing confinement and deviatoric stresses. This stress hardening behaviour is due to good interlock between particles and would lead to good mechanical performance under traffic loading. On the other hand, samples with small D60 and high fines content showed a significant decrease of stiffness when bulk stress increased evidencing stress softening behaviour. Such mechanical behaviour is caused by poor interlock between particles. Small particles, in an aggregate structure that includes excessive amount of fines, would not be able to achieve proper interlock needed to distribute applied stresses with minimum deformation. This mechanism is apparent in Figure 5.4-b and Figure 5.4-c which shows slippage of aggregates during the resilient modulus testing. Comparing the resilient behaviour of UGM-1(9) and UGM-1(9.7) shows that a slight increase in D60 from 5.5mm to 7.4mm could result in changing the resilient behaviour from stress softening to stress hardening as shown in Figure 5.7 and Figure 5.8. Ahmed et al. (2018) discussed the effect of UGM resilient behaviour on M_R regression coefficients and mentioned that a positive value of K2 indicates stress hardening behaviour. In this study, it was found that a higher K2 value indicates a more evident stress softening behaviour, as the material becomes more dependent on bulk stress. The stress hardening and stress softening phenomena, of the studied materials, are presented in Figure-5.7 to 5.20.

a) UGM-1(9.7) **b) UGM-1(12.3)**

c) UGM-1(14.5) **d) UGM-2(6.4)**

Figure 5.4 UGM specimens after resilient modulus testing showing signs of aggregate distortion and excessive deformation in samples with high fines UGM-1(12.3) and UGM-1(14.5)

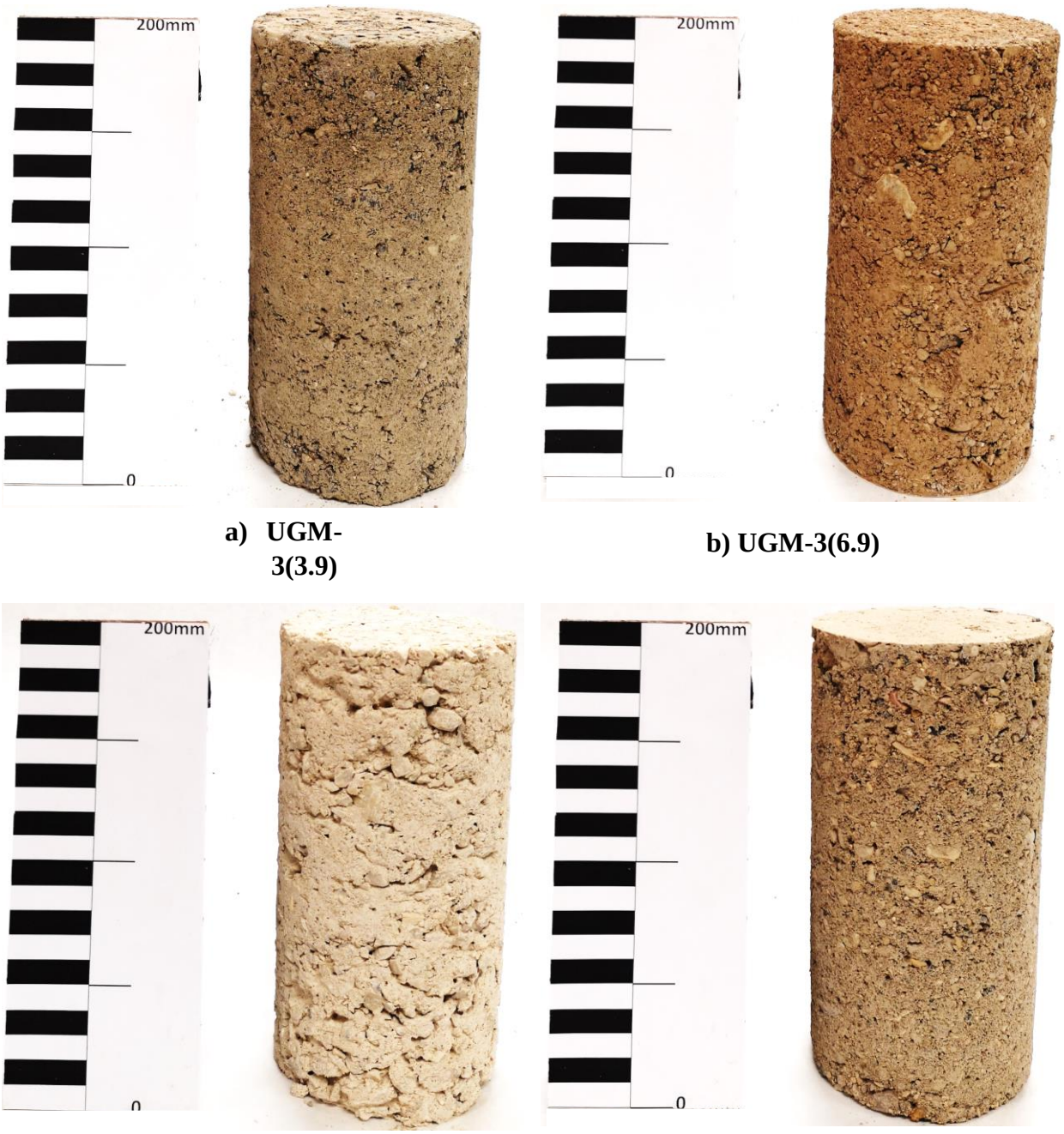

a) UGM-3(3.9)

b) UGM-3(6.9)

c) UGM-3(7.1)

d) UGM-4(3.3)

Figure 5.5 UGM Specimens after resilient modulus testing

UGM-4(7.8)

Figure 5.6 UGM-4(7.8) specimen after resilient modulus testing showing signs of fine particles migration due to large pore structure.

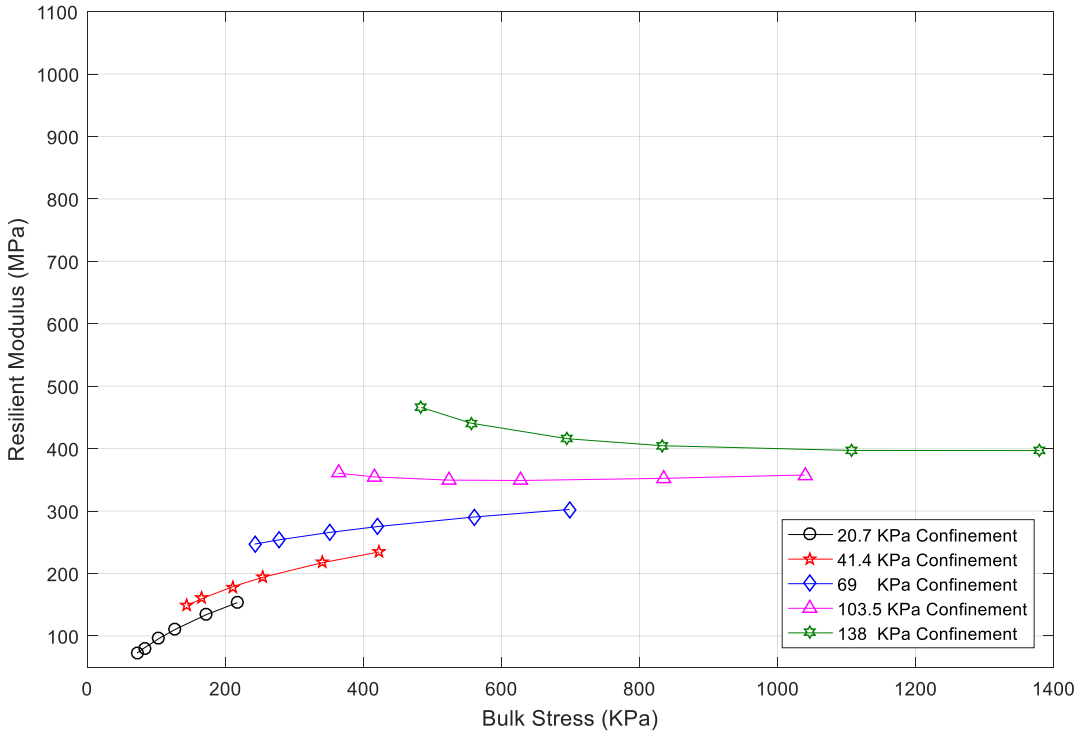

Figure 5.7 Bulk stress vs. resilient modulus for UGM-1(9)

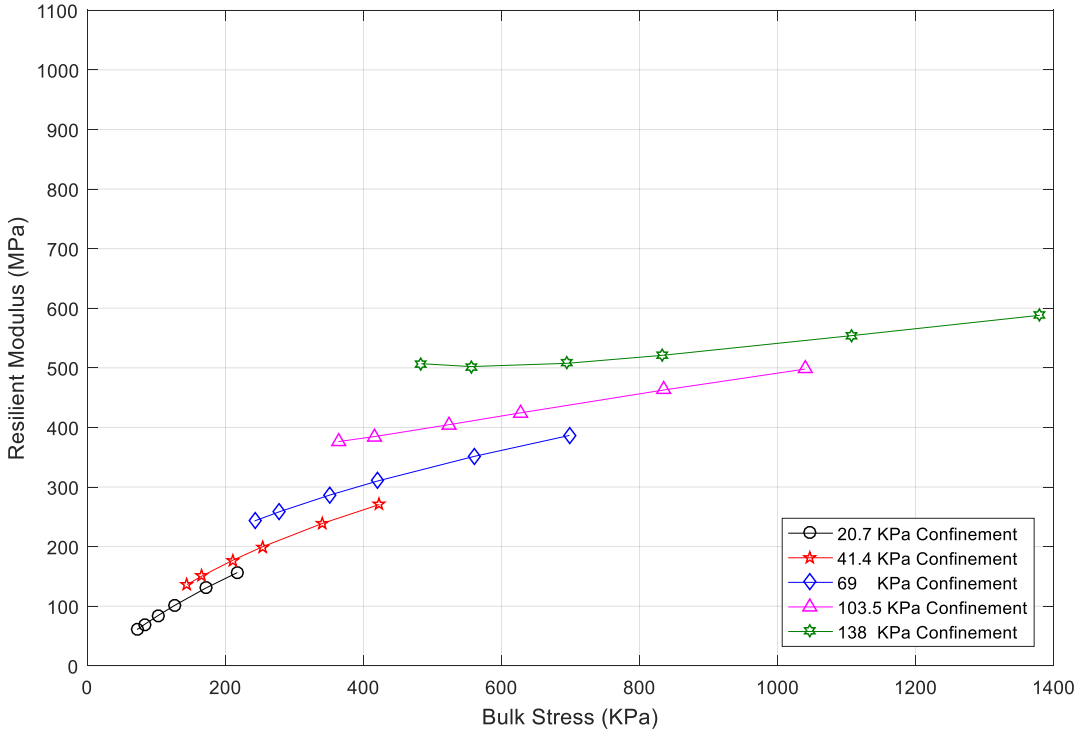

Figure 5.8 Bulk stress vs. resilient modulus for UGM-1(9.7)

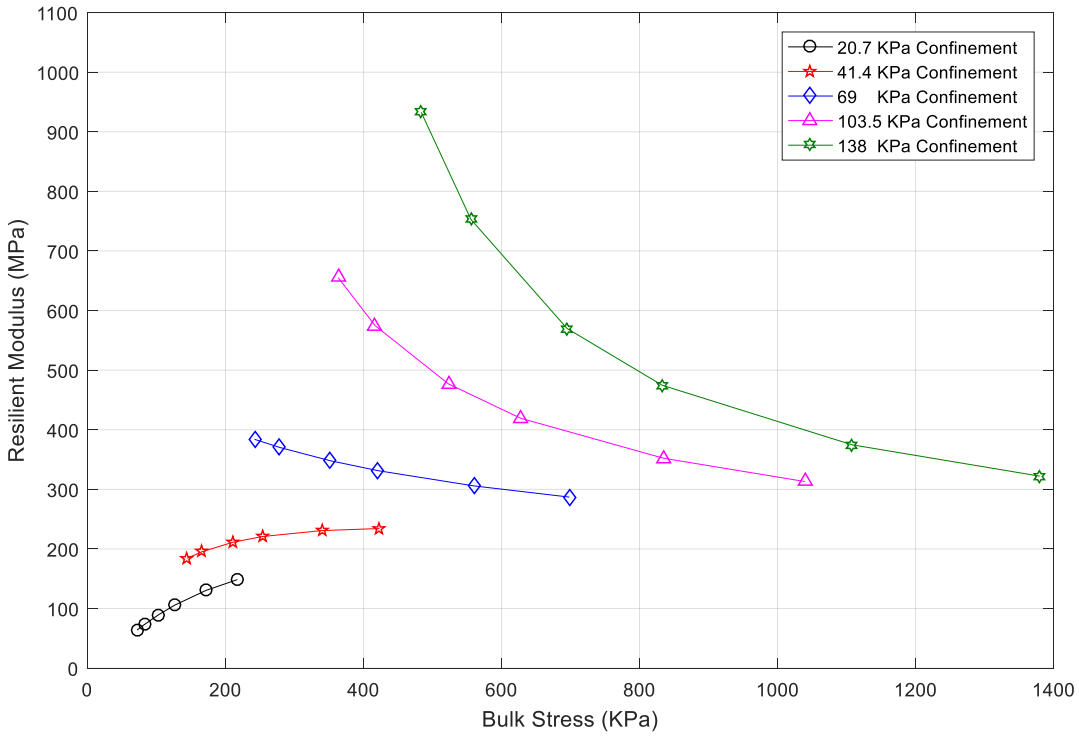

Figure 5.9 Bulk stress vs. resilient modulus for UGM-1(12.3) showing obvious signs of stress softening

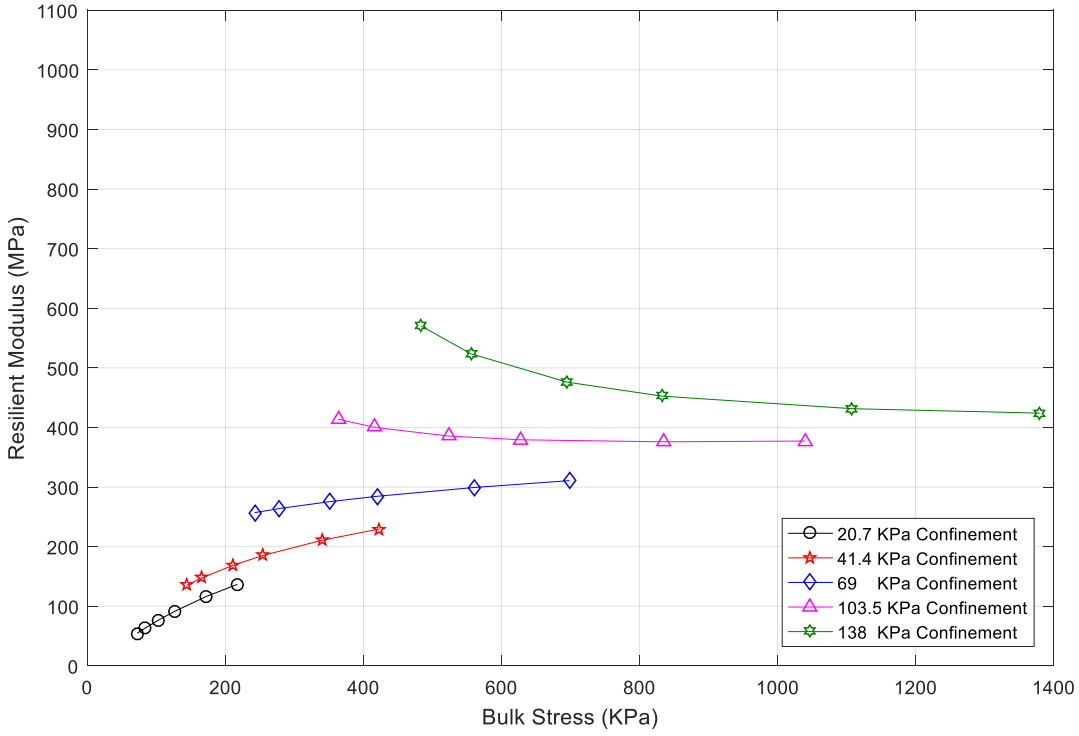

Figure 5.10 Bulk stress vs. resilient modulus for UGM-1(14.5)

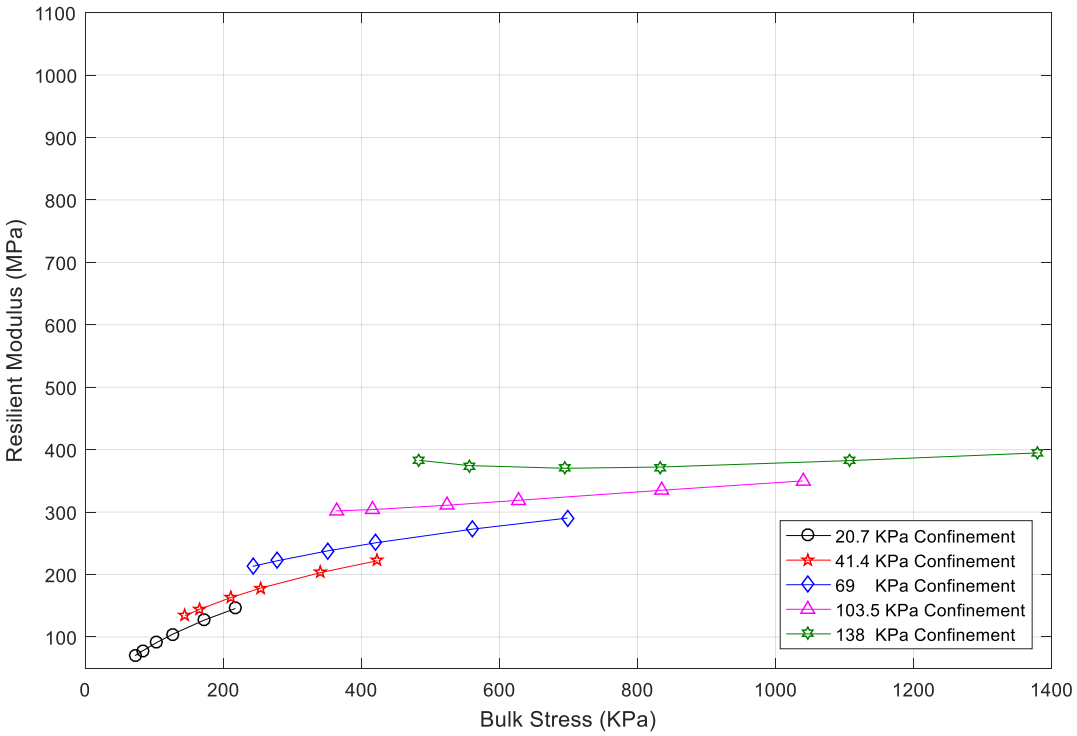

Figure 5.11 Bulk stress vs. resilient modulus for UGM-1(10.5)

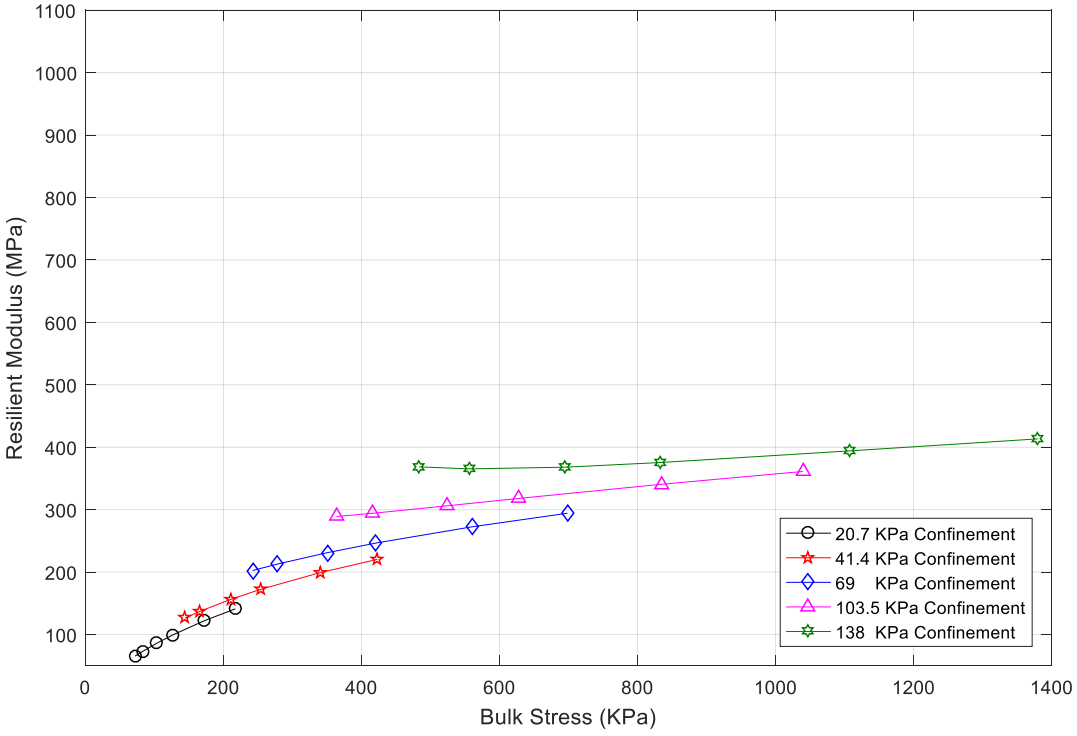

Figure 5.12 Bulk stress vs. resilient modulus for UGM-1(16)

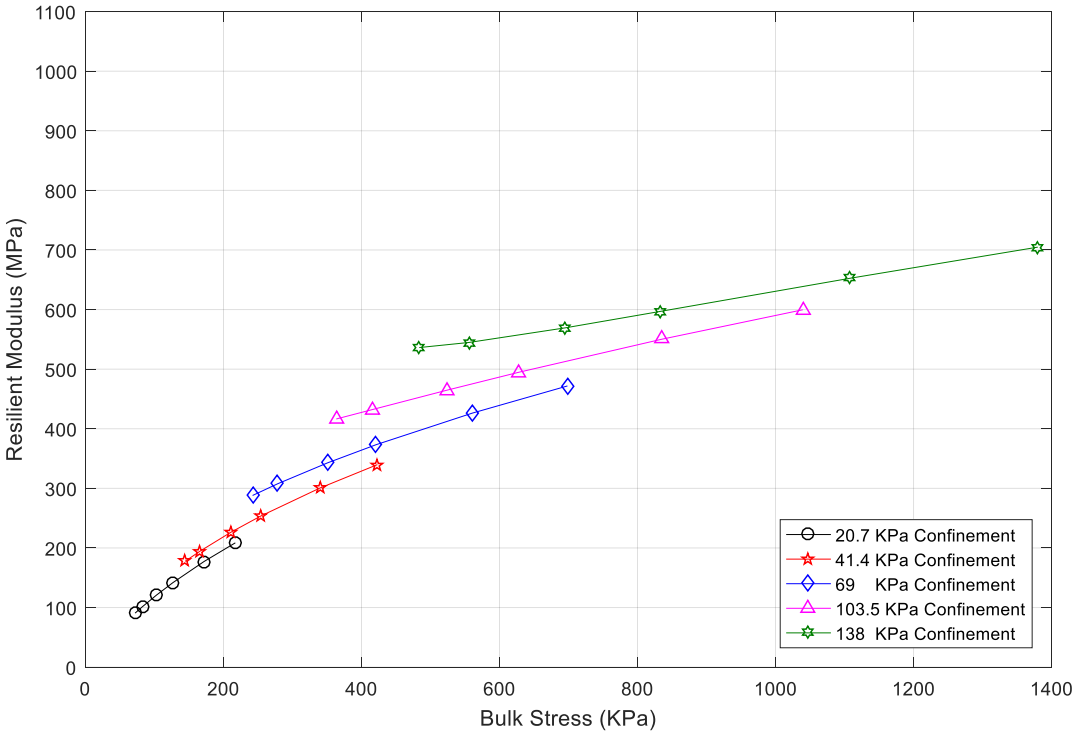

Figure 5.13 Bulk stress vs. resilient modulus for UGM-2(3.5)

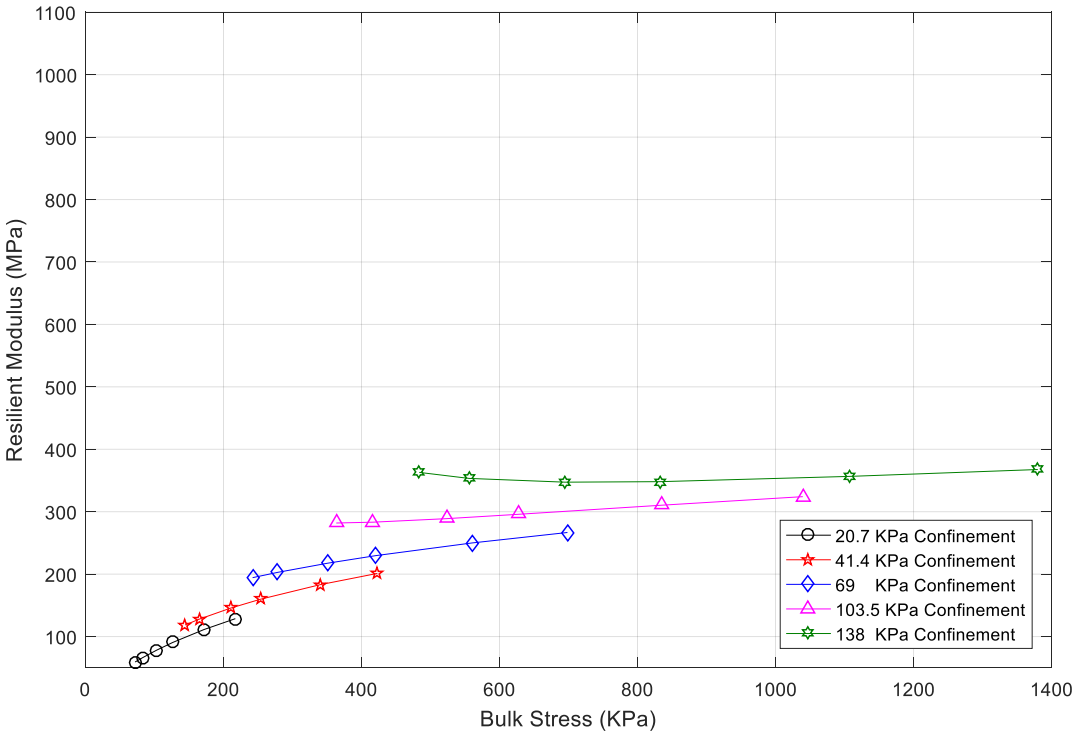

Figure 5.14 Bulk stress vs. resilient modulus for UGM-2(4)

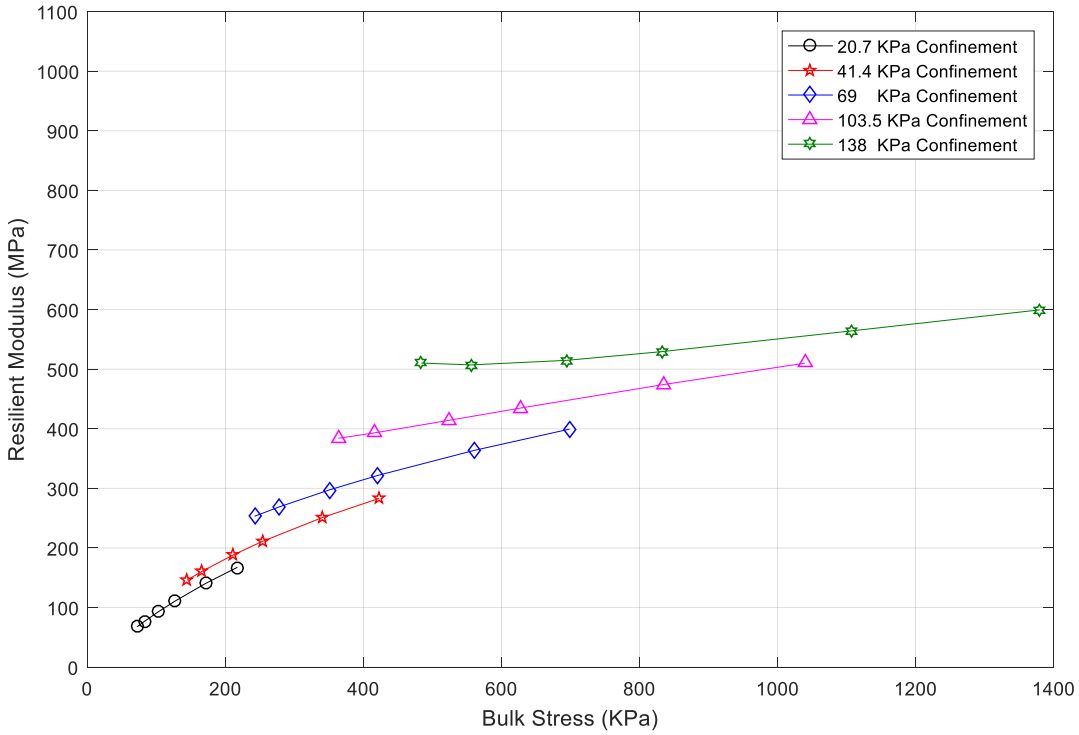

Figure 5.15 Bulk stress vs. resilient modulus for UGM-2(6.4)

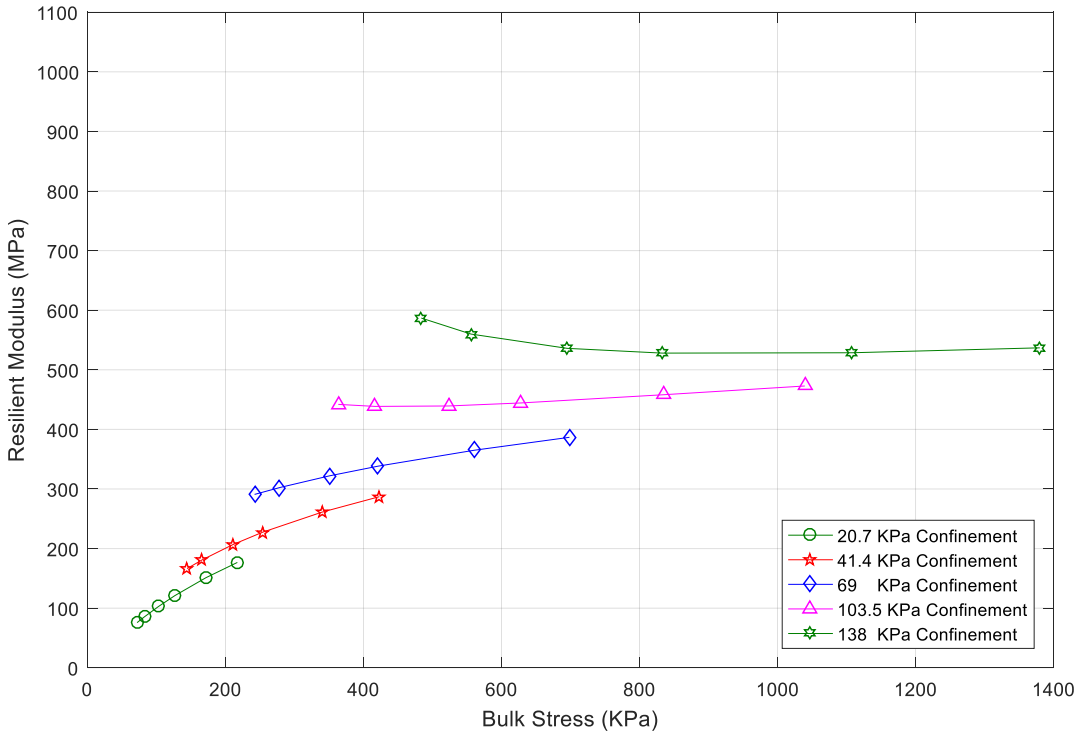

Figure 5.16 Bulk stress vs. resilient modulus for UGM-3(3.9)

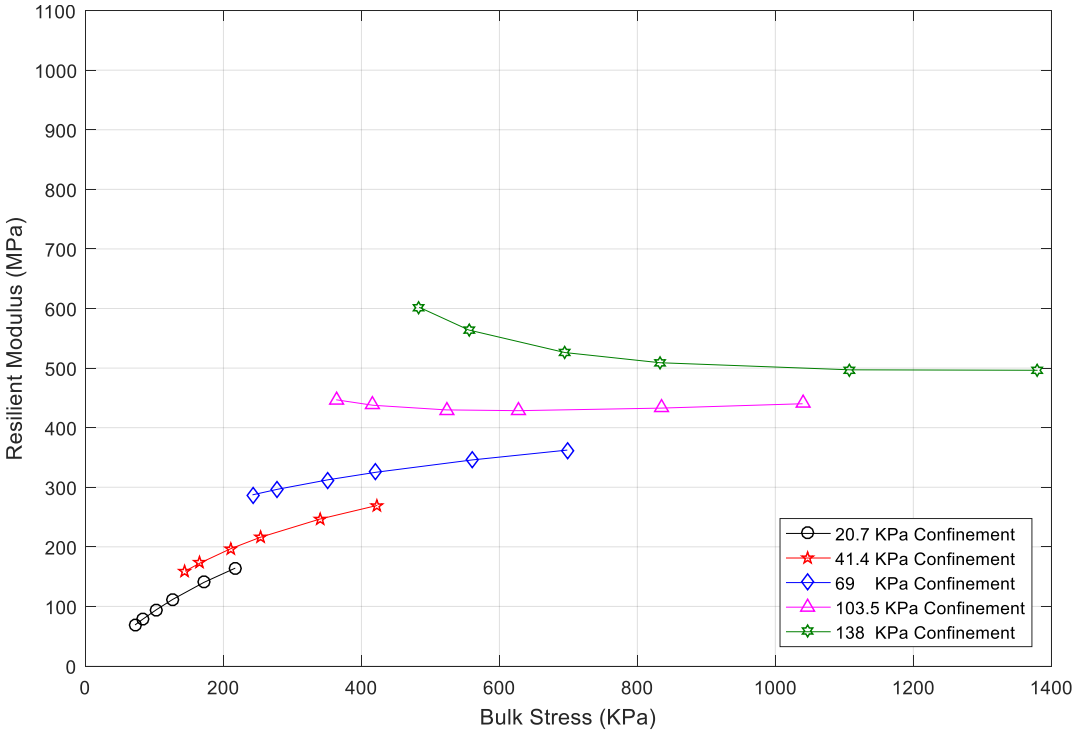

Figure 5.17 Bulk stress vs. resilient modulus for UGM-3(6.9)

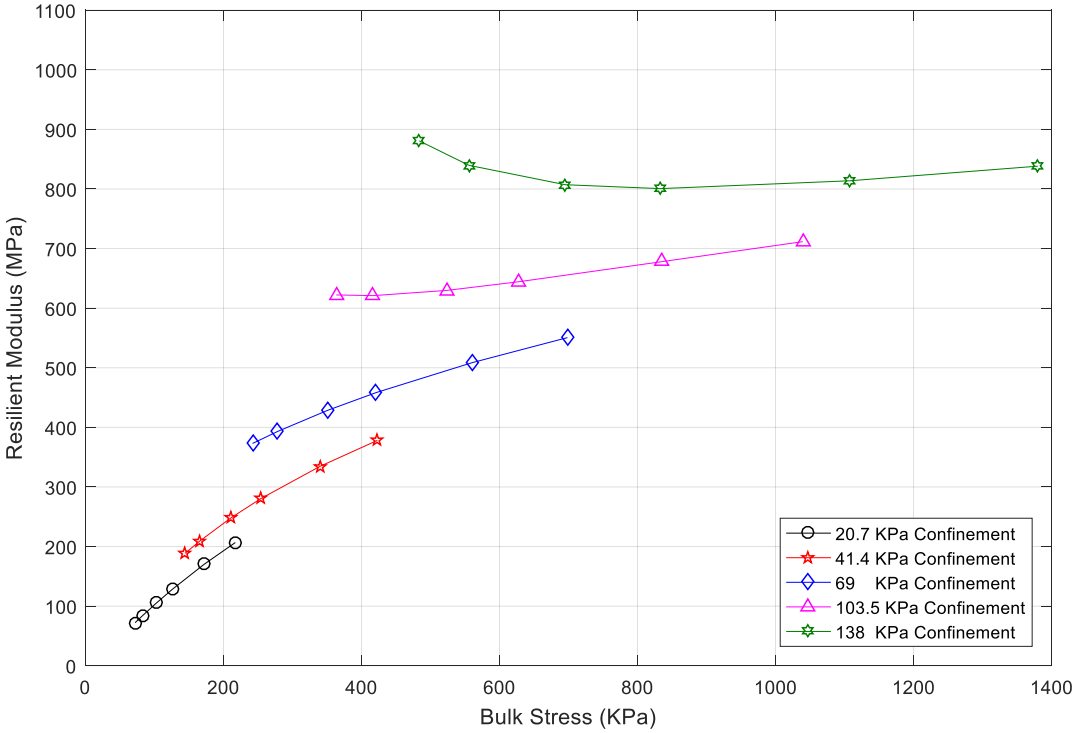

Figure 5.18 Bulk stress vs. resilient modulus for UGM-3(7.1)

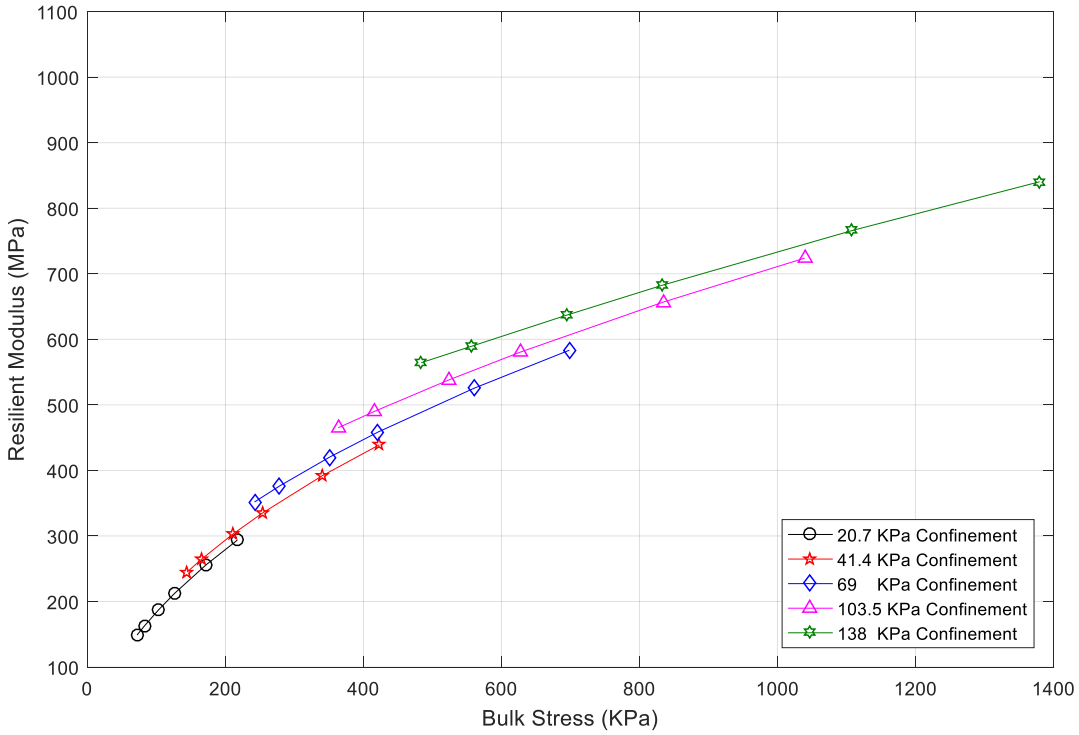

Figure 5.19 Bulk stress vs. resilient modulus for UGM-4(3.3) showing obvious signs of stress hardening.

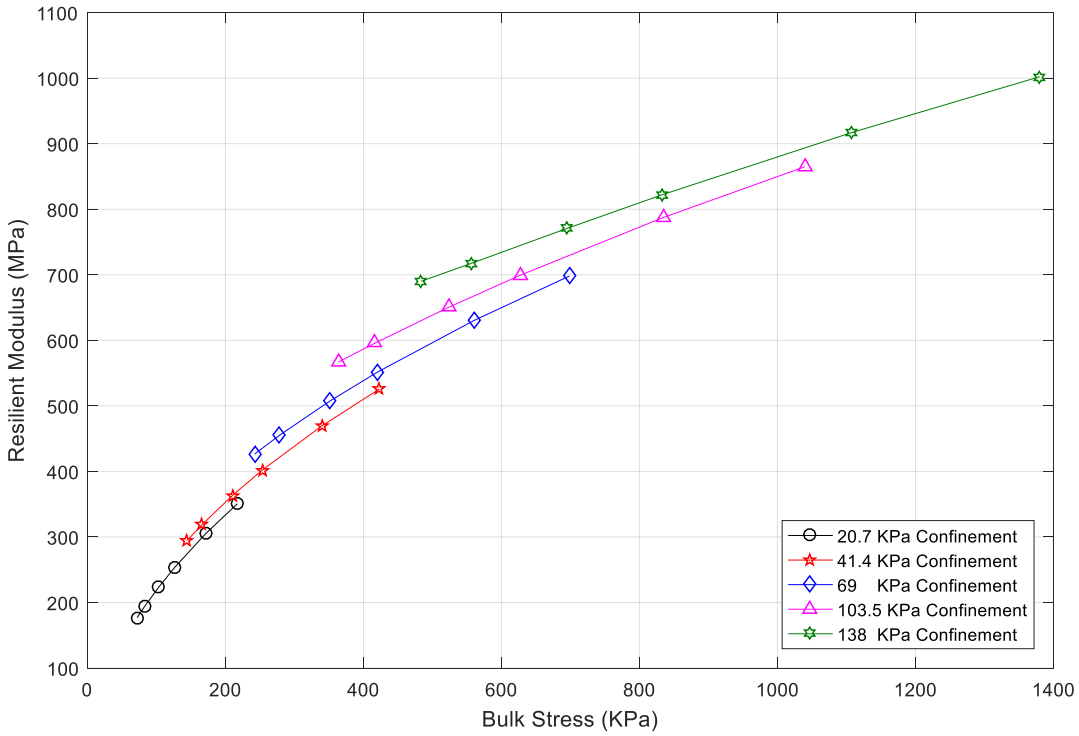

Figure 5.20 Bulk stress vs. resilient modulus for UGM-4(7.8) showing obvious signs of stress hardening.

5.2.5 Stability of UGM during Compaction

According to the statistical analysis done in the previous sections, an increased D10 and D60 was found to have positive effects on drainage and mechanical performance for the UGM gradation bands included in this study. However, such increase may affect the stability of the aggregate structure. The stability of the aggregate structure may be evaluated based on the coefficient of uniformity parameter. For the materials in this study, it was noticed that when the value of Cu falls below 30, the aggregates would demonstrate signs of poor stability during construction as well as difficulty to achieve and retain compaction. Based on field observation of several highway construction projects in Manitoba, materials UGM-1(12.3), UGM-3(6.9), and UGM-3(7.1) were found to provide stable surface during construction with no signs of shoving or rutting due to construction traffic, while UGM-4(3.3) and UGM-4(7.8) showed difficulty achieving and retaining density with some signs of instability.

The compaction effort was qualitatively observed in the laboratory, during MR specimen preparation, by recording the mechanical effort needed to achieve compaction higher than 95%, and a level (uniform) lift surface. The desired compaction was achieved by using a mechanical vibratory compactor with 2,000 blows/minute. Based on the required compaction effort to achieve 95% of the proctor density, samples requiring more than 60 blows per lift were considered difficult to compact. Table 5.5 shows that there is agreement between field and laboratory observation for stability and ease of compaction, and the results also show that Cu parameter can be a good indicator of UGM stability and ease of compaction.

It was also observed that materials with a gravel-to sand ratio (G/S) higher than two, tend to show signs of aggregate attrition (Figure 5.21) during compaction, as well as signs of fine particle

migration and segregation. Such high values of G/S result from a gradation having close values between P_4 and P_{200}, suggesting a gradation gap in the secondary aggregate structure.

Table 5.5 Stability and Compaction Effort

Sample ID	Cu	G/S	Compaction blows per lift
UGM-1(9)	67.5	0.94	<30
UGM-1(9.7)	78.0	1.71	30 to 60
UGM-1(12.3)	98.3	0.82	<30
UGB-1(14.5)	132	1.01	<30
UGM-2(3.5)	24.6	0.82	30 to 60
UGM-2(6.4)	29.9	1.27	30 to 60
UGM-3(3.9)	18.6	1.68	>60
UGM-3(6.9)	35.1	1.18	30 to 60
UGM-3(7.1)	46.6	1.89	30 to 60
UGM-4(3.3)	28.7	1.79	>60
UGM-4(7.8)	25.4	3.23	>60

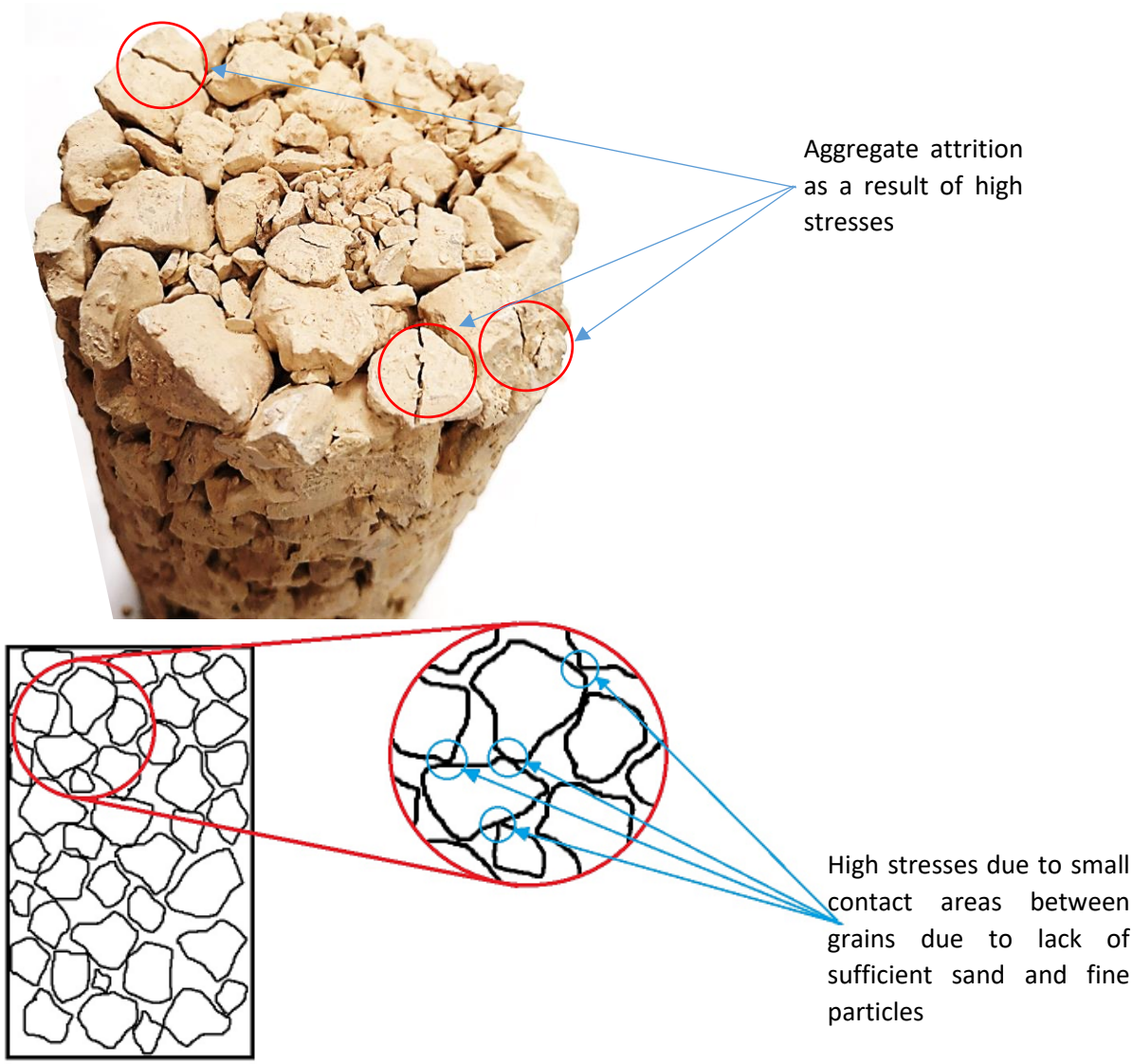

Figure 5.21 Specimen UGM-4(7.8) showing aggregate attrition due to compaction as a result of gradation gap in the secondary aggregate structure.

5.3 Field Testing for UGM Stiffness

UGM stiffness was assessed in the field by using FWD testing. The tests were performed after the construction of the base layer on PTH-10 and PTH-75. 40KN load drop was used on 450mm loading plate to simulate the stress generated by half a standard axle load. Equation 2.12 was used to calculate the surface modulus which is referred to as E_{FWD}.. Vennapusa et al. (2015) studied FWD deflection data for unpaved gravel roads in Missouri, and recommended 40KN load drop for accurate representation of traffic loads. The average of 21 data points for each location are reported in Table 5.6. Correlations between surface E_{FWD} and laboratory measured M_R can be established with more field measurements paired with laboratory testing of local materials.

$$E = \frac{2*(1-\mu^2)*\sigma*a}{D_0} \qquad \textbf{(Eq. 2.12)}$$

Table 5.6 Field measurements of surface layer modulus

Material ID	Location	Underlying Layer	Lab Measured M_R (MPa)	E_{FWD} (MPa)
UGM-1(12.3)	PTH-10	Class "C" Granular	183	154
UGM-3(6.9)	PTH-10	Class "C" Granular	184	188
UGM-4(3.3)	PTH-75	Rubblized Concrete	299	450

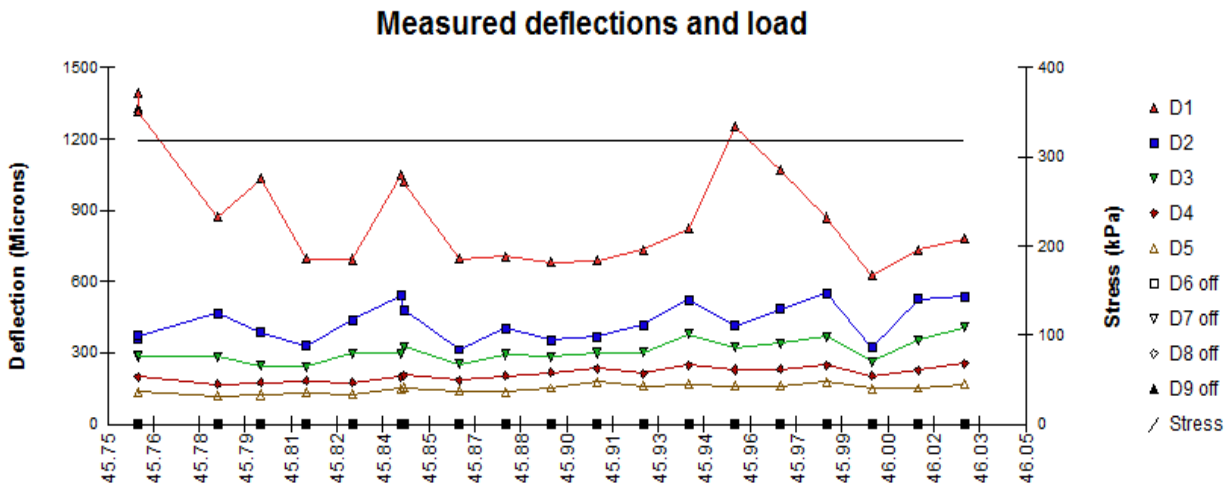

a)

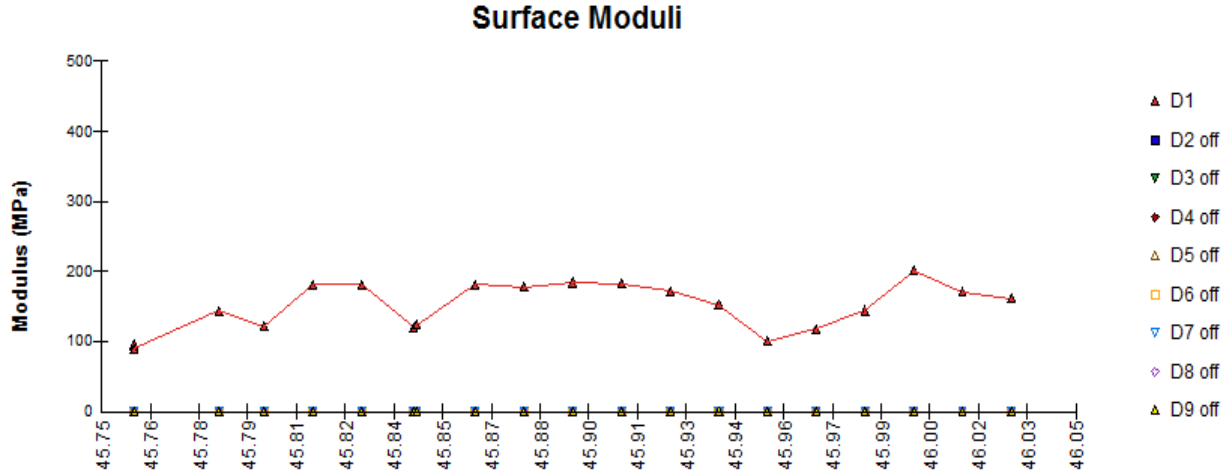

b)

Figure 5.21 FWD measured deflections and calculated surface moduli for PTH-10-South Curve "UGM-1(12.3)"

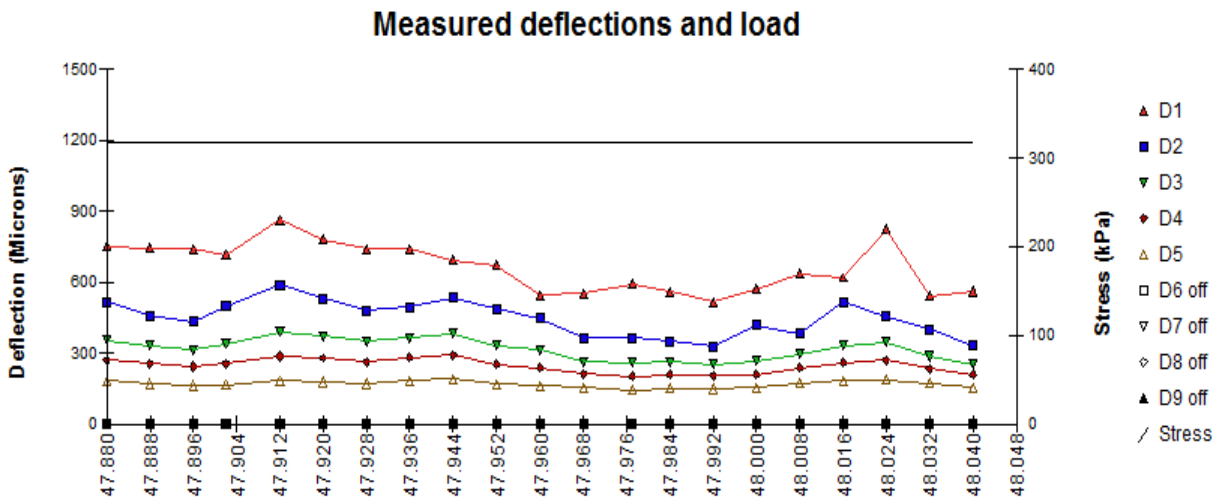

a)

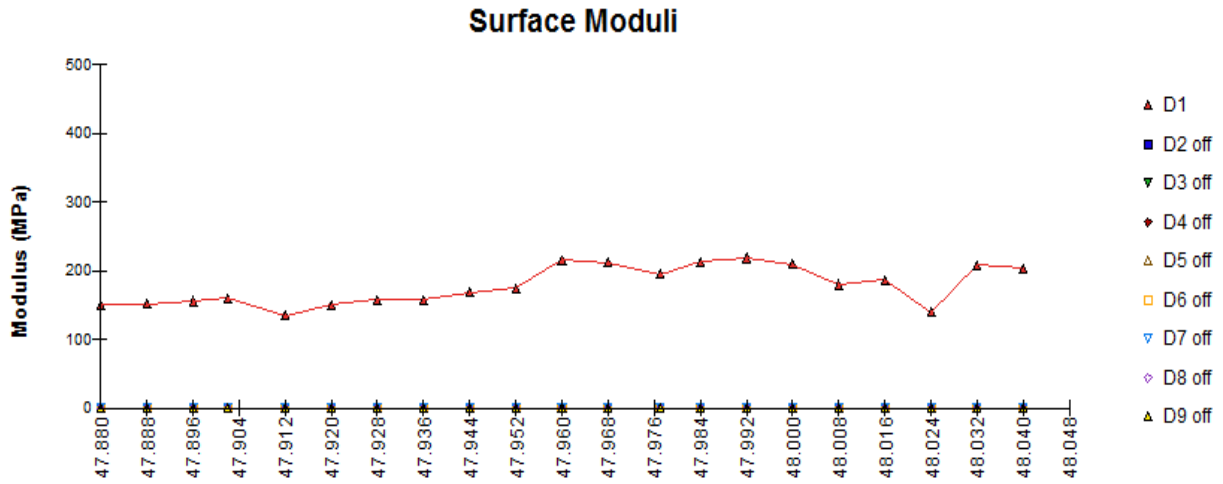

b)

Figure 5.22 FWD measured deflections and calculated surface moduli for PTH-10-North Curve "UGM-3(6.9)"

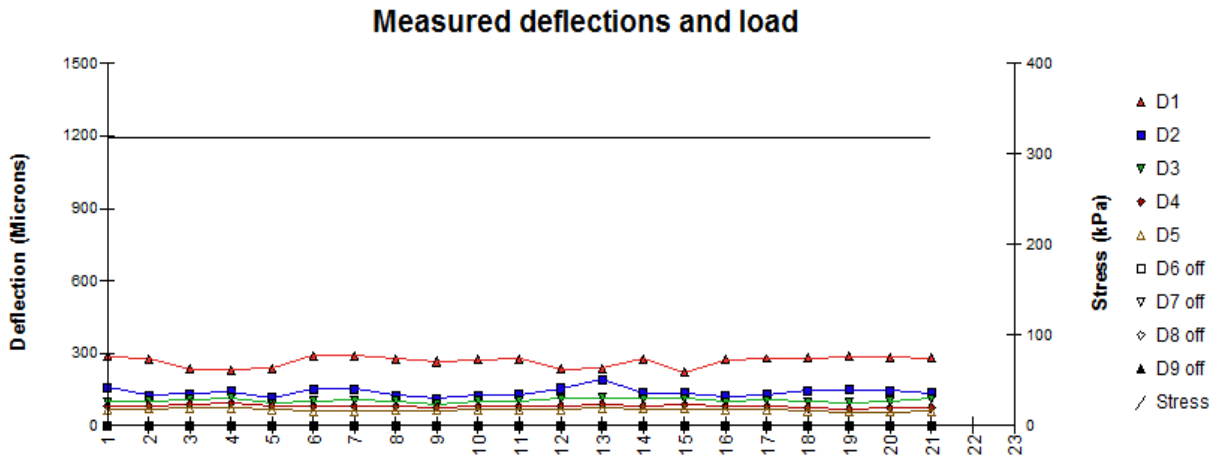

a)

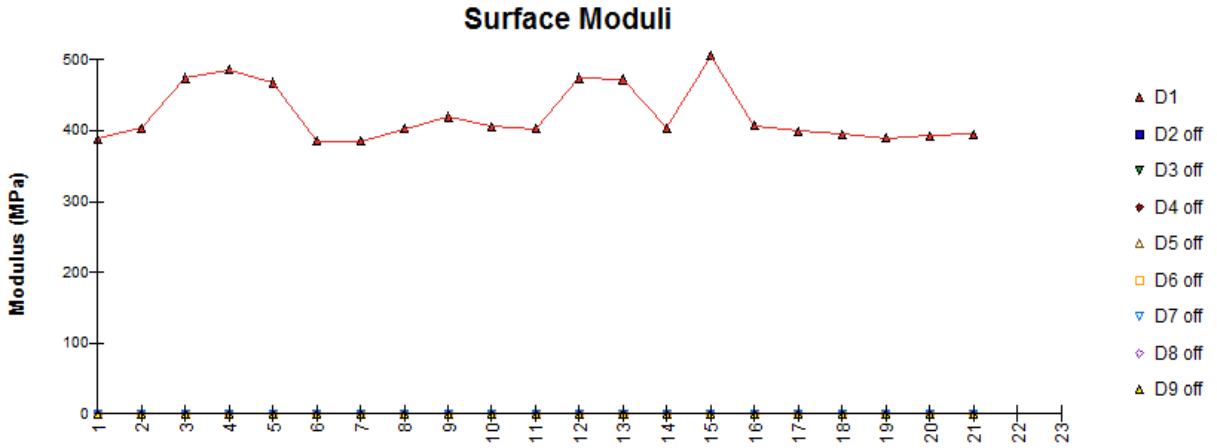

b)

Figure 5.23 FWD measured deflections and calculated surface moduli for PTH-75 "UGM-4(3.3)"

5.4 Plastic Behaviour of UGM

In pavement structures, UGM layers experience stresses that exceed their elastic limits along their service life. Therefore, it is important to characterize the plastic behaviour of UGM under cyclic loading. Figure 5.25 to Figure 5.28 show the relationship between the accumulation of plastic strain and load repetitions. The plotted values are the average between two tests for each material. It is noted that deformation behaviour progresses in two different stages. At the first stage (post

compaction), it can be noted that a high increase in plastic strain under few load cycles. As the permanent strain accumulation rate decreases, the material progresses to the second stage. The permanent strain in this stage is almost constant with increasing load repetitions. These curves are used to determine the permanent deformation properties of each material. Werkmeister's criteria was used to evaluate the shakedown behaviour of each UGM sample (S. Werkmeister, 2003);

Range A: Plastic Shakedown	$\varepsilon_{p(5000)} - \varepsilon_{p(3000)} < 4.5 \times 10^{-5}$
Range B: Plastic Creep	$4.5 \times 10^{-5} < \varepsilon_{p(5000)} - \varepsilon_{p(3000)} < 40 \times 10^{-5}$
Range C: Incremental Collapse	$\varepsilon_{p(5000)} - \varepsilon_{p(3000)} > 40 \times 10^{-5}$

The results of the shakedown analysis are reported in Table 5.7 and it shows that the average shakedown characterization, for all tested materials, fall in the Range-B limits. This indicates that the tested UGM would perform well with limited permanent deformation due to repeated loads during their service life, given optimum moisture conditions throughout their service life.

Permanent deformation test data was fitted to the three-parameter model in Eq-2.11. It was found that the model provides good fit for the UGM test data with a R^2 value of higher than 0.9 in all samples. Eq-2.11 is applied in the performance model in MEPDG for rutting prediction. Nonlinear regression techniques were used to calculate the permanent deformation regression coefficients, (ε_o, ρ, and β), for each material, which can be used as input parameters in MEPDG.

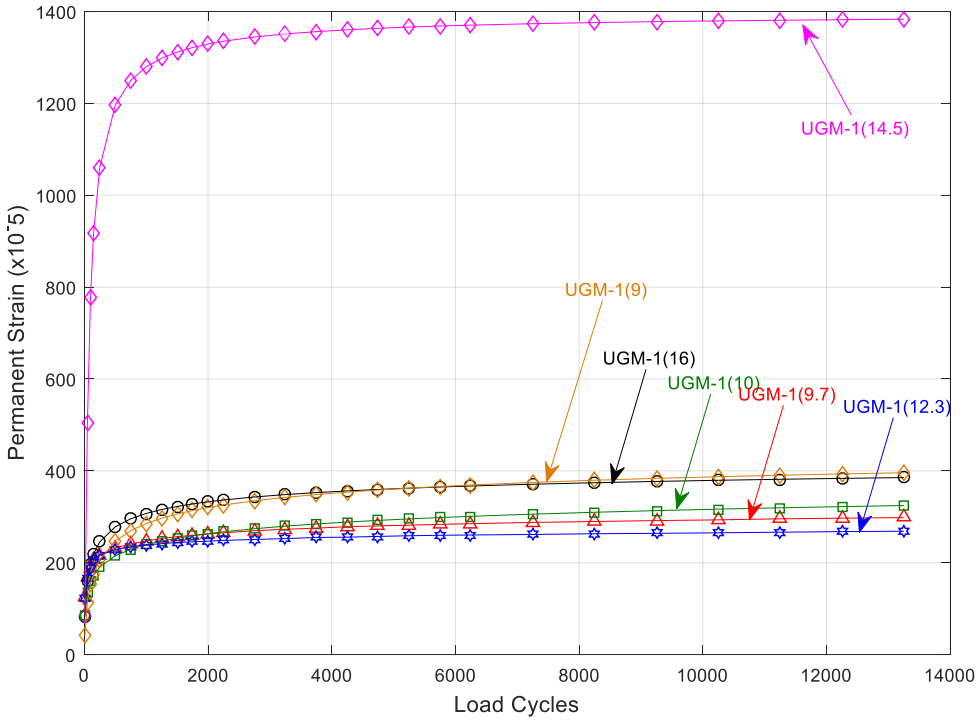

Figure 5.24 Permanent deformation accumulation of UGM-1 samples

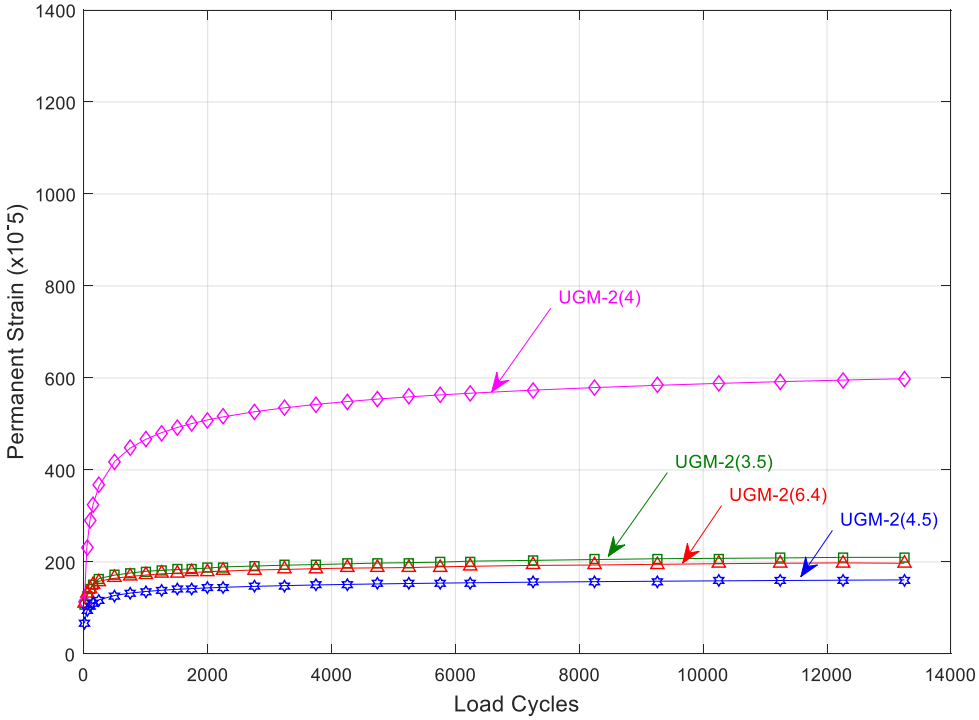

Figure 5.25 Permanent deformation accumulation of UGM-2 samples

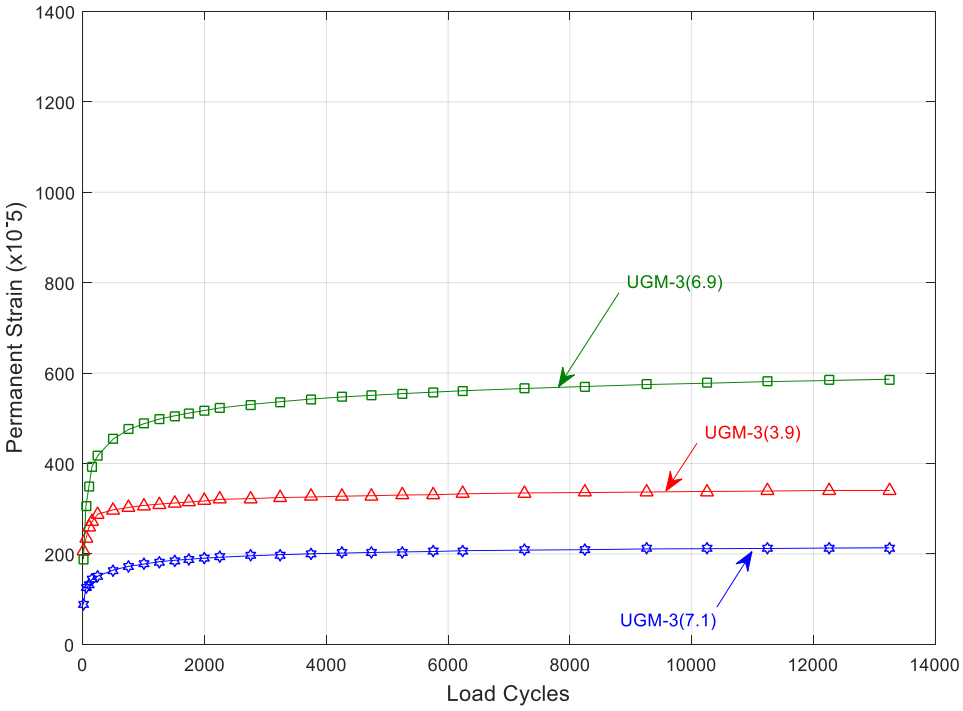

Figure 5.26 Permanent deformation accumulation of UGM-3 samples

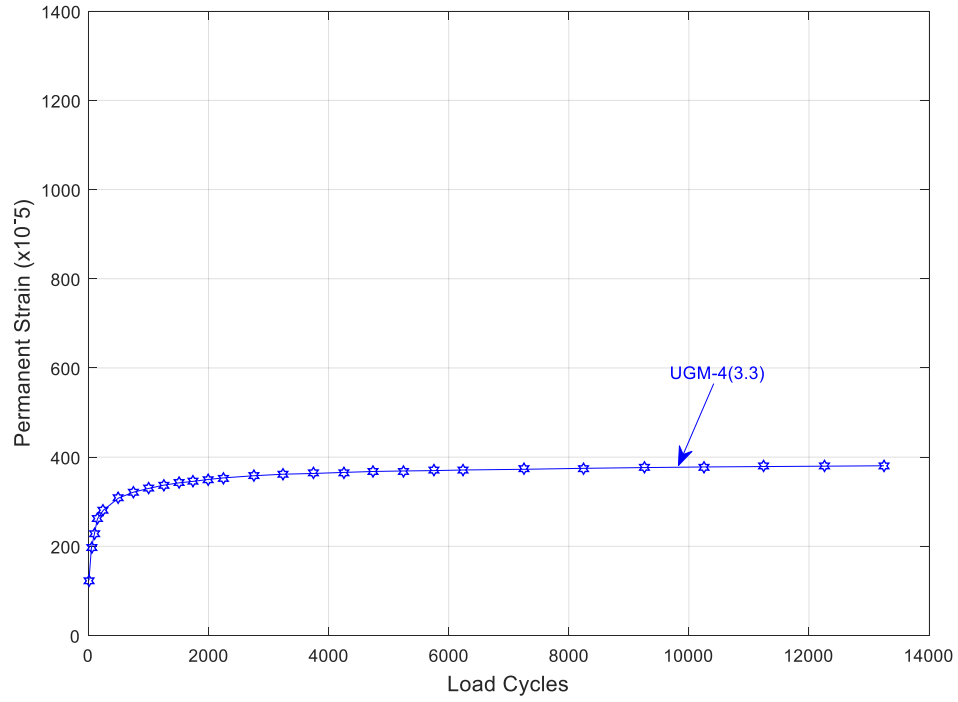

Figure 5.27 Permanent deformation accumulation of UGM-4 samples

Table 5.7 Plastic behaviour characterization

Sample ID	Permanent Deformation Parameters			Shakedown Parameters		Shakedown Behaviour
	ε_o	ρ	β	$\varepsilon_{13,000}$ (x 10-5)	$\varepsilon_{5,000} - \varepsilon_{3,000}$ (x 10-5)	
UGM-1(9)	4.628	58.58	0.3133	385	15.3	Plastic Creep
UGM-1(9.7)	3.951	19.61	0.1941	290	10.3	Plastic Creep
UGM-1(12.3)	2.911	6.787	0.3222	266	5.2	Plastic Creep
UGM-1(14.5)	14.06	49.62	0.7719	1387.02	18.6	Plastic Creep
UGM-1(10.5)	5.621	396.5	0.1706	323.87	16.9	Plastic Creep
UGM-1(16)	5.152	187.1	0.313	392.5	21.6	Plastic Creep
UGM-2(3.5)	2.858	10.28	0.1642	210	6.5	Plastic Creep
UGM-2(4)	7.34	77.16	0.3083	597.44	25.7	Plastic Creep
UGM-2(4.9)	NA	NA	NA	NA	NA	NA
UGM-2(6.4)	2.629	4.01	0.1546	200	5.3	Plastic Creep
UGM-2(4.5)	1.99	14.71	0.2278	160.79	4.9	Plastic Creep
UGM-3(3.9)	3.972	1.475	0.2073	340	7.2	Plastic Creep
UGM-3(6.9)	6.835	23.37	0.2908	581	18.2	Plastic Creep
UGM-3(7.1)	2.86	23.38	0.1997	215	7.4	Plastic Creep
UGM-4(3.3)	4.248	20.99	0.3532	382	10.1	Plastic Creep
UGM-4(7.8)	NA	NA	NA	NA	NA	NA

NA = Test was not conducted

Chapter 6 Conclusions and Recommendations

6.1 Summary

Towards the objective of evaluating the mechanical and drainage performance of UGM used by Manitoba Infrastructure, a series of laboratory and field testing, as well as theoretical analysis have been carried out. The mechanical behaviour of UGM was characterized by laboratory testing of the resilient modulus and permanent deformation. While the drainage behaviour was characterized by measuring the hydraulic conductivity and calculating the time required to drain 50% of the moisture from a given pavement structure.

Ten UGM samples were collected from different highway construction sites in Manitoba and the Yukon. The samples represent four base coarse specifications for the two Jurisdictions. Two updated gradation ranges were adopted by Manitoba Infrastructure and used in provincial trunk highway construction projects which allowed for both laboratory and field investigation of their performance. Standard proctor tests and sieve analysis were conducted by the transportation agencies providing the UGM, and the test data was used to complete this research.

In addition to the samples tested in this investigation, previous test data from Soliman, (2015) were used to conduct a statistical analysis. The analysis provided means to point out the physical properties that most significantly influence mechanical and drainage behaviour of compacted UGM. Test data was also used to assess the accuracy of hydraulic conductivity prediction models for the purpose of improving pavement design reliability.

6.2 Conclusions

- The drainage performance characterized by the hydraulic conductivity and time-to drain showed that the quality of drainage improved significantly in UGM gradation bands that allow larger maximum aggregate size and limited amounts of fines. UGM-4 gradation band, which specifies a maximum aggregate size of 37.5mm and fines content of 3 to 6, was found to have the highest average hydraulic conductivity in the studied gradations. However, materials from that gradation band showed signs of compaction difficulties and instability. While UGM-3 gradation band, specifying 25mm maximum aggregate size and fines content of 6 to 8, had no signs of instability and an overall fair quality of drainage.
- In UGM, the primary aggregate structure is responsible for creating pores which are filled by particles from the secondary aggregate structure. The secondary aggregate structure would significantly influence the pore structure and therefore control permeability. Based on the statistical analysis, conducted on test data from this research, it was found that D_{10} was a significant indicator of UGM hydraulic conductivity with a correlation coefficient of 0.65 and p-vale of 0.006.
- Applying hydraulic conductivity test data to study three hydraulic conductivity prediction models, commonly used to estimate the drainage performance of compacted UGM, lead to finding that the Moulton model provides the closest approximations to laboratory measured hydraulic conductivity. The model takes into account material properties as well as gradation parameters to estimate the hydraulic conductivity. However, the Moulton model was found to continuously underestimate the hydraulic conductivity of limestone materials. Due to the non-plastic nature of the fines and due to the crushed shape of the aggregates.

- The Double Ring Infiltrometer test method proved to be a simple and cost-effective method to provide in-situ hydraulic conductivity values that are comparable to laboratory measured values. The in-situ measurements of hydraulic conductivity conducted on PTH-10 and PTH-75 provided field confirmation of the improved drainage performance of updated gradation bands.
- UGM with better drainage performance were found to perform mechanically well under moisture conditions that approach saturation. Samples with higher hydraulic conductivity were able to dissipate excess pore water pressure during resilient modulus testing resulting in a smaller reduction in stiffness than in samples with lower hydraulic conductivity.
- The mechanical performance characterized by the resilient modulus for UGM has been found to improve significantly in gradations with larger nominal maximum aggregate size (NMAS) and lower fines content. UGM-4 gradation band, which specifies NMAS of 37.5mm and fines content of 3% to 6%, was found to have the highest average resilient modulus of about 327MPa. However, materials from that gradation band showed signs of compaction difficulties and instability. While UGM-3 gradation band, specifying 25mm NMAS and fines content of 6% to 8%, had no signs of instability and an average resilient modulus of about 194MPa.
- UGMs having coarse gradations and small amount of fines exhibited stress hardening behaviour with no signs of stress softening under different states of stress. Gradations with smaller particle sizes and higher fines content showed more obvious stress softening behaviour. Such mechanical behaviour is caused by poor interlock between grains. Small grains, in an aggregate structure that includes excessive amount of fines, would not be able

to achieve proper interlock needed to distribute applied stresses with minimum deformation.

- The interlock capacity between gravel size particles plays a primary role in the resilient mechanical response of UGM. Based on the statistical analysis, conducted on the data from this research, it was found that at a confidence level of 95%, the influence of aggregate size on stiffness can be captured by the D60 parameter. The corresponding correlation coefficient was 0.8 with a p-value of 0.0002.
- Plastic mechanical behaviour was characterized by the permanent deformation response using RLT test with 13,000 load cycles which could only capture the early age performance of the material. The shakedown approach, which depends on the rate of plastic strain accumulation, was used to evaluate the long-term performance of UGM. At OMC, all materials were found to fall under the plastic creep range which indicates desirable rutting resistance as a base material.
- Based on the analysis of laboratory test data from hydraulic conductivity and resilient modulus tests, it was found that a gradation band which allows D60 greater than 8mm and D10 greater than 0.2mm would result in good mechanical and drainage performance, (M_R > 200MPa, Time-to drain < 5 days).
- Gravel-to Sand ratio was found to be a significant indicator of stiffness, but not of drainage. However, G/S ratio in the range of 1.5 to 1.9 was found to ensure stability of the primary aggregate structure while maintaining good mechanical and drainage performance.
- Coefficient of uniformity was found reflect aggregate stability and ease of compaction. Samples with Cu less than 30 showed signs of instability during field construction and compaction difficulty during laboratory specimen preparation.

6.3 Future Considerations

This research has evaluated the drainage and mechanical performance of UGM through laboratory and field testing. Future research in the same context should take the following points in consideration:

- UGM specifications should reflect desired field performance. Transportation agencies can achieve such link between specifications and performance by employing performance related testing (hydraulic conductivity, resilient modulus, and permanent deformation) in the characterization of drainage and mechanical performance of UGM. Using the corresponding measured material properties in design would improve the reliability of pavement designs.
- During the evaluation of drainage performance of UGM samples in this research, it was observed that limestone samples consistently provided higher drainage values than gravel samples with the similar D_{10} and D_{60}. Further investigation needs to be conducted to point out the mineralogical properties responsible for the difference in performance.
- The hydraulic conductivity test setup, in the Pavement Research laboratory at the University of Manitoba, utilizes a submergible pump which maintains a constant head in a small reservoir that feeds into the test specimen. Such setup was found to significantly increase the water temperature ($30^{o}C$) in the constant head reservoir which leads to higher difference between corrected and measured hydraulic conductivity values. Future research should consider heat transfer alternatives to prevent heat buildup the constant head reservoir.
- The double ring infiltrometer field testing method was used in three locations to validate the drainage performance measured in the laboratory. Though the classified drainage

quality was found to be comparable between field and laboratory results, the hydraulic conductivity values differed substantially. Future research should consider more field testing paired with laboratory measurements of hydraulic conductivity in order to establish a reliable correlation between the two testing methods.

- Research observation during laboratory compaction of UGM samples showed that the coefficient of uniformity can be used to indicate the stability of the material under construction traffic. Additional research should be conducted to investigate the relationship in order to reduce construction costs while improving the performance of base materials.
- In the evaluation of plastic mechanical response, RLT testing was used to subject UGM samples to 13,250 load cycles at a single stress ratio. This number of loading cycles was chosen as a balance between accuracy and testing duration. Permanent deformation tests with longer duration and varying stress ratio should be considered in future research to validate the shakedown prediction.
- Evaluation of plastic behavior of UGM should be carried out under varying moisture conditions to assess the plastic behaviour of local UGM under different environmental conditions.

References

Abhijit, P., & Patil, J. (2011). Effects of Bad Drainage on Roads. Civil and Environmental Research, 1(1), 1–7.

Ahmed, M. U., Hasan, M. M., & Tarefder, R. A. (2018). Investigating Stress Dependency of Unbound Layers Using Falling-Weight Deflectometer and Resilient Modulus Tests. Geotechnical Testing Journal, 39(6), 954–964.

Ahmeduzzaman, M. (2016). Performance based characterization of virgin and recycled aggregate base materials. MSc. Thesis, Department of Civil Engineering, University of Manitoba.

Angell, D. J. (1988). Technical Basis for the Pavement Design Manual. Brisbane, Main Roads Department. Report no. RP165, Queensland, Australia.

ARA Inc ERES Consultants Division. (2004). Guide for Mechanistic Empirical Design of New and Rehabilitated Pavement Structures. Champaign, Illinois.

Arnold, G., Werkmeister, S., & Alabaster, D. (2007). The Effect of Grading on the Performance of Basecourse Sggregate. Land Transport New Zealand Report 325. Christchurch, New Zealand.

Ashtiani, R. (2009). Anisotropic characterization and performance prediction of chemically and hydraulically bounded pavement foundations, PhD Thesis. Texas A&M University.

ASTM. (2009). D3385-9, Standard Test Method for Infiltration Rate of Soils in Field Using Double-Ring Infiltrometer. ASTM International, West Conshohocken, PA, 2009.

ASTM (2015) D5856-15, Standard Test Method for Measurement of Hydraulic Conductivity of Porous Material Using a Rigid-Wall, Compaction-Mold Permeameter, ASTM International, West Conshohocken, PA, 2015

Ba, M., Tinjum, J. M., & Fall, M. (2015). Prediction of permanent deformation model parameters of unbound base course aggregates under repeated loading. Road Materials and Pavement Design, 16(4), 854–869.

Bennert, T., & Maher, A. (2005). The Development of a Performance Specification for Granular Base and Subbase Material. Federal Highway Adminstration, Report no. FHWA-NJ-2005-003, Piscataway, NJ.

Bilodeau, J. P., & Doré, G. (2012). Relating resilient behaviour of compacted unbound base granular materials to matrix and interlock characteristics. Construction and Building Materials, 37, 220–228.

Bilodeau, J. P., Dore, G., & Pierre, P. (2009). Pavement Base Unbound Granular Materials Gradation Optimization. In Bearing Capacity of Roads, Railways and Airfields. 8th International Conference (pp. 145–154). Champaign, IL, United States: CRC Press, Balkema.

Bilodeau, J. P., Dore, G., & Schwarz, C. (2011). Effect of seasonal frost conditions on the permanent strain behaviour of compacted unbound granular materials used as base course. International Journal of Pavement Engineering, 12(5), 507–518.

Blaschke, B. C., Afferton, K. C., & Willett, T. (1993). AASHTO Guide for Design of Pavement Structures 1993. Washington, D.C.: American Association of State Highways and Transportation Offecials.

Boadu, F. K. (2000). Hydraulic Conductivity of Soils from Grain-Size Distribution: New Models. Journal of Geotechnical and Geoenvironmental Engineering, 180(August), 739–746.

Bouchedid, M., & Humphrey, D. (2005). Permeability of base material for Maine roads. Transportation Research Records, 1936, 142–149.

Bree, J. (1967). Elastic-plastic behaviour of thin tubes subjected to internal pressure and intermittent high-heat fluxes with application to fast-nuclear-reactor fuel elements. The Journal of Strain Analysis for Engineering Design, 2(3), 226–238.

Cedergren, H. R. (1974). Methodology and Effectivness of Drainage Systems for Airfield

Pavements. Construction Engineering Research Laboratory. U.S. Army Corps of Engineers, Technical Report C-13.

Cedergren, H. R. (1988). Why all important pavements should be well drained. Transportation Research Record, (1188), 56–62.

Christopher, B. C., & Zhao, A. (2001). Design Manual for Roadway Geocomposite Underdrain Systems. Contech Construction Products INC. Rosewell, GA.

Christopher, B. R., & McGuffey, V. (1997). NCHRP synthesis of highway practice no.239: Pavement subsurface drainage systems. National Research Council, Washington, D.C.

Christopher, B. R., Schwartz, C., & Boudreau, R. (2006). Geotechnical Aspects of Pavements. Federal Highway Adminstration, Report no. FHWA NHI-05-037. Woodbury, MN.

Davich, P., Labuz, J., Guzina, B., & Drescher, B. (2004). Small Strain and Resilient Modulus Testing of Granular. Minnesota Department of Transportation, Research Services Section. St. Paul, MN.

Diefenderfer, P., Abhijit, P., & Patil, J. (2001). Six adverse effects of bad drainage on roads. Civil and Environmental Research, (1), 1, 1-17.

Eijkelkamp Agrisearch Equipment. (2015). Double Ring Infiltrometer: Operating Instructions. Document09.04, Giesbeek, Netherlands. 1–9.

Elsayed, A. S., & Lindly, J. K. (1996). Estimating Permeability of Untreated Roadway Bases. Transportation Research Record, 1519(9), 11–18.

Erlingsson, S., Baltzer, S., Baena, J., & Bjarnason, G. (2009). Measurement Techniques for Water Flow. In A. Dawson (Ed.), Water in Road Structures (p. P436). New York City. NY. USA.: Springer.

Federal Highway Administration. (1992). Drainable Pavement Systems, Participant Notebook. Publication no. FHWA-SA-92-00. Washington, D.C. 20590.

Garcia-Rojo, R., & Herrmann, H. J. (2005). Shakedown of Unbound Granular Material. Granular Matter, 7(2–3), 109–118.

George, K., & Uddin, W. (2000). Subgrade characterization for highway pavement design.

Mississippi Department of Transportation, Report no. FHWA/MS-DOT-RD-00-131. Jackson, MS, USA.

Gu, F., Zhang, Y., Luo, X., Sahin, H., & Lytton, R. L. (2017). Characterization and prediction of permanent deformation properties of unbound granular materials for Pavement ME Design. Construction and Building Materials, 155, 584–592.

Hall, K. T., & Crovetti, J. A. (2007). Effects of Subsurface Drainage on Pavement Performance: Analysis of the SPS-1 and SPS-2 Field Sections. Transportation Research Board. Washington, D.C.

Hazen, A. (1911). Discussion of "Dames on sand formation," by A.C. Koenig. Transactions of the American Society of Civil Engineers, (73), 199–203.

Heukelom, W., & Klomp, A. (1962). Dynamic Testing as a Mmeans of Controlling Pavements During and After Construction. In International Conference on the Structural Design of Asphalt Pavements (pp. 495–510). Ann Arbor, Michigan.

Hoffman, M., & Thompson M. (1982). Backcalculating nonlinear resilient moduli from deflection data. Transportation Research Record, 852, 42–51.

Hoppe, E. J. (1996). The Influence of Fines on Strengh and Drainage Characteristics of Aggregate Bases. Virginia Transportation Research Council. Chariottsbille, VA.

Hossain, M. S., & Lane, D. S. (2015). Development of a Catalog of Resilient Modulus Values for Aggregate Base for Use With the Mechanistic- Empirical Pavement Design Guide (MEPDG). Virginia Center for Transportation Innovation and Research, Report no. VCTIR 15-R13. Charlottesville, VA.

Ji, Y., Siddiki, N., Nantung, T., & Kim, D. (2012). Evaluation of resilient modulus of subgrade and base materials in indiana and its implementation in MEPDG. Transportation Research Board 2012 Annual Meeting (pp. 1–21). Washington, DC United States.

Kamal, M. A., Dawson, A. R., Farouki, T., Hughes, D. A. B., & Shaa'at, A. A. (1993). Field and Laboratory evaluation of the mechanical behaviour of unbound granular materials in pavements. Transportation Research Record No. 1406, (pp. 88–97).

Kaye, & Laby. (1995). Tables of Physical & Chemical Constants (16th ed.). Middlesex, UK: The National Physical Laboratory. Retrieved from www.kayelaby.npl.co.uk

Kim, S.-H., Tutumluer, E., Little, D. N., & Kim, N. (2007). Effect of gradation on nonlinear stress-dependent behaviour of a sandy flexible pavement subgrade. Journal of Transportation Engineering, 133(10), 582–589.

Kim, S., Little, D. N., & Masad, E. (2005). Simple methods to estimate ingerent and stress-induced anisotropic level of aggregate base. Transportation Research Record, 1913, 24–31.

Klute, A. (1965). Laboratory Measurement of Hydraulic Conductivity of Saturated Soil. Physical and Mineralogical Properties, Including Statistics of Measurement and Sampling (9.1). Madison, WI: American Society of Agronomy, Soil Science Society of America. https://doi.org/10.2134/agronmonogr9.1.frontmatter

Kolisoja, P. (1997). Resilient deformation characteristics of granular materials. PhD. Thesis, Department of Civil Engineering, Tampere University of Technology.

Lal, R., & Shukla, M. K. (2004). Principles of Soil Physics. (E. Paul & J. Ladd, Eds.) (5th ed.). New York, NY: Marcel Dekker, Inc. Retrieved from PP. 334

Lekarp, F., Isaccson, U., & Dawson, A. (2000a). State of the art: 1: Resilient response of unbound aggregates. Journal of Transportation Engineering, 126, 66–75.

Lekarp, F., Isaccson, U., & Dawson, A. (2000b). State of the art. II: Permanent strain response of unbound aggregates. Journal of Transportation Engineering, 126(1), 76–83.

Liang, R. Y. (2007). Evaluation of Drainable Bases Under Asphalt Pavements. Fediral Highway Adminstration, Report No. FHWA/OH-2007/10. Akron, OH.

Mallela, J., Titus-Glover, L., & Darter, M. . (2000). Considerations for providing subsurface drainage in jointed concrete pavements. Transportation Research Record, 1709, 1–10.

Moulton, L. K. (1980). Highway subdrainage design. Fediral Highway Adminstration, Report no. FHWA-TS-80-224. Morantown, WV.

Nazzal, M. D., Mohammad, L. N., & Austin, A. (2011). Evaluation of the Shakedown Behaviour of Unbound Granular Base Materials. In Geo-Frontiers (pp. 4752–4761). American Society

of Civil Engineers (ASCE).

Nazzal, M., & Mohammad, L. (2010). Estimation of Resilient Modulus of Subgrade Soils Using Falling Weight Deflectometer. Transportation Research Record: Journal of the Transportation Research Board, 2186, 1–10.

Nishizawa, T. (2012). A Prediction Method of Plastic Deformation Development of Subbase and Subgrade in Concrete Pavement. In Transportation Research Board 91st Annual Meeting. Washington, DC.

Oda, M. (1974). A Mechanical and Statistical Model of Granular Materials. Japanese Society of Soil Mechanics and Foundation Engineering, 14(1), 13–27.

Osouli, A., Chaulagai, R., Tutumluer, E., & Shoup, H. (2019). Strength Characteristics of Crushed Gravel and Limestone Aggregates with up to 12 % Plastic Fines Evaluated for Pavement Base / Subbase Applications. Transportation Geotechnics, 18, 25–38.

Ping, V., Changqin, L., & Yang, Z. (2001). Implementation of resilient modulus in the Florida flexible pavement design procedure. Florida Department of Transportation, Report WPI#051078

Powell, W., Potter, J., Mayhew, H., & Nunn, M. (1984). The structural design of bituminous roads. Transport and Road Research Laboratory, Report.1132. Crowthorne, UK.

Raad, L., Minassian, G., & Gartin, S. (1992). Characterization of saturated granular bases under repeated loads. Transportation Research Record, 1369, 73–82.

Rahman, M., & Erlingsson, S. (2015). A model for predicting permanent deformation of unbound granular materials. Road Materials and Pavement Design, 16(3), 653–733.

Randolph, B. W., Cai, J., Heydinger, A. G., & Gupta, J. D. (1981). Laboratory Study of Hydraulic Conductivity for Coarse Aggregate Bases. Transportation Research Record, 1519, 19–27.

Schreuders, H. (1989). Implication of aggregates in the design, construction, and performance of flexible pavements. (H. Schreuders & C. Marek, Eds.), ASTM International. Philadelphia, PA.

Sharma, S., & Das, A. (2008). Backcalculation of pavement layer moduli from falling weight deflectometer data using an artificial neural network. Canadian Journal of Civil Engineering, 35, 57–66.

Sharp, R. W. (1985). Pavement Design Based on Shakedown Analysis. Transportation Research Board, 1022, 99–107.

Sherard, J. L., Dunnigan, L. P., & Talbot, J. R. (1984). Basic properties of sand and gravel filters. Journal of Geotechnical Engineering, 110, 684–700.

Simmons, C. T. (2008). Henry Darcy (1803 – 1858): Immortalised by his scienti fi c legacy. Hydrogeology Journal, 16, 1023–1038.

Soliman, H. (2015). Modelling of the resiliant and permanent deformation behaviour of subgrade soils and unbound granular material. PhD. Thesis, Department of Civil Engineering, University of Manitoba.

Soliman, Haithem, and Ahmed Shalaby. 2015. "Permanent Deformation Behaviour of Unbound Granular Base Materials with Varying Moisture and Fines Content." Transportation Geotechnics 4: 1–12.

Soliman, Haithem, and Ahmed Shalaby. 2016. "Validation of Long-Term Pavement Performance Prediction Models for Resilient Modulus of Unbound Granular Materials." Transportation Research Record (2578): 29–37

Stolle, D., Peijun, G., & Ying, L. (2009). Resilient modulus properties of granular highway materials. Canadian Journal of Civil Engineering, 36(4), 639–654.

Suits, D., Goddard, J. B., & Baldwin, J. S. (1999). Testing and Performance of Geosynthetics in Subsurface Drainage. STP-1390, ASTM 100 Barr Harbor Drive West Conshohocken, PA

Tao, M., & Abu-Farsakh, M. (2008). Effect of Drainage in Unbound Aggregate Bases on Flexible Pavement Performance. Fediral Highway Adminstration, Report no. FHWA/LA.07/429. Baton Rouge, Luisiana.

Thom, N. H., & Brown, S. F. (1987). Effect of moisture on the structural performance of a crushed-limestone road base. Transportation Research Record, 1121, 50–56.

Thompson, M. R., & Robnett, Q. L. (1979). Resilient properties of subgrade soils. Journal of

Transportation Engineering, ASCE, 105(1), 71–89.

Tutumluer, E. (2013). Practices for Unbound Aggregate Pavement Layers. National Cooperative Highway Research Program, NCHRP Synthesis 445. Washington, D.C.

Ullidtz, P. (1987). Pavement Analysis (19th ed.). New York. NY. USA.: Elsevier Science Publishing Company Inc.

Uz, V. E., Saltan, M., & Gokalp, I. (2015). Comparison of DCP , CBR , and RLT Test Results for Granular Pavement Materials and Subgrade with Structural Perspective. In International Symposium on Non-Destructive Testing in Civil Engineering (NDT-CE). Berlin, Germany.

Van Til, C. J., McCullough, B. F., & Vallegra, B. A. (1972). Evaluation of AASHTO Interim Guides for Design of Pavement Structures. National Cooperative Highway Research Program, NCHRP Report.128, Oakland, California.

Vavrik, W. R., Huber, G., Pine, W. J., Carpenter, S. H., & Bailey, R. (2002). Bailey Method for Gradation Selection in Hot-Mix Asphalt Mixture Design. Transportation Research Circular, E-C044(October), 34.

Vennapusa, P. K. R., Asce, M., & White, D. J. (2015). Performance Assessment of Secondary-Roadway Infrastructure in Iowa after 2011 Missouri River Flooding. Journal of Infrastructure Systems, 21(4), 1–11.

Werkmeister, S. (2003). Permanent deformation behaviour of unbound granular materials.PhD. Thesis, University of Technology, Dresden, Germany.

Werkmeister, S., Dawson, A., & Wellner, F. (2004). Pavement design model for unbound granular materials. Journal of Transportation Engineering, 130(5), 665–741.

Werkmeister, S., Dawson, A., & Wellner, F. (2005). Permanent Deformation Behaviour of Granular Materials and the Shakedown Concept. Transportation Research Record, (1), 75–81.

Xiao, Y., Chen, L., Zhang, Z., Lyu, D., Tutumluer, E., & Zhang, J. (2016). Laboratory validation of a gradation design concept for sustainable applications of unbound granular materials in pavement construction. Construction and Building Materials, 129, 125–139.

Xiao, Y., Tutumluer, E., Qian, Y., & Siekmeier, J. (2012). Gradation Effects Influencing Mechanical Properties of Aggregate Base-Granular Subbase Materials in Minnesota. Transportation Research Record, 2267, 14–26.

Yau, A., & Quintus, H. L. Von. (2002). Study of LTPP Laboratory Resilient Modulus Test Data and Response Characteristics. Fediral Highway Adminstration Report no. FHWA-RD- 02-051 Austin, TX.